



EUROPEAN  
COMMISSION

European  
Research Area

# Carbon-14 Source Term

## CAST



<sup>14</sup>CAST

## WP5 Review of Current Understanding of Inventory and Release of C14 from Irradiated Graphite (D5.5)

Author(s):

Nelly Toulhout, Ernestas Narkunas, Borys Zlobenko, Daniela Diaconu, Laurent Petit, Stephan Schumacher, Stephane Catherin, Mauro Capone, Werner von Lensa, Gabriel Piña, Steve Williams, Johannes Fachinger, Simon Norris

Editor: Simon Norris

Date of issue of this report: 15/07/2015

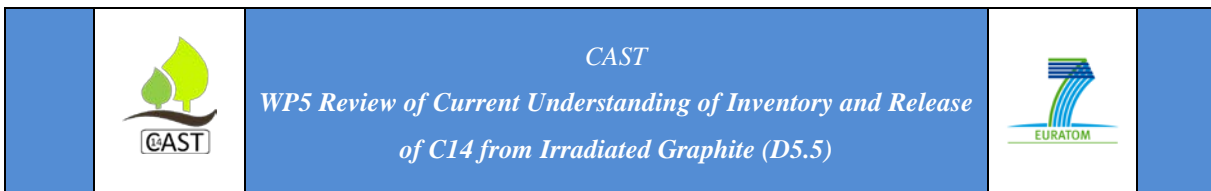
The project has received funding from the European Union's European Atomic Energy Community's (Euratom) Seventh Framework Programme FP7/2007-2013 under grant agreement no. 604779, the CAST project.

### Dissemination Level

PU	Public	X
RE	Restricted to the partners of the CAST project	
CO	Confidential, only for specific distribution list defined on this document	







## ***CAST – Project Overview***

The CAST project (CARbon-14 Source Term) aims to develop understanding of the potential release mechanisms of carbon-14 from radioactive waste materials under conditions relevant to waste packaging and disposal to underground geological disposal facilities. The project focuses on the release of carbon-14 as dissolved and gaseous species from irradiated metals (steels, Zircalloys), irradiated graphite and from ion-exchange materials.

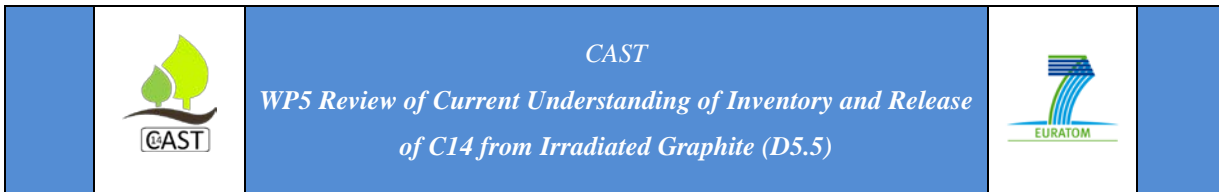
The CAST consortium brings together 33 partners with a range of skills and competencies in the management of radioactive wastes containing carbon-14, geological disposal research, safety case development and experimental work on gas generation. The consortium consists of national waste management organisations, research institutes, universities and commercial organisations.

The objectives of the CAST project are to gain new scientific understanding of the rate of release of carbon-14 from the corrosion of irradiated steels and Zircalloys and from the leaching of ion-exchange resins and irradiated graphites under geological disposal conditions, its speciation and how these relate to carbon-14 inventory and aqueous conditions. These results will be evaluated in the context of national safety assessments and disseminated to interested stakeholders. The new understanding should be of relevance to national safety assessment stakeholders and will also provide an opportunity for training for early career researchers.

For more information, please visit the CAST website at:

<http://www.projectcast.eu>





CAST		
Work Package: 5	CAST Document no. 5.5	Document type: R
Task: 5.1	CAST-2014-D5.5	R = report, O = other
Issued by: RWM		Document status:
Internal no. :		FINAL

Document title
<b>WP5 Review of Current Understanding of Inventory and Release of C14 from Irradiated Graphite (D5.5)</b>

## Executive Summary

The European Commission project CAST (CARbon-14 Source Term) commenced in 2013. Work Package 5 of CAST considers irradiated graphite and related carbon-14 behaviour and is led by Radioactive Waste Management Limited (RWM) (UK).

It is important that this Work Package is cognisant of existing understanding of carbon-14 in irradiated graphite and its release under disposal conditions, in particular information available from the European Commission project ‘Treatment and Disposal of Irradiated Graphite and other Carbonaceous Waste (CARBOWASTE). CARBOWASTE was launched in 2008 and terminated in March 2013. It addressed the retrieval, characterisation, treatment, reuse and disposal of i-graphite, including other carbonaceous waste such as non-graphitised carbon materials or pyrocarbon. The safety and environmental assessments related to irradiated graphite disposal as undertaken in the CARBOWASTE project confirmed there is sufficient understanding to justify site-specific studies on the disposal of graphite wastes in surface or geological disposal facilities, and that there is sufficient underpinning understanding at a generic level to be confident that graphite waste can be disposed in a manner such that relevant radiological protection regulations can be attained.

The objective of CAST WP5 is to understand the factors determining release of carbon-14 from irradiated graphite under disposal conditions (to include surface disposal facilities and geological disposal facilities). This is to be achieved by:

- Determining the carbon-14 inventory and concentration distribution in irradiated graphites, and factors that may control these;
- Measuring the rate and speciation of carbon-14 release to solution and gas from irradiated graphites in contact with aqueous solutions; and
- Determining the impact of selected waste treatment options on carbon-14 releases and relating this to the nature of carbon-14 in irradiated graphite.

To ensure knowledge and understanding from the CARBOWASTE project is thoroughly considered in the CAST project, Task 5.1 is being undertaken in the first year of CAST. This task is the subject of the current report, and has the aim to:

- Review CARBOWASTE and other relevant R&D activities to establish the current understanding of inventory and release of carbon-14 from irradiated graphites.

The current report is an output of Task 5.1, and represents Deliverable 5.5 of the CAST project. This report presents, in Section 2, contributions from various CAST organisations on respective current irradiated graphite research activities. Links to precedent work, e.g. as undertaken as part of the CARBOWASTE project, are presented where relevant. Each organisation report in Section 2 is written to be ‘stand-alone’; the common report reference list provides a good indication of the wealth of information currently accessible relating to irradiated graphite.

Irradiated graphite knowledge is presented in this report covering the following topics:

- Irradiated graphite characterisation – examples of current studies;
- Thermal annealing of irradiated graphite – example of current study;
- Exfoliation of irradiated graphite – example of current study;
- Release of  $^{14}\text{C}$  compounds from i-graphite in alkaline environment;
- Graphite corrosion;
- Leaching of irradiated graphite – examples of current studies.

Key points from the work reported herein include:



CAST

WP5 Review of Current Understanding of Inventory and Release  
of C14 from Irradiated Graphite (D5.5)



- Water-uptake tests have shown that, although virgin graphite exhibits little water-ingression and quasi-hydrophobic behaviour, irradiated graphite, as well as heat-treated graphite, behaves in a hydrophilic manner;
- Extrapolation of thermal-annealing and ion bombardment work on implanted  $^{13}\text{C}$  to  $^{14}\text{C}$  and its  $^{14}\text{N}$  precursor suggests that  $^{14}\text{N}$  tends to migrate to the free surfaces where it is partially released under the effect of temperature. Most of the  $^{14}\text{C}$  formed by activation of the remaining  $^{14}\text{N}$  might be located close to free surfaces (open pores). The sole influence of heat at UNGG reactor temperatures (200 – 500°C) did not promote  $^{14}\text{C}$  release. However, both  $^{14}\text{N}$  and  $^{14}\text{C}$  should be released through radiolytic corrosion when located close to free surfaces. The results strengthen the conclusion that the  $^{14}\text{C}$  inventory remaining in French irradiated graphites has been mainly produced through the activation of  $^{13}\text{C}$ .
- Only a small fraction of the total  $^{14}\text{C}$  inventory seems to be released on leaching in solution under simulated disposal conditions over timescales of up to 3 to 4 years. The total fractional releases and rates of release over experimental timescales are dependent on the source of irradiated graphite. The majority of release occurs to the solution phase; small amounts of gaseous phase releases have been measured. Leaching studies show an initial fast release followed by an approach to a steady state with a very low incremental release rate. Crushing may increase the accessibility of  $^{14}\text{C}$  to water but volatile  $^{14}\text{C}$  may be lost during crushing. Even when harsh acidic conditions are applied, <30% of the  $^{14}\text{C}$  inventory is released over experimental timescales. This points to the likelihood that there are two forms of  $^{14}\text{C}$  in irradiated graphite: leachable (with the leachability depending on accessibility to leachant) and non-leachable (inaccessible, probably part of graphite matrix);
- Under alkaline conditions  $^{14}\text{C}$  is released to the solution phase in hydrocarbon/organic forms as well as inorganic ( $^{14}\text{CO}_2$ /carbonate) forms under alkaline conditions. Evidence from French and UK studies show that some  $^{14}\text{C}$  is released to the gas phase under high-pH conditions. Gas phase releases include both

volatile  $^{14}\text{C}$ -hydrocarbon/organics (probably  $^{14}\text{CH}_4$ ) and  $^{14}\text{CO}$  at high pH.  $^{14}\text{CO}_2$  is also released from solution at near-neutral pH. The form of gaseous  $^{14}\text{C}$  release is affected by redox conditions with a lower redox seeming to favour  $^{14}\text{C}$ -hydrocarbon/organic compounds;

- Carbon-14 is mainly homogeneously-distributed throughout the graphite matrix, arising primarily from the activation of  $^{13}\text{C}$ , with a smaller proportion heterogeneously distributed on surfaces and enriched in hotspots;
- The chemical form of  $^{14}\text{C}$  is primarily elemental and bound covalently in the graphite structure. Thus the removal of the bulk of the  $^{14}\text{C}$  would only occur by oxidation, with conversion to either  $^{14}\text{CO}$  or  $^{14}\text{CO}_2$ . However the graphite matrix is extremely resistant to oxidation at repository temperatures and is unlikely to undergo oxidation once conditions have become anaerobic after closure. Kinetic and mechanistic studies undertaken to understand the corrosion behaviour of graphite under disposal conditions, as well as the natural analogues of graphite deposits in nature, show that the graphite has an extreme long life time. Only strong oxidative environments would lead to measurable graphite corrosion rates. Work to date indicates that significant graphite corrosion requires high dose rates of ionising radiation that would not be expected for irradiated graphite even in the form of spent HTR fuel.

## Contents

Executive Summary	i
1 Introduction	1
2 Organisation Summaries of Current Understanding of the Inventory of Carbon-14 in Irradiated Graphite and its Release	5
2.1 Centre National de la Recherche Scientifique (CNRS/IN2P3) laboratory: Institute of Nuclear Physics of Lyon (IPNL)	5
2.2 Lithuanian Energy Institute (LEI)	8
2.3 State Institution “Institute of Environmental Geochemistry National Academy of Science of Ukraine” (IEG NASU)	13
2.4 Regia Autonoma pentru Activitati Nucleare (INR)	14
2.4.1 Review the outcome of CARBOWASTE in the Romanian context	14
2.4.2 Review of <sup>14</sup> C content and speciation and their correlation with impurity content and irradiation history in the MTR i-graphite	16
2.4.3 Conclusions	24
2.5 Agence Nationale pour la gestion des déchets radioactifs / EDF (Andra / EDF)	26
2.6 Agenzia Nazionale per le Nuove Technologie, L’Energia e lo Sviluppo Economico Sostenibile (ENEA)	28
2.6.1 Italian Nuclear Graphite	28
2.6.2 Sample preparation and preliminary characterisation	30
2.6.3 Procedure description	31
2.6.4 Results	33
2.7 Forshungzentrum Juelich GmbH (FZJ)	34
2.7.1 Inventory of i-Graphite in Germany	34
2.7.2 Waste acceptance criteria for KONRAD	42
2.7.3 I-Graphite disposal in the ASSE test repository	45
2.7.4 Review of CARBOWASTE and CarboDISP	46
2.8 Centro de Investigaciones Energéticas Medioambientales y Tecnológicas (CIEMAT)	52
2.8.1 Samples investigate at CIEMAT	55
2.8.2 Characterisation Methods developed and applied at CIEMAT	56
2.8.3 Structural Characterization on i-graphite	69
2.8.4 Organic Molecules contents	75
2.8.5 Chemical Treatment by Inorganic Agents	81
2.9 Radioactive Waste Management (RWM) summary	89
2.9.1 Introduction	89
2.9.2 The Inventory of Carbon-14 in irradiated graphite in the UK Radioactive Waste inventory	90
2.9.3 Leaching studies of carbon-14 release from irradiated graphites	92
2.9.4 Early UK graphite leaching experiments	97
2.9.5 Japanese Tokai graphite leaching studies	99
2.9.6 UK Leaching studies of irradiated graphites	100
2.9.7 French leaching studies of irradiated graphites	106
2.9.8 Leaching of UK graphites as a potential chemical pre-treatment	109
2.9.9 Other relevant information	111

2.9.10	<b>Discussion</b>	<b>115</b>
2.9.11	<b>Summary of current understanding of carbon-14 releases from graphite on immersion in water</b>	<b>118</b>
2.9.12	<b>Conceptual Model for Carbon-14 Release from Irradiated Graphites</b>	<b>120</b>
2.10	<b>Furnaces Nuclear Applications Grenoble (FNAG) summary</b>	<b>121</b>
2.10.1	<b>Introduction</b>	<b>121</b>
2.10.2	<b>Background</b>	<b>121</b>
2.10.3	<b>Behaviour of graphite in aqueous phases at high <math>\gamma</math>-dose rates</b>	<b>122</b>
2.10.4	<b>Oxidation products of graphite corrosion</b>	<b>129</b>
2.10.5	<b>Long term scenario Water intrusion and Coated Particle damage in HTR fuel pebbles</b>	<b>130</b>
2.10.6	<b>Conclusions</b>	<b>134</b>
3	<b>Summary</b>	<b>135</b>
	<b>References</b>	<b>143</b>



## 1 Introduction

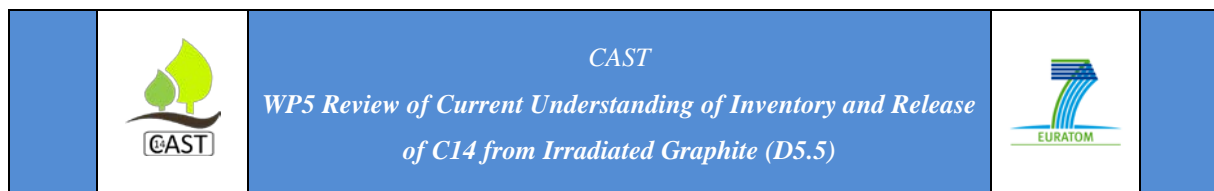
The utilization of nuclear graphite in reactors as moderator, reflector or operational material leads to an accumulation of radioactivity by neutron activation both of constituent elements of the graphite and of impurities. Radionuclide inventories at reactor end-of-life depend on a number of factors including impurity contents, irradiation history, reactor temperature and cooling gas composition. The principal long lived radionuclide species present are  $^{14}\text{C}$  and  $^{36}\text{Cl}$ , with shorter-lived species including  $^3\text{H}$ ,  $^{60}\text{Co}$  and small quantities of fission products and actinides. A fraction of these radionuclides is released during reactor operation due to temperature and radiolytic graphite corrosion. After removal from the reactor, irradiated nuclear graphite still remains radiotoxic for hundreds of thousands of years because of the presence of long-lived species such as  $^{36}\text{Cl}$  and actinides. Today about 260,000 tonnes of irradiated graphite have been accumulated worldwide (IAEA, 2010).

Irradiated graphite waste and other waste products are being, and will be, stored for many years in interim storage sites, with the associated burden for active radioprotection and site surveillance. Disposal of radioactive waste forms a key part of international policy for long-term radioactive waste management. Disposal can be implemented by isolating the waste from the biosphere in a surface disposal facility (SDF), or in a deep geological disposal facility (GDF). The irradiated graphite waste itself, whether treated or not, will likely be encapsulated in waste packages as part of the disposal process, which further provides for long term stability.

In order to assess whether irradiated graphite (i-graphite) can be disposed of as waste without or with further treatment, either in a GDF<sup>1</sup> or a SDF, it is necessary to assess its behaviour under disposal conditions. Disposal conditions are influenced by the natural hydrogeological environment and by the waste package and other engineered barriers. Release and subsequent transport in solution and in a gaseous phase may need to be considered for carbon-14.

---

<sup>1</sup> A geological disposal facility can also be referred to as a repository, where the disposal facility is envisaged as being at depth in a suitable geological environment.



The European Commission project CAST (CARbon-14 Source Term) commenced in 2013 and is investigating carbon-14 and its release from irradiated steels, Zircalloys and graphites and from spent ion-exchange resins. Work Package 5 of CAST considers irradiated graphite and related carbon-14 behaviour and is led by Radioactive Waste Management (UK). It is important that this Work Package is cognisant of existing understanding of carbon-14 in irradiated graphite and its release under disposal conditions, in particular information available from the European Commission project 'Treatment and Disposal of Irradiated Graphite and other Carbonaceous Waste (CARBOWASTE)'. CARBOWASTE was launched in 2008 and terminated in March 2013 [Banford et al., 2008; von Lensa et al., 2011]. It addressed the retrieval, characterisation, treatment, reuse and disposal of i-graphite, including other carbonaceous waste such as non-graphitised carbon materials or pyrocarbon. CARBOWASTE was structured into six Work Packages (WPs):

- WP1 Integrated waste management approach;
- WP2 Retrieval and segregation;
- WP3 Characterisation and modelling;
- WP4 Treatment and purification;
- WP5 Recycling and new products;
- WP6 Disposal behaviour of graphite and carbonaceous wastes.

In CARBOWASTE, the study of the disposal properties and disposability of irradiated graphite and carbonaceous wastes was subdivided in four strongly interlinked tasks undertaken within Work Package 6 of that project [Grambow et al., 2013]:

- Task 6.1 Disposal behaviour of graphite wastes
- Task 6.2 Disposal behaviour of carbonaceous wastes
- Task 6.3 Improving disposal behaviour by suitable waste packages
- Task 6.4 Assessment of waste performance under disposal conditions in the long term

The safety and environmental assessments related to irradiated graphite disposal as undertaken in the CARBOWASTE project confirmed there is sufficient understanding to justify site-specific studies on the disposal of graphite wastes in an SDF or a GDF, and that

there is sufficient underpinning understanding at a generic (non site-specific) level to be confident that graphite waste can be disposed in a manner such that relevant radiological protection regulations can be attained. Confidence that a GDF or a SDF can be developed is built on understanding of how multiple barriers – engineered barriers and natural barriers - can work together to ensure safety, and there is confidence that, for specific site and disposal concept, an optimised design that meets all environmental safety requirements can be developed.

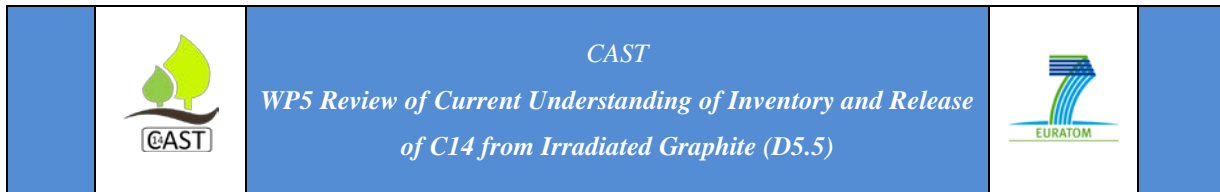
Residual uncertainties for irradiated graphite disposal, which could be progressed via future research, were identified as part of the assessment studies undertaken in CARBOWASTE [Grambow et al., 2013]. Such future research could assist in optimisation studies for an SDF or a GDF. Grambow et al. emphasise that, even in the absence of such future work, there is a sufficient understanding of irradiated graphite to conclude with confidence, on the basis of work undertaken in the EC CARBOWASTE project, that irradiated graphite waste can be safely disposed in a wide range of disposal systems.

The objective of CAST Work Package 5 is to understand the factors determining release of  $^{14}\text{C}$  from irradiated graphite under disposal conditions. This is to be achieved by:

- Determining the  $^{14}\text{C}$  inventory and concentration distribution in irradiated graphites, and factors that may control these;
- Measuring the rate and speciation of  $^{14}\text{C}$  release to solution and gas from irradiated graphites in contact with aqueous solutions; and
- Determining the impact of selected waste treatment options on  $^{14}\text{C}$  releases and relating this to the nature of  $^{14}\text{C}$  in irradiated graphite.

To achieve these objectives, five tasks are to be undertaken:

- Task 5.1 – Review of CARBOWASTE and other relevant R&D activities to establish the current understanding of inventory and release of  $^{14}\text{C}$  from i-graphites;
- Task 5.2 – Characterisation of the  $^{14}\text{C}$  inventory in i-graphites;
- Task 5.3 – Measurement of release of  $^{14}\text{C}$  inventory from i-graphites;
- Task 5.4 – New wasteforms and  $^{14}\text{C}$  decontamination techniques for i-graphites; and
- Task 5.5 – Data interpretation and synthesis – final report.



The current report is an output of Task 5.1, and represents Deliverable 5.5 of the CAST project. This report presents, in Section 2, contributions from various CAST organisations on respective current i-graphite research activities. Links to precedent work, e.g. as undertaken as part of the CARBOWASTE project, are presented where relevant. Each organisation report in Section 2 is written to be ‘stand-alone’; the common report reference list provides a good indication of the wealth of information currently accessible relating to irradiated graphite.

## 2 Organisation Summaries of Current Understanding of the Inventory of Carbon-14 in Irradiated Graphite and its Release

### 2.1 Centre National de la Recherche Scientifique (CNRS/IN2P3) laboratory: Institute of Nuclear Physics of Lyon (IPNL)

Previous work carried out at IPNL is part of the PhD work of Silbermann [Silbermann, 2013; Silberman et al., 2014]. The aim of this work was to obtain data on  $^{14}\text{C}$  inventory, localization and speciation in irradiated graphite in order to be able to anticipate its behaviour during disposal. More specifically, it aimed to understand the behavior of  $^{14}\text{C}$  during reactor operation by discriminating the effects of temperature and irradiation.

We have implemented an indirect approach to study the behavior of  $^{14}\text{C}$ . This approach is based on  $^{13}\text{C}$  implantation used to simulate  $^{14}\text{C}$ .  $^{13}\text{C}$  implantation results in a disordering of the graphite structure. We can consider that  $^{13}\text{C}$  stops at an interstitial position or at a vacancy and may therefore be representative of the  $^{14}\text{C}$  displaced from its original site due to recoil during neutron irradiation. We have also implanted samples with  $^{14}\text{N}$  to study the behavior of nitrogen as a main precursor of  $^{14}\text{C}$ . The implantations were performed in both cases into graphite samples whose surfaces had been previously polished. The implantation fluence for each element is of  $F=6.10^{16}$  at/cm<sup>2</sup> corresponding to 5at.% at the projected range  $R_p$ . They result in Gaussian-like profiles with respective projected ranges  $R_p$  centered at around 300 nm for  $^{13}\text{C}$  and 450 nm for  $^{14}\text{N}$ . In both cases, implantation creates damage in the graphite structure estimated to some displaced atoms (dpa) according to SRIM software<sup>2</sup> (Ziegler et al., 2008). Thus, the amount of dpa's created by ion implantation is of the same order as that induced by neutron irradiation in most UNGG (Uranium Naturel Graphite Gaz) reactors. The analyses of the implanted species were carried out by SIMS before and after the treatments in order to study the evolution of their profiles or to map the implanted elements as well as the native nitrogen impurity. The modification of the graphite structure

---

<sup>2</sup> SRIM is the acronym for Stopping and Range of Ions in Matter. It is a group of computer programs which calculate interaction of ions with matter. SRIM is based on a Monte Carlo simulation method and is very popular in the ion implantation research and technology community and also used widely in other branches of radiation material science.

was followed by Raman microspectrometry. Moreover, XPS measurements were carried out to study the speciation of the native (non-implanted) nitrogen.

Virgin graphite samples issued from the moderator of the Saint Laurent A2 French UNGG reactor were used to carry out annealing experiments.

Two types of experiments were carried out:

- 1) Annealing up to 1600°C of implanted graphite samples in vacuum or inert atmosphere.
- 2) Annealing at 500°C of implanted graphite samples in a gas simulating the UNGG gas (composition: 97.43 vol. % CO<sub>2</sub>, 2.5 vol. % CO, 500 vpm CH<sub>4</sub>, 100 vpm O<sub>2</sub> and 100 vpm H<sub>2</sub>). In this configuration, the gas and the graphite/gas interface were simultaneously irradiated with helium ions. This induces gas radiolysis as well as an energy deposit at the implanted graphite/gas interface (the value of the electronic stopping power induced by the helium ions at the gas/graphite interface is of  $S_e \sim 400\text{keV}/\mu\text{m}$ , this value being of the same order as mean values induced by recoil atoms after neutron irradiation).

The following main conclusions may be inferred from the obtained results:

- High concentration levels (above 200 at.ppm) of native nitrogen have been measured close to the free surfaces. This nitrogen is in the form of CN (C-N, C=N or C≡N) compounds. Moreover, the implanted <sup>14</sup>N tends to migrate towards the free surfaces under the effect of temperature. Part of the nitrogen tends to be released at 500°C.
- Annealing at temperatures ranging up to 1300°C does not induce any migration of the implanted <sup>13</sup>C. Temperatures as high as 1600°C are required for its diffusion (diffusion coefficient around  $D \sim 10^{-19} \text{ m}^2 \cdot \text{s}^{-1}$ ). When the implanted graphite is simultaneously irradiated and heated, the presence of methane prevents the graphite surface from gasification. As soon as the methane has been consumed through gas radiolysis, the gas/graphite interface begins to be gasified. CO<sub>2</sub> is radiolysed and the thereby formed O• radicals promote graphite surface consumption through oxidative corrosion. Thus in our experiment, radiolytic corrosion has led to the partial or total

loss of the implanted  $^{13}\text{C}$  or  $^{14}\text{N}$ . Moreover, a greater impact of corrosion has been observed for the binder rather than for the coke grains.

Finally, the extrapolation of our results to  $^{14}\text{C}$  and the  $^{14}\text{N}$  precursor suggests that:

- $^{14}\text{N}$  tends to migrate to the free surfaces where it is partially released under the effect of temperature ( $500^\circ\text{C}$ ). Therefore, most of the  $^{14}\text{C}$  formed by activation of the remaining  $^{14}\text{N}$  might be located close to free surfaces (open pores).
- The sole influence of heat at UNGG reactor temperatures ( $200 - 500^\circ\text{C}$ ) did not promote  $^{14}\text{C}$  release. On the contrary, both  $^{14}\text{N}$  and  $^{14}\text{C}$  should have been released through radiolytic corrosion when located close to free surfaces.
- Our results strengthen the conclusions of [Poncet et al., 2013] arguing that the remaining  $^{14}\text{C}$  inventory in French irradiated graphites has been mainly produced through the activation of  $^{13}\text{C}$ .

## **2.2 Lithuanian Energy Institute (LEI)**

For Lithuania, the main carbon-14 source is irradiated graphite from Lithuanian nuclear power plant at Ignalina site. Ignalina NPP, located in the north-eastern part of Lithuania, has two Units with RBMK-1500 water-cooled graphite-moderated channel-type power reactors. Both units are under decommissioning now. The core of one RBMK-1500 reactor contains about 1900 t of graphite. Graphite is used as a moderator and reflector of neutrons (GR-280 grade graphite blocks, ~1800 t). It is also used for positioning of technological channels in the reactor core (GRP-2-125 grade graphite rings/sleeves, ~100 t) [Almenas et al. 1998].

During the EC 7<sup>th</sup> FP Project CARBOWASTE, C-14 activity inventories were numerically estimated for the graphite blocks and rings/sleeves of the Unit 1 by Lithuanian Energy Institute (LEI) [Narkunas et al., 2013a]. Due to the lack of representative information on the materials compositions of the RBMK-1500 reactor graphite (and in order to assess the impact of the impurities on the induced activity), two cases were defined for the neutron activation analysis – materials' compositions with maximal and with minimal reported concentrations of impurities. The long-lived C-14 is one of the most important radionuclides in the activated RBMK reactors graphite and is mainly formed due to the carbon (raw material) and nitrogen (impurity) activation. The propagation of the helium-nitrogen cooling gas mixture (which circulates around RBMK reactor graphite stack) into the graphite pores may additionally increase the quantity of nitrogen impurity and consequently increase C-14 production. Therefore, a conservative estimation of possible nitrogen impurity content coming from the cooling gases of RBMK-1500 reactor graphite stack was also done, and as a result, an axial distributions of induced C-14 activities in the RBMK-1500 reactors' graphite blocks and rings/sleeves were achieved. The summarised results of the study are presented in Table 2.2.1.

**Table 2.2.1: Summarised Results on Modelled C-14 Activities in the Ignalina Unit 1 Reactor Graphite**

Assumption	Min. C-14 activity, Bq/g	Max. C-14 activity, Bq/g	Avg. C-14 activity, Bq/g
<b>Modelling of Ignalina NPP Unit 1 reactor's graphite blocks (GR-280 grade graphite)</b>			
No nitrogen impurities in graphite	–	$7.0 \times 10^4^*$	–
Minimal initial nitrogen impurities in graphite matrix	$1.8 \times 10^4^*$	$7.2 \times 10^4^*$	$5.2 \times 10^4^*$
Maximal initial nitrogen impurities in graphite matrix	$1.2 \times 10^5^*$	$5.0 \times 10^5^*$	$3.6 \times 10^5^*$
Maximal initial nitrogen impurities in graphite matrix and nitrogen is present in all open graphite pores	–	$8.6 \times 10^5^*$	–
Maximal initial nitrogen impurities in graphite matrix and nitrogen is present in all (open and closed) graphite pores	–	$9.9 \times 10^5^*$	–
<b>Modelling of Ignalina NPP Unit 1 reactor's rings/sleeves graphite (GRP-2-125 grade graphite)</b>			
No nitrogen impurities in graphite	$1.5 \times 10^4^*$	$6.1 \times 10^4^*$	$4.3 \times 10^4^*$
Maximal initial nitrogen impurities in graphite matrix** and nitrogen is present in all open graphite pores	–	$6.5 \times 10^5^*$	–
Maximal initial nitrogen impurities in graphite matrix** and nitrogen is present in all (open and closed) graphite pores	–	$6.8 \times 10^5^*$	–

\*) – These activities are minimal, maximal or average in axial direction in the region of the reactor active core;

\*\*\*) – Assuming the same concentration of nitrogen impurity as for GR-280 grade graphite – 70 ppm, because there was no data on initial nitrogen impurity in GRP-2-125 grade graphite.

From the point of view of C-14 release from irradiated graphite, the results may also be interpreted in the way, that there could be four major fractions of C-14 release/removal from irradiated RBMK reactors graphite. The first, and likely the most difficult to remove is the fraction of C-14 coming from C-13 activation in graphite matrix, which can be in the order of  $10^4$  Bq/g for both graphite grades. The second fraction is associated with activation of nitrogen impurities, which are incorporated in the virgin graphite matrix. This fraction of C-14 looks like also difficult to remove from irradiated graphite and may be in the order up

to  $10^5$  Bq/g, depending on the initial nitrogen impurity concentration. The third and fourth fractions are related to the nitrogen adsorption/penetration from cooling gases into the graphite pores and its activation. The fraction of C-14 being produced in the open pores may be in the order of  $10^5$  Bq/g for the most conservative case, whereas in the closed pores it may be  $\sim 3$  and  $\sim 7$  times lower for GR-280 and GRP-2-125 grade graphites respectively. These fractions of C-14 looks like the easiest fractions to remove (the fraction from open pores being more easy), as the produced C-14 is probably only adsorbed on the surfaces of the graphite pores and as free gases inside them, without being incorporated into the graphite matrix.

Some experimental measurements of C-14 inventory in the RBMK-1500 reactor graphite were performed by Centre for Physical Sciences and Technology (CPST) within the frame of CARBOWASTE Project [Narkunas et al., 2013b]. The measurements were performed for the specimens of graphite rings/sleeves taken from the regions of active core, top and bottom reflectors. So, the calibration of LEI-developed numerical models against these experimental activity measurement results was performed too. It was done by the reverse activation modelling way, i.e. the initial concentration of nitrogen impurity during the modelling was altered until the modelled activities of C-14 matched best the measured ones (so called “explanatory” nitrogen impurity concentration was defined). As measurements were made for three different positions, the best match was obtained by the help of the least squares method, i.e. the “explanatory” nitrogen concentration was the one that gave the minimal sum of the squares of the differences between measured and modelled activities in all three positions. The comparison of the modelled specific activities of C-14 in the graphite rings/sleeves (using estimated “explanatory” 13 ppm concentration of nitrogen impurity) showed very good agreement with the measured results. Modelled specific activities of C-14 were the same as measured ones (including measurement errors):

- $\sim 1.30 \times 10^5$  Bq/g in the graphite rings/sleeves in the region of active core, while measured activity was  $\sim 1.3 \pm 0.2 \times 10^5$  Bq/g;
- $\sim 1.66 \times 10^4$  Bq/g in the graphite rings/sleeves in the region of top reflector, while measured activity was  $\sim 1.3 \pm 0.4 \times 10^4$  Bq/g;

- $\sim 2.32 \times 10^4$  Bq/g in the graphite rings/sleeves in the region of bottom reflector, while measured activity was  $\sim 2.4 \pm 0.6 \times 10^4$  Bq/g.

CPST also reported calculated nitrogen impurity of  $15 \pm 4$  ppm, which gives the closest results of their modelling in comparison with measurements. This quantity of  $15 \pm 4$  ppm for nitrogen is also in good agreement with LEI determined “explanatory” concentration of 13 ppm nitrogen. There was no published data on initial nitrogen impurity content in GRP-2-125 grade graphite, but estimated “explanatory” concentration (13 ppm) was less than possible maximal calculated concentration of nitrogen in graphite pores (46 ppm) and less than maximal reported concentration for GR-280 grade graphite (70 ppm). More information on performed numerical and experimental investigations of C-14 inventories in RBMK-1500 graphite are presented in CARBOWASTE Deliverables [Narkunas et al., 2013a, Narkunas et al., 2013b].

A short leaching test for RBMK graphite was performed at the very end of the CARBOWASTE project too. The results of this leaching test of two samples of graphite bushing from RBMK-1500 reactor thermal channel during three months were presented in CARBOWASTE Deliverable [Druteikiene et al., 2013]. The leaching test of C-14 from irradiated graphite bushing of Ignalina Nuclear Power Plant (INPP) RBMK-1500 reactor (Unit 1) was planned according to the ISO method of leach testing of immobilized radioactive waste solids and was performed by CPST and Ignalina NPP staff. For the test, two alkaline leaching solutions (pH=7.5 and pH=10) were prepared by addition of a controlled amount of NaOH to distilled water. The leached amount of C-14 after a one day soak in alkaline water solution corresponded to  $\sim 0.03$  % of the total C-14 activity. Leaching rates for both experiments during the first day was about twice that of the leaching rate after twelve days and more than three times higher than that at later times. This meant that there were two fractions of C-14 in the irradiated graphite, one of which was loosely trapped. As nitrogen was used to flush the graphite stacks of the RBMK reactors, therefore it could be expected that its activation reaction mostly occurred on the surface. This fact enabled us to propose that the loosely trapped fraction of C-14 was due to the presence of weakly bounded C-14 atoms on the surface of irradiated graphite, which were produced from

nitrogen. Furthermore, the increase of the water solution alkalinity from pH=7.5 to pH=10 enhanced notably (more than 2 times) leaching rate after two months.

LEI also studied the relation between treatment and disposal on the performance of RBMK-1500 graphite disposed of in crystalline rocks [Narkuniene et al., 2012]. Modelling of C-14 migration in the near field and far field was performed with the source term based on LEI modelling results on the RBMK-1500 inventory using different illustrative release rates to represent possible differences between non-treated and treated graphite and conceptual models developed. The importance of waste leaching rate was studied within the context of different performances of the engineered barriers (in terms of sorption, limited solubility) and considering possible graphite encapsulation in cementitious material. The latter reflects possible packaging options: with grouting and without grouting. It was found that the importance of waste leaching rate depends on several aspects: on the performance of the backfill and of the natural barrier system (in terms of its impact on the attenuation of the radionuclide flux). The impact of the options (treatment vs no treatment of graphite) on the C-14 flux to geosphere was not straightforward. To understand the option of non-treatment vs. treatment the inventory, leaching rates, barrier performance and migration conditions all need to be considered.

An independent programme (out of the frame of CARBOWASTE Project) of graphite sampling from the graphite stack of Unit 1 was developed by INPP staff, and sampling was accomplished at the end of 2013 year. This work also included some leaching experiments for several radionuclides. However, the measured radionuclide inventories and leaching tests results are not publically available.

### **2.3 State Institution “Institute of Environmental Geochemistry National Academy of Science of Ukraine” (IEG NASU)**

For Ukraine, the main radiocarbon source is irradiated graphite from the Chernobyl Nuclear Power Plant. The ChNPP is a decommissioned nuclear power station about 14 km northwest of the city of Chernobyl, and 110 km north of Kyiv (Kiev). The ChNPP had four RBMK reactor units. The commissioning of the first reactor in 1977 was followed by reactor No. 2 (1978), No. 3 (1981), and No.4 (1983). Reactors No.3 and 4 were second generation units, whereas Nos.1 and 2 were first-generation units. RBMK is an acronym for "High Power Channel-type Reactor" of a class of graphite-moderated nuclear power reactor with individual fuel channels that uses ordinary water as its coolant and graphite as its moderator. The combination of graphite moderator and water coolant is found in no other type of nuclear reactor.

The approved «ChNPP Decommissioning Program» establishes a preferred decommissioning strategy.

A report [Zlobenko et al., 2014] has recently been prepared for the EC CAST project (Deliverable D5.3) that presents information on graphite characterisation being undertaken as part of the ChNPP Decommissioning Program. Work considering chemical decontamination of graphite is reported, as is the overall graphite waste management approach.

## 2.4 Regia Autonoma pentru Activitati Nucleare (INR)

The main objective of the INR in WP5 is to update the inventory of C-14 in the irradiated graphite arising from TRIGA 14MW reactor thermal column and to define the associated source term, not only as total amount of C-14 but also as inorganic/organic ratio.

In this regard, the INR activities consist in a review of the current knowledge achieved in the understanding of the speciation of C-14 from irradiated graphite used in research reactors and the experimental data on C-14 leaching rate and its chemical forms in the context of deep geological disposal.

Irradiated graphite from TRIGA 14MW reactor was investigated in CARBOWASTE and showed significant C-14 and Cl-36 activities that impose its deep geological disposal. Preliminary performance assessment initially considered for a near surface disposal was based on C-14 release rates in liquid and gas provided by literature. These values are specific to irradiated graphite irradiated under environmental, thermal, irradiation conditions quite different than in the TRIGA 14MW thermal column. Specific data on C-14 release from TRIGA i-graphite are therefore needed to define the source term both as total release rate and as organic/inorganic ratio.

### 2.4.1 Review the outcome of CARBOWASTE in the Romanian context

In Romania, the first detailed investigation of the irradiated graphite from the TRIGA 14MW research reactor started under the CARBOWASTE project. Combining experimental data on C-14 activity with numerical calculations, a preliminary inventory of the C14 was estimated to be  $3 \cdot 10^{10}$  Bq [Iorgulis et al. 2013].

Experimental work demonstrated the C-14 activity decreases along the thermal column due to the thermal neutron flux attenuation (Figure 2.4.1) from  $10^5$  Bq/g in the first row next to the reactor core to  $2 \cdot 10^2$  Bq/g in the middle of the column (Table 2.4.1), but is quite uniformly distributed inside a brick, with values ranging between  $0.9 \cdot 10^3$  to  $1.9 \cdot 10^3$  Bq/g being measured on different samples from a graphite block in CARBOWASTE [Diaconu et al., 2013].

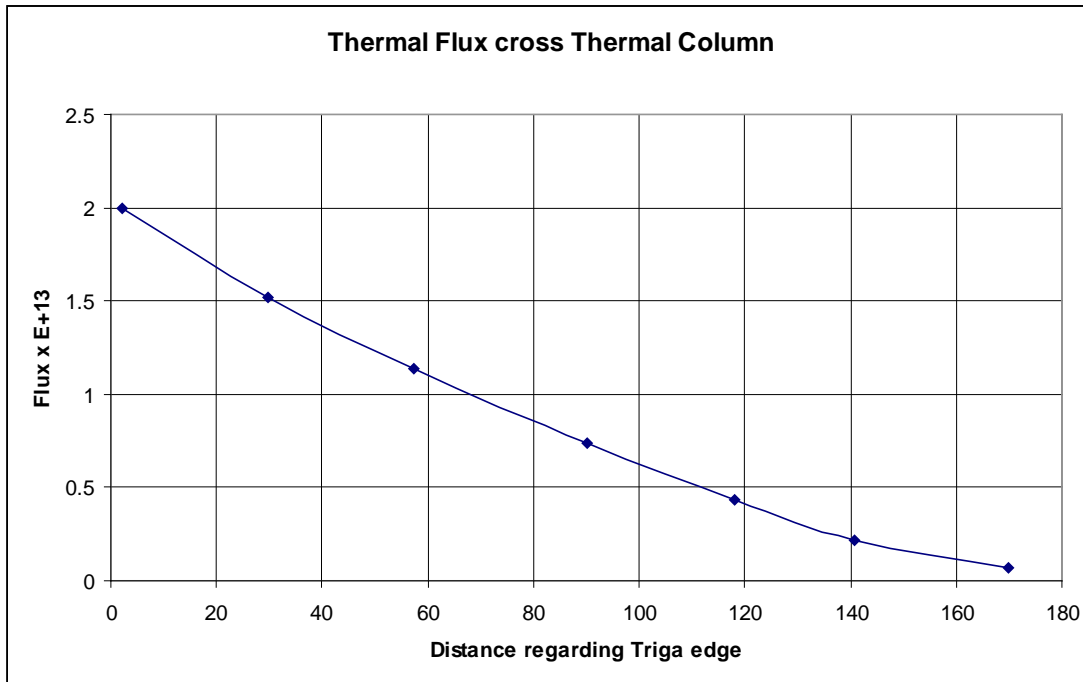


**Figure 2.4.1. Thermal flux variation along the thermal column**

**Table 2.4.1. Predicted C-14 and H-3 activities for different positions along the thermal column**

Radionuclide	Predicted Activity (Bq/g)		
	First row	Sample location	Column centre
H 3	3.89E+05	0.973E+04	2.87E+03
C 14	1.12E+05	0.958E+03	2.82E+02
Cl36	8.21E+03	7.66E+01	2.25E+01

Work done by ICN in CARBOWASTE proposed and assessed as a first approach for i-graphite management its disposal in a near surface facility. The C-14 radiological impact assessed using conservative release rates provided by literature did not exceed the dose limit [Constantin et al., 2013].

The C1-36 content estimated numerically based on impurity content gives a total amount of around  $8.5 \cdot 10^9$  Bq, which exceeds the Waste Acceptance Criteria (WAC) established for the near surface repository (MAAL=10 Bq/g) in Romania. The radiological impact was also above the maximum limit imposed by the regulatory body [Constantin et al., 2013].

Therefore, the most relevant outcomes of the INR work done by ICN under CARBOWASTE consisted of:

- the first estimation of the inventory of the i-graphite arising from the TRIGA thermal column;
- a methodology for inventory assessment applicable to other MTR thermal columns;
- an assessment of the radiological impact of C-14 and C1-36 for a near surface repository using very conservative assumptions;
- a proposed management strategy for the i-graphite based on some preliminary evidence.

Starting from this point, the INR targets in CAST project are to define the C-14 source term specific for the TRIGA 14MW thermal column in different deep geologic environments (since a host rock is not yet selected) with a special focus on the estimation of the C-14 organic/inorganic ratio based on laboratory leaching experiments.

## **2.4.2 Review of $^{14}\text{C}$ content and speciation and their correlation with impurity content and irradiation history in the MTR i-graphite**

### 2.4.2.1 Reviewed sources

In this task INR reviewed data on MTR i-graphite in order to identify possible correlations of the C-14 content and its speciation with impurity content and irradiation history. The objective of this review was to achieve a synthesis of available information in the literature on C-14 specific for the irradiated graphite arising from research reactors, related to:

- the experimental data on the release of  $^{14}\text{C}$  in different environments and conditions environment,
- chemical speciation;

- processes and factors that determine the release of  $^{14}\text{C}$  from graphite as organic or inorganic compounds, and
- correlations of the reports of two species ( $^{14}\text{C}$  from graphite as organic or inorganic compounds) with the content of impurities and irradiation history.

To properly use this information to the i-graphite specific to thermal columns of research reactors, an in-depth understanding of conditions leading to the production of organic and inorganic species in irradiated graphite and the possible correlation with the impurity content was firstly required.

The review started with the CARBOWASTE scientific reports dedicated to  $^{14}\text{C}$  release during heat treatments [von Lensa, 2011] or in solutions specific to disposal environments [Vendé, 2012]. Besides data obtained in CARBOWASTE project, information in other documents or synthesis reports [Marshall et al., 2011; Carlsson et al., 2014; IAEA, 2006] have been reviewed. The studies providing an analysis of the state-of-the-art in this area were:

- Key Processes and Data for the Migration of  $^{14}\text{C}$  Released from a cementitious Repository [Jackson and Yates, 2011].
- Longer-term release of carbon-14 from Irradiated Graphite [Marshall et al., 2011].
- Chemical Aspects on the final disposal of Irradiated Graphite and aluminum - A literature survey [Carlsson et al., 2014].
- Characterization, Treatment and Conditioning of Radioactive Graphite from Decommissioning of Nuclear Reactors [IAEA, 2006].

#### 2.4.2.2 C-14 Speciation

It is well known that the sorption and solubility of  $^{14}\text{C}$  is influenced by its speciation.  $^{14}\text{C}$  can be released from waste (including i-graphite) either as an organic or inorganic compound, having different radiologic impacts and needing different approaches in performance assessment models. Therefore, when  $^{14}\text{C}$  is considered for disposal, further clarifications are needed to distinguish between its organic and inorganic species [Marshall et al., 2011].

The necessity to distinguish between carbon species results from different behavior of each species in relation to environmental engineering and geological barriers mentioned by all the studies dedicated to the analysis of carbon species in relation to their disposal [Marshall et al., 2011; Carlsson et al., 2014; IAEA, 2006; Jackson and Yates, 2011]. CH<sub>4</sub> does not form carbonates in cement barriers and crosses them without any retention, becoming therefore the most interesting of the carbon compounds in terms of radiological impact. The *organic forms* of carbon that could be found in disposal conditions are:

- CH<sub>4</sub> - methane
- C<sub>2</sub>H<sub>6</sub> - ethane
- C<sub>2</sub>H<sub>4</sub> - ethene
- C<sub>2</sub>H<sub>2</sub> - acetylene

to whom oxygen-containing molecules with short sequence such as aldehydes, ketones and alcohols can be added.

*Inorganic species* associated with potential releases of <sup>14</sup>C include:

- CO<sub>3</sub><sup>-2</sup> - carbonate
- CO<sub>2</sub> - carbon dioxide
- HCO<sup>-3</sup> bicarbonate
- H<sub>2</sub>CO<sub>3</sub> - carbonic acid

Under deep disposal conditions, both stable carbon and <sup>14</sup>C may be released in the near field of radioactive waste in different forms:

- carbon dioxide / carbonate / bicarbonate;
- methane,;
- organic molecules; it is considered that these species will not persist in the long term but could react to form methane or carbon dioxide.

<sup>14</sup>C species that can be released during the long-term disposal of irradiated graphite waste depend on the nature, history and irradiation conditions and on the near field characteristic of the geological environment.

The processes leading to  $^{14}\text{C}$  release from a deep geological repository identified by previous studies and summarized in [Vendé, 2012] are:

- corrosion of metals
- degradation of irradiated graphite
- degradation of organic matter
- microbial activity
- radiolysis
- conversion between organic and inorganic forms

Experts generally agree that the slow degradation of irradiated graphite can produce mainly  $\text{CO}_2$  and  $\text{CH}_4$  containing  $^{14}\text{C}$ .  $\text{CO}_2$  formation is mainly associated with oxidizing environment, while  $\text{CH}_4$  formation is favored by a reducing environment [Vendé, 2012].

$\text{CH}_4$  can also result from  $\text{CO}_2$  reducing by autotrophic microbial processes using hydrogen. In a geological repository,  $\text{H}_2$  is generated by metals corrosion and by radiolysis. In the case of metals the  $\text{CH}_4$  formation is explained by  $\text{H}_2$  generation due to corrosion, followed by its consumption by microbes which generate methane. Under microbial activity,  $\text{CO}_2$  can also be converted to  $\text{CH}_4$ .

#### 2.4.2.3 C-14 release rate

Experimental studies in the CARBOWASTE project performed by different laboratories demonstrated there is as a  $^{14}\text{C}$  fraction in graphite available for a quicker release and a fraction that is almost inert. The first one was associated with  $^{14}\text{C}$  resulting from the activation of  $\text{N}_2$  adsorbed on the surface of graphite particles. The inert fraction could be associated to the  $^{14}\text{C}$  resulted from  $^{13}\text{C}$  activation located either in the crystal lattice or as interstitials between the graphene layers.

$^{14}\text{C}$  release in liquid phase of less than  $<0.1\%$  has been measured in hyper-alkaline solutions by CEA corresponding mainly to the oxidizing species.  $^{14}\text{C}$  is mainly released in liquid phase both as inorganic (65%) and organic (35%) [Carlsson et al., 2014].

SUBATECH studies on  $^{14}\text{C}$  release in hyper-alkaline solutions on SLA2 samples, at room temperature and  $50^\circ\text{C}$ , lasting up to 821 days, coupled with species investigation, showed also very small release rates, the total cumulative fraction ranging for different graphite samples between 0.26 to 0.5% of  $^{14}\text{C}$  inventory with 0.1 to 0.15% in liquid phase, of which around 75% was inorganic  $^{14}\text{C}$  [Vendé, 2012]. The release variation with time suggested a two stage process: an initial quick step at high rate ( $0.9 - 2 \cdot 10^{-3}\%$  inventory / day during the first 21 days), followed by a slow stage with a linear release rate of around  $2 \cdot 10^{-4}\%$  inventory /day.

This two-stage process is confirmed by CEA studies on irradiated graphite from different reactors. The two stages could be associated with the initial release of the more labile species arising from the  $^{14}\text{N}$  impurities or from the  $^{13}\text{C}$  from different depositions, while the second stage is most probably linked to  $^{14}\text{C}$  created in the matrix [Carlsson et al., 2014].

The same kinetics was found by the experiments developed in the UK on BEP0 graphite, which showed a clear decrease of the  $^{14}\text{C}$  organic compounds release rate with time, in a solution of sodium hydroxide at an initial pH value of 13 [Marshall et al., 2011].

Quantitatively, the total amount of  $^{14}\text{C}$  released in the *gas phase* represented  $5.33 \cdot 10^{-3}\%$  from the total inventory and consisted of  $^{14}\text{CO}$  (representing 78%) and  $^{14}\text{C}$  organic (22%). The release rate over the first period of 0.057 Bq/h decreased to only 0.007 Bq/h in the last stage. The ratio of  $^{14}\text{CO}$  /organic  $^{14}\text{C}$  remained almost similar along the release period, ranging between 2.5 and 3.9. Fitting data in a first order function (1), a cumulative release of gas reaching a plateau was obtained at about  $5 \cdot 10^{-3}\%$  of the total inventory [Marshall et al., 2011].

$$a(t) = fA(1 - e^{-kt}) \quad (1)$$

where  $a$  is the total activity released up to time  $t$ ,  $A$  is the initial activity in the graphite, and  $f$  and  $k$  are fitted parameters ( for CO model  $f = 4.2 \cdot 10^{-5}$ ,  $k = 3.8 \cdot 10^{-4} \text{ hr}^{-1}$ , for organic  $^{14}\text{C}$  model  $f = 1.2 \cdot 10^{-5}$ ,  $k = 4.1 \cdot 10^{-4} \text{ hr}^{-1}$ )

These data also suggest an initial release of readily volatile  $^{14}\text{C}$  species. UK specialists suggest that in the long term, the  $^{14}\text{C}$  released accumulated in this stage could be more

important even at this very low rate, but long term measurements are needed to clarify this assumption [Marshall et al., 2011].

But the larger part of the  $^{14}\text{C}$  released during the leaching test representing 0.10% of the total inventory was found in the *liquid phase* and consisted mainly in  $\text{CO}_2$ . It should be noted that in parallel with  $^{14}\text{C}$ , tritium release was also measured in both gas and liquid phases, both in the form of organic and inorganic. The data showed that most of the tritium released from graphite remained in the aqueous phase (as in the case of  $^{14}\text{C}$ ) [Marshall et al., 2011].

The major conclusion of these studies is  $^{14}\text{C}$  and C stable release is slow, and it is controlled by the release rate.

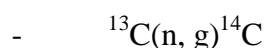
Canadian experience on  $^{14}\text{C}$  produced in CANDU reactors found that some  $^{14}\text{C}$  atoms produced in the graphite can be chemically bond by hydrogen, nitrogen or oxygen. Irradiation of  $\text{N}_2$  used as filling gas showed  $^{14}\text{C}$  creation and its fast conversion to simple hydrocarbons and C-N compounds [Carlsson et al., 2014].

Other information on the irradiated graphite from research reactors are provided by Magnusson and his collaborators [Carlsson et al., 2014]. They studied the distribution between organic and inorganic in different parts of the research reactor graphite and demonstrated clearly the existence of both species, in a ratio organic/inorganic of around 1:2.

It is worth mentioning also that some studies pointed out that the initial rapid release of gaseous  $^{14}\text{C}$  under alkaline conditions from intact graphite was not seen for crushed graphite [Marshall et al., 2011].

#### 2.4.2.4 Nitrogen contribution to $^{14}\text{C}$ in i-graphite

$^{14}\text{C}$  is produced in the irradiated graphite from  $^{13}\text{C}$ ,  $^{14}\text{N}$  and  $^{17}\text{O}$  according to the following nuclear reactions:



- $^{14}\text{N}(n, p) ^{14}\text{C}$
- $^{17}\text{O}(n, \alpha) ^{14}\text{C}$

It is well known that the reaction  $^{14}\text{N}(n, p) ^{14}\text{C}$  is the main contributor to  $^{14}\text{C}$  due to the high neutron reaction cross section and isotopic abundance of  $^{14}\text{N}$  (Table 2) as shown in Table 2.4.2 [Hou, 2005].

**Table 2.4.2. Nuclear parameters for neutron activation production of  $^{14}\text{C}$  and their relative contributions**

Radionuclide	Abundance (%)	Cross section (barn)	Concentration of target element	Relative contribution
$^{14}\text{N}$	99.63	1.83	40 ppm	1
$^{13}\text{C}$	1.10	0.0014	100%	0.21
$^{17}\text{O}$	0.04	0.24	100 ppm	$1.03 \cdot 10^{-4}$

Our previous simulations [Iorgulis et al., 2013] have shown a high degree of uncertainty in C-14 accumulation predictions vis-a-vis of the  $\text{N}_2$  amount in graphite. The inverse calculation method for the TRIGA thermal column gave a  $\text{N}_2$  concentration of 0.01%, the same as the value determined by EDS analysis [Diaconu et al., 2013.]. This is almost 2 times higher than the values reported in the literature [Takahasi et al. 2001, Hou, 2005]. More precise determination of  $\text{N}_2$  concentration is very important to an accurate estimation of the C-14 inventory.

$\text{N}_2$  concentration could be also important if a correlation could be found between the  $^{14}\text{C}$  created by the activation of the adsorbed  $\text{N}_2$  and the  $^{14}\text{C}$  release rate, due to the weaker bond of these atoms placed on the graphite grains surface, compared to the  $^{14}\text{C}$  derived from  $^{13}\text{C}$  activation within the graphite grains [Takahasi et al. 2001, Hou, 2005].

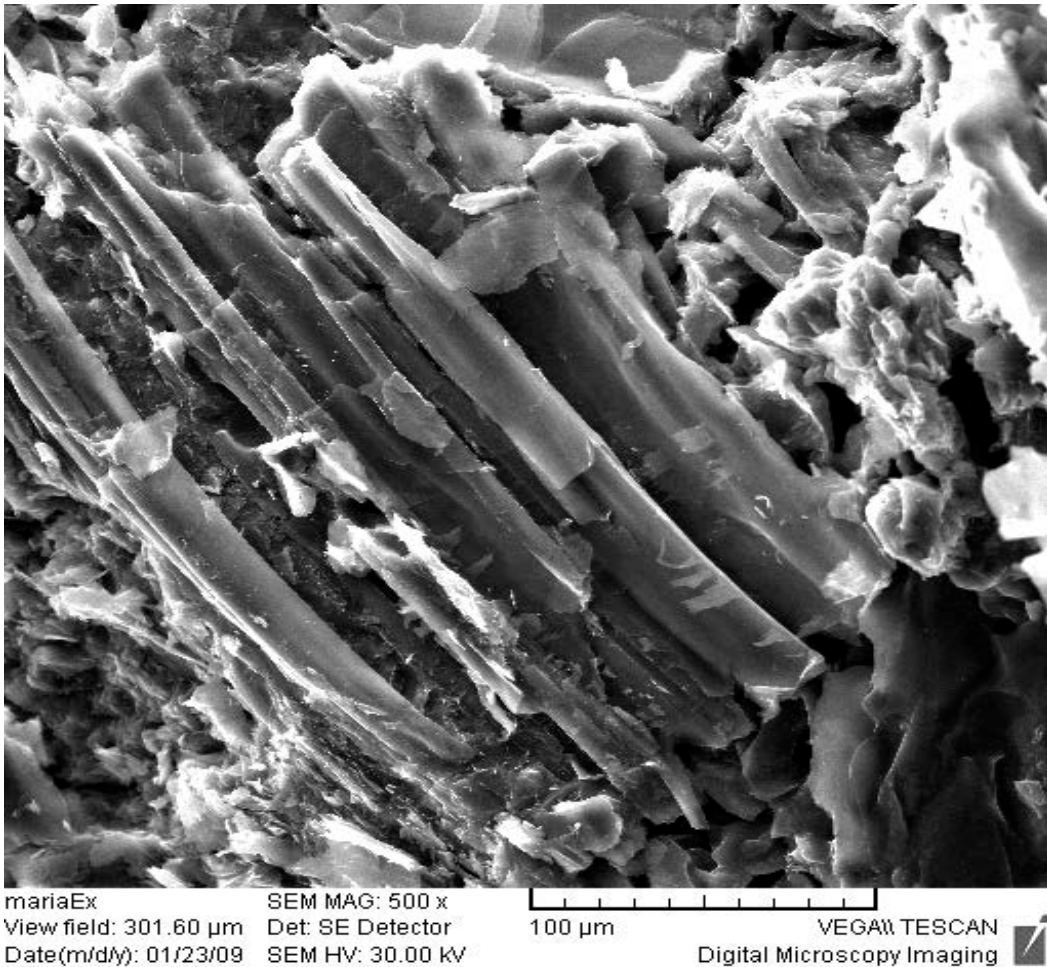


**Figure 2.4.2. Graphite morphology: parallel plates of the basal planes**

[Takahasi et al, 2001]

Takahashi and co-workers [Takahasi et al, 2001] tried to correlate the  $^{14}\text{C}$  release rate with the graphite morphology and impurities. Analysis of nitrogen distribution in depth suggested that its molecules are adsorbed on the graphite surface by weak interactions. In around 50nm its concentration can decrease from 100 to 40ppm. The special morphology of graphite parallel plates (Figure 2.4.2) acts as a barrier against in-depth nitrogen penetration.

The high graphitization degree determines a very high thermodynamic stability, which prevents decomposition in disposal conditions. Therefore, the  $^{14}\text{C}$  released from irradiated graphite can be associated only with the activated nitrogen, initially adsorbed on the graphite surface.

Summarizing, this review of publicly available results on C-14 compounds released from irradiated graphite in alkaline environment (specific to a cement-based geological disposal) showed a large agreement on the following:

- only a very small fraction of the C-14 is released (less than 0.1%).
- this release can be very probable correlated with the C-14 activated from the nitrogen adsorbed on the surface of the graphite.
- both organic and inorganic C-14 species are released in alkaline solutions, their amounts depending on the irradiation history and graphite properties.
- C-14 amount released in liquid phase seems to be larger than C-14 amount released in gas phase.
- CO<sub>2</sub> dominates the C-14 release in liquid phase, while CO and CH<sub>4</sub> are considered the major compounds released in gas phase.
- either in liquid or gas, C-14 leaching rate decreases in time with 1-2 orders of magnitude, trending to establish a very slow release rate; the process could be quite well described by a first-order kinetics function.
- chemical mechanisms leading to CO<sub>2</sub>, CO, CH<sub>4</sub> formation are not clearly understood: the graphite could react with the oxygen solved in the water to form CO<sub>2</sub>, while methane formation could be associated with strong reducing conditions.
- Canadian studies on the CANDU filling gas (N<sub>2</sub>) pointed out that the C-14 atoms created in graphite can be chemically bound with hydrogen, nitrogen or oxygen. They revealed the formation of C-14 atoms which have been quickly converted to simple hydrocarbons or carbon-nitrogen compounds.

### 2.4.3 Conclusions

The most relevant outcomes of the INR work done by ICN under CARBOWASTE relevant for the Romanian context are:

- the first estimation of the inventory of the i-graphite arising from the TRIGA thermal column.

- a methodology for inventory assessment applicable to other MTR thermal columns.
- an assessment of the radiological impact of C-14 and Cl-36 for a near surface repository in very conservative assumptions.
- a proposed management strategy of the i-graphite based on some preliminary evidences.

The experimental results of different tests on C14 release in alkaline solutions published in the literature indicate the presence of both inorganic and organic  $^{14}\text{C}$  species. Release kinetics are specific to each species and depend on the properties of graphite, the history and conditions of irradiation.

The amount of  $^{14}\text{C}$  released into the environment depends on the chemical form in which it is released from the graphite. The  $^{14}\text{C}$  organic species show a tendency to release as the gaseous form, for example, methane (although organic carbon release in solution occurs), while the inorganic  $^{14}\text{C}$  as  $^{14}\text{CO}_2$  is prone to precipitate on the solid matrix of the repository barriers to form, for example, calcium carbonate.

Most of the experimental tests indicated that the total release of  $^{14}\text{C}$  in hyper alkaline solutions is dominated by inorganic species ( $\text{CO}_2$ ) which is mostly in the liquid phase.

The proposed mechanism for explaining release carbon species from i-graphite is the water catalyzed oxidation with oxygen dissolving to form  $\text{CO}_2$ , but there is still no clear understanding of the processes leading to the formation of either species.

Quantitative data on the  $^{14}\text{C}$  organic / inorganic ratio and  $^{14}\text{C}$  released from irradiated graphite of nuclear power plants (which generates huge volumes of waste) reported in the literature are still scarce, very few of them referring to graphite irradiated in the thermal column of research reactors.

## 2.5 Agence Nationale pour la gestion des déchets radioactifs / EDF (Andra / EDF)

The following French available data on the leaching of carbon 14 have been reviewed and the conclusions drawn are given below.

Graphite origin	Date of experiment	Duration	Leaching liquid	Gaseous phase	Graphite form	Operational conditions
G2 moderator	1990	90 days	Deionised pure water, 20°C	Hermetic vessel, air atmosphere	Solid (~630 g)	Dynamic
SLA2 sleeve	1999	455 days	Industrial water pH=7.2	Hermetic vessel, air atmosphere	Solid (<10g)	Dynamic
BUA1 moderator	2003	455 days	Lime water, 20°C	Hermetic vessel, inert gas purge (N <sub>2</sub> )	Solid (~10g)	Semi-dynamic
BUA1 moderator	2003	455 days	Deionised water, 20°C	Hermetic vessel, inert gas purge (N <sub>2</sub> )	Solid (~10g)	Semi-dynamic
BUA1 moderator	2003	144 days	Deionised water, 40 °C	Hermetic vessel, inert gas purge (N <sub>2</sub> )	Solid (~10g)	Semi-dynamic
G2 moderator	2007	455 days	Deionised and lime water, 20°C	Hermetic vessel, inert gas purge (Ar)	Solid (~90g)	Dynamic
G2 moderator	2011....	548 days	NaOH water, 20°C, pH=13	Hermetic vessel, inert gas purge ( Ar)	Powder (50 g)	Semi-dynamic
SLA2 moderator	2011....	551 days	NaOH water, 20°C, pH=13	Hermetic vessel, inert gas purge ( N <sub>2</sub> )	Powder (25 g)	Semi-dynamic

For the graphite stack, the obvious result of the studies carried out on French irradiated graphite is that carbon 14 leaching rate is very slow. In most of cases, a quasi-steady state leach rate appears to be achieved after the elapse of around 100 to 200 days. Over that period, the calculated mean radiocarbon leach rate lies between  $10^{-11}$  and  $10^{-8}$  m.day<sup>-1</sup> (meters per day). The reasons of the variability of this radiocarbon leach rate are still not clear. The studies were carried out on graphite from different origins and with different operational histories.

A faster carbon 14 leach rate seems to be observed for sleeve graphite (operational waste) which represents a small part of the total inventory in carbon 14. More investigation is needed to clarify this particular behavior of carbon 14 of the irradiated sleeve graphite.

The nature of the leaching liquid (deionised or lime or soda water ) does not evidence any clear impact on the carbon 14 leaching behaviour but a significant part of the results is below the quantification limits of the method used for the measurement of carbon 14 in the leaching liquid. To obtain significant results (above the quantification limit) it is necessary to use sufficient masses of trepanned samples that are not always available and to use a suitable methodology for leaching liquid sampling and carbon 14 measurements.

Concerning the implications of these studies for other i-graphite, it seems important to remember that the results obtained on the radionuclide behavior might depend on the history and on the background behind the used i-graphite. The results obtained on one studied i-graphite cannot be directly and simply extended to other i-graphites.

Further results concerning the chemical forms of the leached carbon 14 will be the object of the CAST deliverable D5.8 by Andra entitled « Synthesis report on carbon 14 speciation in solution and gas from French graphite waste ».

## 2.6 Agenzia Nazionale per le Nuove Technologie, L'Energia e lo Sviluppo Economico Sostenibile (ENEA)

### 2.6.1 Italian Nuclear Graphite

Although Italy has constructed four commercial reactors, only one (Latina) was graphite moderated. All of these commercial reactors are shut down; So.G.I.N. (the Italian main WMO) is now responsible for their decommissioning. It is estimated that about 2,100 t of i-graphite will arise from the decommissioning of the Magnox-type Latina reactor. The radionuclide composition of the irradiated graphite is based on predictions that are similar to the UK's Magnox reactor values.

The main production characteristics are listed in the Table 2.6.1.

**Table 2.6.1 Latina NPP nuclear graphite manufacturing characteristics**

<b>Manufacturer</b>	<b>Head Wrightson Processes Ltd. (Yarm, Yorkshire, UK)</b>
Production Date	November 1961
Type	PGA Graphite, grade A and B
Moderator	Grade A, density 1.75 g/cm <sup>3</sup> , cross section 4.0 mb
Reflector	Grade B, density 1.64 g/cm <sup>3</sup> , cross section 4.5 mb

Within the CARBOWASTE Project, as part of an agreement between ENEA and So.G.I.N., ENEA received 15 cylindrical samples from Latina NPP to start developing a process of chemical decontamination by organic solvents treatments ultrasound assisted. They were taken from the drilling of the core in two different radial positions (channel 7 and 8): from each sample were removed both the surface layer exposed to the fuel channel and the innermost layer; the approximate mean weight is 5 g [Piña et al., 2013].

The removal of the layer exposed to the channel ensures that the activity present in the

sample is representative only of the contribution due to neutron activation<sup>3</sup>.

In Table 2.6.2 the masses of the samples, after the outer layer removal, are reported; the mean diameter is 1.7 cm and the mean height is about 1.0 cm (see Figure 2.6.1).

**Table 2.6.2 - Irradiated-Graphite Samples weights in grams (g)**

<b>08F08</b>							
A1/C3	A1/C4	A1/I2	A1/I3	A1/S1	A1/S2	A1/S3	
3.5476	4.4188	4.1437	4.2189	2.0567	3.9708	3.5290	
<b>07S07</b>							
G2/C3	G2/C4	G2/I1	G2/I2	G2/I3	G2/S1	G2/S2	G2/S3
3.3065	3.7149	3.3451	3.6853	3.5436	4.1867	4.3726	3.9471

As mentioned, 7 samples came from the Channel 8 (08F08), while the other 8 samples from Channel 7 (07S07); For each of these 2 groups, the samples came from different level origins named: S, Upper, C, Central and I, Bottom.



**Figure 2.6.1 - One of the i-Graphite samples from Latina NPP**

<sup>3</sup> The removal of the layer has been done only to remove the “contamination products”; the study was

## 2.6.2 Sample preparation and preliminary characterisation

All the samples used in this work were crushed and then finely ground. From each of them a representative homogenous aliquot was taken and weighted.

Radiocarbon has been measured by Liquid Scintillation Counting after pre-treatment of an aliquot of each samples by Microwave Assisted Digestion in Teflon closed vessels with acid mixture. Each aliquot of these solutions has been added with Scintillation Cocktail and measured by Liquid Scintillation Analyser TDCR HIDEX 300SL in Dual-Label Mode with <sup>14</sup>C Reference Standards. The results are shown in the Table 2.6.3.

**Table 2.6.3 - Radiocarbon characterisation of the Latina NPP (by LSC)**

Sample	Bq/g	unc.
08F08A1/C3	312.9	±12.1
08F08A1/S3	306.2	±7.5
07S07G2/S3	1467.7	±7.8
07S07G2/S1	793.9	±11.7
08F08A1/I3	260.9	±2.2
07S07G2/C3	1471.6	±9.1
08F08A1/S1	160.4	±12.5
07S07G2/S2	1497.7	±7.5
08F08A1/C4	82.2	±6.1
07S07G2/I3	237.1	±9.6
07S07G2/C4	238.9	±9.7
08F08A1/I2	167.8	±13.0
08F08A1/S2	72.1	±4.7
07S07G2/I1	292.7	±7.2
07S07G2/I2	1241.3	±11.1

---

interested in all the activation products, not only the C14 coming from C13 or N14 or O17.

The i-graphite from Latina NPP, similar to all the graphite coming from moderators exposed to a neutron flux (for Latina NPP is up to  $5 \times 10^{22}$  n/cm<sup>2</sup>), presents a wide range and amounts of activation products.

This distribution of activated elements concerns the bulk of the samples, mainly in the closed porosity or between the typical graphite layers. Anyway, there are not usually involved chemical bonds. In order to achieve an exhaustive and valid extraction for activation products, it is important to increase the surface area of the sample. This should allow to the solvent to reach the inner layers/areas (i.e. closed pores, crystallites, etc.) and extract contaminants in solution.

### 2.6.3 Procedure description

The principle is based on the main idea is to apply an exfoliation-like process on the graphite by organic solvents (liquid-phase exfoliation) to produce un-functionalized and non-oxidized graphene layers in a stable homogeneous dispersion [Capone et al., 2013]. This process, helped by mild sonication, consists in separating the individual layers in a more or less regular manner. Such a separation, being sufficient to remove all the inter-planar interactions, thanks to the dipole-induced/dipole interactions between graphenes and organic solvents, results in a dispersion of the graphite in a workable media. This facilitates processing, treatment and easy characterization for the contaminants recoveries (Figure 2.6.2).

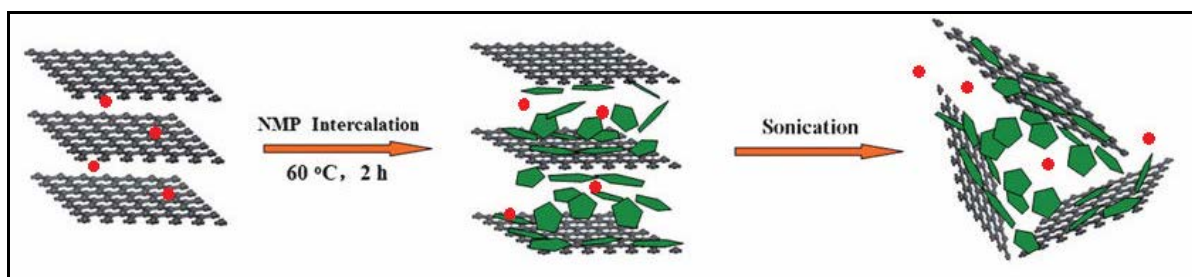


**Figure 2.6.2 - Representation of the main steps for the graphite exfoliation process promoted by organic solvents and ultrasound assisted**

Moreover, no oxidation process is performed nor super-strong acid actions. This would lead

to non-oxidized products so the graphite would be completely recovered as it is.

The overall procedure is characterized by the following main steps:

- Organic Solvents choice;
- Low-power Sonication time;
- Centrifugation/Extraction;
- Removal Efficiency (as % of the recovered activities after treatment with respect to the original values before the treatment).

In order to overcome the van der Waals-like forces between graphite layers to yield a good exfoliation and dispersing the resulted graphene sheets in a stably liquid media, highly polar organic solvents have to be used.

It is started to test the process considering the three common and widely used dipolar Solvents for their good solvency abilities:

- N,N-Dimethylacetamide (DMA)
- N,N-Dimethylformamide (DMF)
- N-Methyl-2-pyrrolidone (NMP)

After sonication, the filtered solution were analysed by LSC/beta-Spectrometry and the removal efficiencies with respect to the original  $^{14}\text{C}$  contents have been calculated. The results are shown in the Table 2.6.4.

**Table 2.6.4 - Overviews of Removal Efficiencies for Radiocarbon**

<sup>14</sup> C	Before	After					
		in DMA		in DMF		in NMP	
	Bq/g	Bq/g	Rem. Eff (%)	Bq/g	Rem. Eff (%)	Bq/g	Rem. Eff (%)
08F08A1/C3	312,87	3,38	1,08	3,70	1,18	46,22	14,77
08F08A1/S3	306,18	11,44	3,74	1,61	0,52	71,89	23,48
07S07G2/S3	1467,70	20,01	1,36	0,77	0,05	80,58	5,49
07S07G2/S1	793,90	13,73	1,73	1,44	0,18	43,39	5,47
08F08A1/I3	260,92	72,99	27,98	20,54	7,87	15,47	5,93
07S07G2/C3	1471,64	21,44	1,46	2,17	0,15	29,19	1,98
08F08A1/S1	160,39	11,92	7,43	1,54	0,96	24,18	15,08
07S07G2/S2	1497,72	15,79	1,05	3,69	0,25	22,40	1,50
08F08A1/C4	82,22	22,48	27,35	3,15	3,83	9,82	11,94
07S07G2/I3	237,11	23,35	9,85	6,71	2,83	4,92	2,07
07S07G2/C4	238,92	7,17	3,00	6,45	2,70	23,96	10,03
08F08A1/I2	167,77	25,59	15,25	3,93	2,34	9,48	5,65
08F08A1/S2	72,12	12,03	16,68	0,88	1,21	8,10	11,23
07S07G2/I1	292,73	29,94	10,23	4,61	1,58	9,76	3,33
07S07G2/I2	1241,34	23,59	1,90	5,72	0,46	56,40	4,54

#### 2.6.4 Results

These first and earliest results (table 2.6.4) show that the removal efficiencies in the experimental conditions we used are best for N,N-Dimethylacetamide (DMA) and N-Methyl-2-pyrrolidone (NMP) for <sup>14</sup>C removal. Further investigations would prove the possibilities to reach an overall process able to optimal removal efficiencies.

A point worth to be assessed is the sonication time plus the sonication power. The energy distributed for mass unit and time in an ultrasound bath is an important point to be investigated in order to reach an exhaustive desegregation (exfoliation-like) of the graphene layers making the intercalated compounds free from the matrix and dissolved in the solvent [Wareing et al., 2013].

## 2.7 Forshungszentrum Juelich GmbH (FZJ)

In Germany, irradiated-graphite (i-graphite) is mainly stemming from the operation of High-Temperature Reactors (HTR), Material Test Reactors (MTR) and of numerous small research or teaching reactors. A limited part of i-graphite has already been disposed in the former salt mine ASSE, acting as a research underground laboratory. The rest is foreseen to be disposed of in the KONRAD repository, which is designed and licenced for radioactive waste with negligible heat generation. The waste acceptance criteria for KONRAD are rather restrictive with regards to radiocarbon and will be explained in more detail. The site for a final HLW repository, which could also be used for i-graphite (e.g. spent HTR fuel), will be selected after having defined the general requirements in a new consensual political, scientific and social approach. Besides the formerly preferred disposal in salt domes (e.g. Gorleben), other types of geological formations (e.g. granite, clay) will be taken into account, too. There are currently two major decommissioning projects underway, which are related to i-graphite, i.e. the AVR (Arbeitsgemeinschaft Versuchs-Reaktor GmbH) and the DIDO MTR, both located at the site of the Research Centre Juelich, which was coordinating the European CARBOWASTE project and the German project on 'Disposal of i-graphite (CarboDISP)'.

### 2.7.1 Inventory of i-Graphite in Germany

#### 2.7.1.1 High-Temperature Reactors

The AVR was the first experimental high temperature reactor of pebble bed type worldwide. The main aim of this experimental reactor was the test of the pebble bed core concept and the test of many different types of pebble shaped fuel elements. It was helium cooled and high-purity graphite was used both as moderator as integral part of the spherical fuel element and as reflector being part of the core structure. AVR started operation in 1967 and its definitive shut-down dates back to 1988. The electrical power output was 15 MW<sub>el</sub> (46 MW<sub>th</sub>). The electrical power was generated by a steam cycle, with a steam generator, on top of the core (see Figure 2.7.2). AVR was equipped with a double wall steel pressure vessel and a gas tight containment. Due to the fact that coated-particle fuel concept (see Figure 2.7.1) was not yet invented when the reactor was designed, no major retention of fission

products was possible in the early fuel element types. Thus, the graphite structures experienced additional contamination by fission products, until the coated-particle fuel was optimized and capable to retain fission products, even at temperatures well above 1000°C. The pebble bed core has a diameter of 3.0 m and an average height of 2.8 m [Association of German Engineers (VDI), 1990]. The outlet temperature of helium was initially maximum 850 °C but, after 1974, it was increased at a nominal maximum of 950 °C, with an inlet temperature of 270°C [see Moormann, 2008].

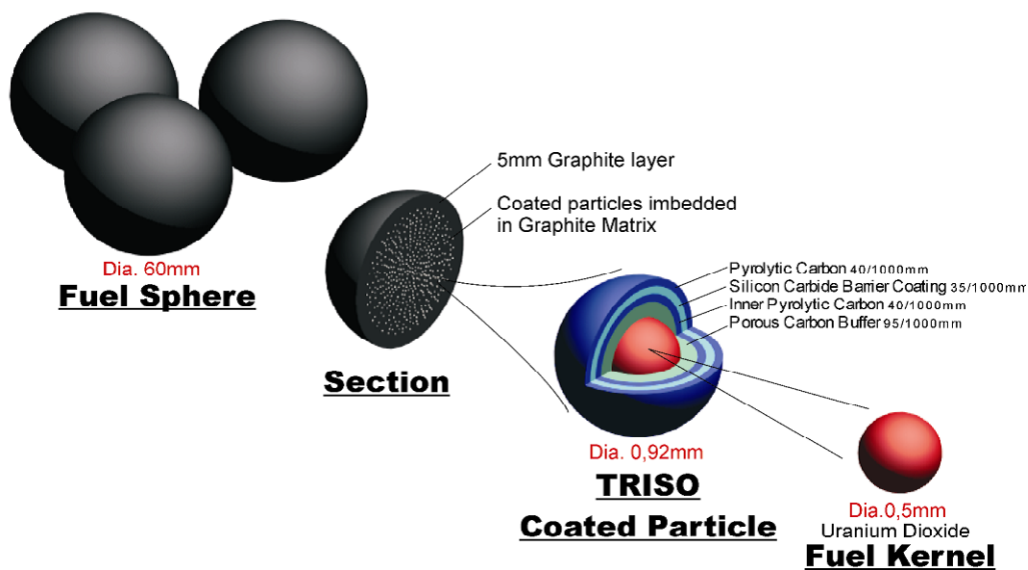


**Figure 2.7.1: Spherical HTR fuel element with coated-particles**

The bottom, side and top reflectors consisted of polycrystalline needle-coke graphite, ARS/AMT grade made by SIGRI-Elektrographit. The graphite reflector wall of 50 cm thickness surrounded the reactor core containing the spherical fuel elements (see Figure 2.7.2). To insulate the external metal structures from high temperatures present in the core, the reflector in turn was enclosed in an insulating carbon brick layer, manufactured with a similar process used to produce graphite but not exceeding about 1200°C to avoid graphitization of the material. This insulating material was less pure and less expensive than nuclear grade graphite. The thickness of the carbon bricks (backed carbon) insulation blocks is 50 cm. The total mass of the graphite used in the reflector amounted to 65 tons and, concerning the carbon bricks, to 157 tons [Association of German Engineers (VDI), 1990].

It will be shown later that this material choice has a crucial impact on the disposal of irradiated-carbonaceous materials, in Germany.

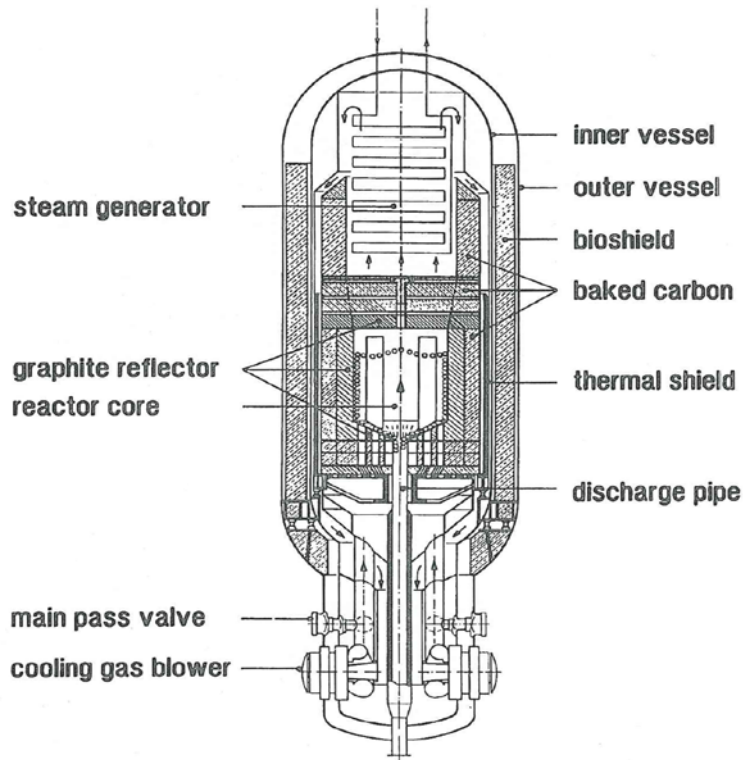


**Figure 2.7.2: AVR Reactor Pressure Vessels and internal structure**

As already mentioned, the AVR was operated with a multitude of different spherical fuel types plus graphite pebbles acting as moderator or absorber elements. The latter (see Figure 2.7.3 dark-grey fraction) were mainly extracted in the first years of operation and disposed in the ASSE test repository.

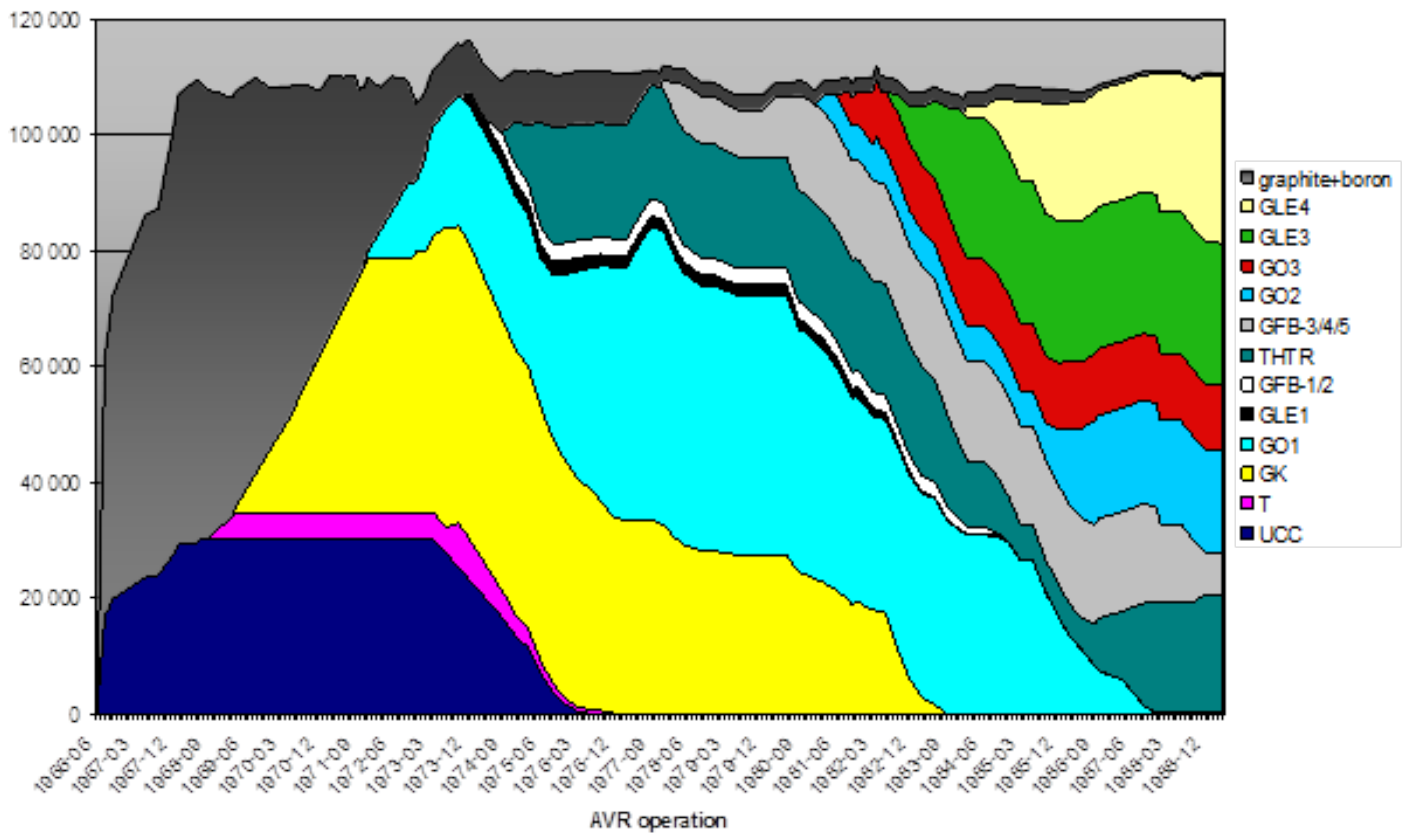


**Figure 2.7.3: Fuel types used in AVR**

After removal of the spent fuel elements the whole inner pressure vessel was filled with a special light concrete to stabilize the core structures and to fix graphite dust produced by fuel friction. In autumn 2014, the 2100 Mg pressure vessel was lifted from its original position in the containment, tilted as illustrated in Figure 2.7.4 and lowered into a horizontal transport device. The transfer to an interim storage facility is planned for Spring 2015. The atmosphere within the pressure vessel has been controlled, after the insertion of concrete. <sup>14</sup>C-labeled methane has been detected and seems to have now reached an equilibrium concentration.

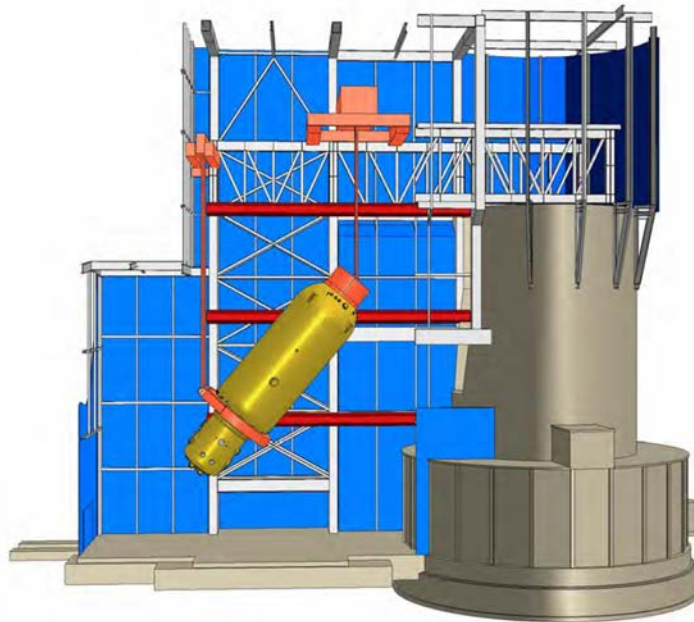


**Figure 2.7.4: Tilting of AVR pressure vessel**

Following the safety report [AVR 2008] for this procedure, the graphite structures contain  $3,6 \cdot 10^{14}$  Bq Tritium and  $4,6 \cdot 10^{12}$  Bq of  $^{14}\text{C}$ . However,  $2,8 \cdot 10^{15}$  Bq Tritium and  $2,8 \cdot 10^{14}$  Bq of  $^{14}\text{C}$  are expected for the carbon brick structures. This means that the disposal of the irradiated carbon brick is the major challenge, for AVR<sup>4</sup>.

The Thorium High-Temperature Reactor (THTR) was an industrial demonstrator for the HTR technology with an electric power of 307,5 MW. The project began in 1971 and was terminated in 1989 after only 423 Full Power Days.

Figure 2.7.5 shows a cross section through the reinforced concrete pressure vessel with the pebble bed reactor core (see Position 1) the steam generators (Position 9) and the blowers (Position 10). THTR 300 was operated with helium as coolant gas with inlet temperatures of

<sup>4</sup> Note Figure 2.7.2, showing AVR Reactor Pressure Vessels and internal structure. This figure indicates separate graphite and carbon brick structures. Graphite is present in the inner part of the side, bottom and top reflectors; the rest of the reflector is made from carbon brick.

250°C entering on top of the core and outlet temperatures of 750°C at the bottom [Wohler and Rautenberg, 1987; Knizia and Simon, 1988].

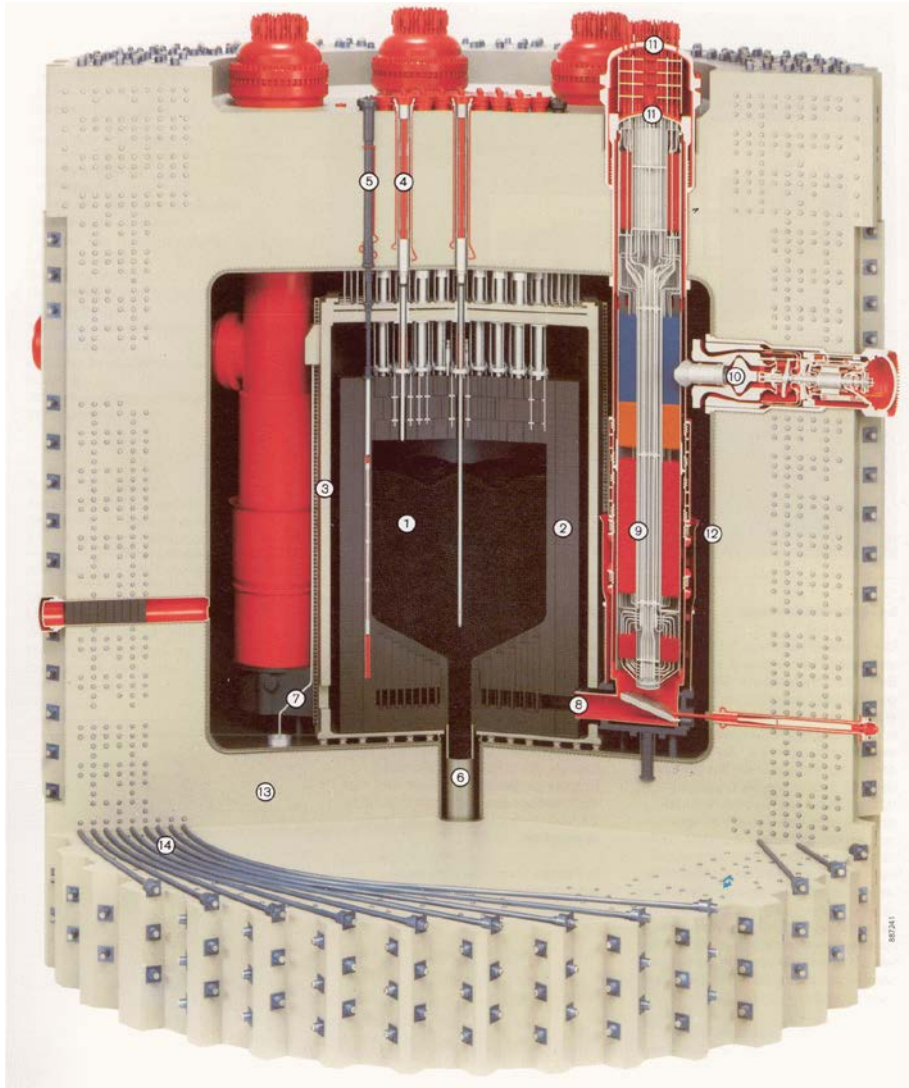


**Figure 2.7.5: THTR-300 cross section**

The ceramic core structures (see Position 2) contain a carbon brick bottom layer and two different graphite grades for the reflector structures. The inner layer consists of Gilsonite graphite PXA2N, whereas PAN graphite made of petrol coke was used in the outer layer. In

total, there are 618,4 Mg of graphite and carbon brick, including moderator/absorber elements (see AVR) and graphite from a burn-up measuring reactor<sup>5</sup>, in the THTR 300.

### **2.7.1.2 Total inventory of i-graphite in Germany**

The following table provides an overview on the i-graphite inventories, in Germany. More than a dozen of SUR 100 teaching reactors have not been listed, as most SUR 100 graphite structures are below exemption limits, due to the extremely low neutron activation.

---

<sup>5</sup> A separate reactor, moderated by graphite, was used to measure the burn-up of each discharged fuel pebble by inserting it into the core of this reactor and evaluating the reactivity change. When the target burn-up was not yet reached, the fuel pebble was recycled to the top of the pebble bed core. The irradiated graphite of this reactor is included in the 618,4 Mg of i-graphite for THTR as well as the moderator pebbles as explained for AVR.

**Table 2.7.1: Inventories of i-graphites in German MTRs & HTRs**

Reactor	Site	Operational	Graphite mass [Mg]
<b>High-Temperature Reactors</b>			
<b>AVR</b>	Jülich	1967-1988	238,1*
THTR	Hamm-Uentrop	1983-1989	618,4 **
<b>MTR</b>			
<b>Argonaut</b> (Ring core)			
SAR	Garching	1959-1968	?
STARK	Karlsruhe	1963-1976	?
Rosendorfer Ringzonenreaktor (RRR)	Rosendorf	1962	?
<b>TRIGA</b>			
FRF-1 / FRF-2	Frankfurt	1958-1968	7,7
FRH	Hannover	1973-1997	1,0
TRIGA HD I/II	Heidelberg	1966-1999	1,6
FRMZ	Mainz	ab 1965	4,4
FRN	Oberschleißheim	1972-1982	27,7
<b>Further Swimming Pool Reactors</b>			
FMRB	Braunschweig	1967-1995	1,5
FRG-1 / FRG-2	Geesthacht	1958-2010 / 1963-1993	11,1
<b>FRJ-1</b>	Jülich	1962-1985	12,9
<b>RFR</b>	Rosendorf	1957-1991	3,9
<b>Heavy-Water Reactors</b>			
<b>FRJ-2</b>	Jülich	1962-2006	30
FR-2	Karlsruhe	1961-1981	?
FRM-1 / FRM-2	München		?
KKN	Niederaichbach	1973-1974	?

\* Incl. Moderator- & absorber elements; \*\* as AVR plus Burn-up Measuring Reactor

Not all i-graphite masses could be exactly identified, due to the fact that information channels to former operators could not be established. The total mass of i-graphite in Germany can be judged to be in the range of 1000 Mg, most of it stemming from the HTRs (856,5 Mg) and the rest from diverse MTR (~ 150 Mg).

I-graphite samples were available and analysed from AVR, FRJ-1 (MERLIN), FRJ-2 (DIDO) and RFR. The tritium and radiocarbon activities are listed in Table 2.7.2.

**Table 2.7.2: Tritium and radiokarbon activities in German MTR & HTR graphites**

C-14	Packaging without specified tightness		Packaging specified tightness					
			annual permeability factor					
			≤ 0,01		≤ 0,001		≤ 0,0001	
	metallic solids	other waste product groups	metallic solids	other waste product groups	metallic solids	other waste product groups	metallic solids	other waste product groups
unspecified	8,4E+12	1,8E+08	9,2E+12	2,0E+08	9,2E+12	2,0E+08	9,2E+12	2,0E+08
volatile content 1% < x ≤ 10%		1,8E+09		2,0E+09		2,0E+09		2,0E+09
<b>volatile content ≤ 1%</b>		1,8E+10		2,0E+10		2,0E+10		2,0E+10

Abundant i-graphite material (~60 kg) for systematic investigations within CAST is only available from the Russian-built Rossendorf research reactor (RFR) and from MERLIN. The samples from block 4 of the RFR thermal column have been chosen for the leaching and treatment tests in CAST as they show a much higher radiocarbon activity compared to block 3 and MERLIN.

### 2.7.2 Waste acceptance criteria for KONRAD

‘Low level and intermediate level radioactive waste with negligible heat generation’ including i-graphite are destined for the KONRAD repository, which is a former iron-ore mine. The total volume of the repository is 303000 cbm. The temperature in the disposal drifts with a total length of 26 km is expected to remain at 50°C because heat generation by the waste is limited. The maximum radiocarbon activity for KONRAD is restricted to  $4 \times 10^{14}$  Bq. This value was based on a former judgement on the expected overall radiocarbon-labelled wastes in Germany. The average  $^{14}\text{C}$  activity per cbm results to  $1,32 \times 10^9$  Bq/cbm, under the assumption that the  $^{14}\text{C}$  activity would be homogeneously distributed over the whole repository volume. The maximum weight of waste containers cannot exceed 20 Mg

with respect to the transport facilities underground. A typical waste container, which could be used for i-graphite disposal in KONRAD is shown in Figure 2.7.6. The operational period for KONRAD is expected to be 40 years.

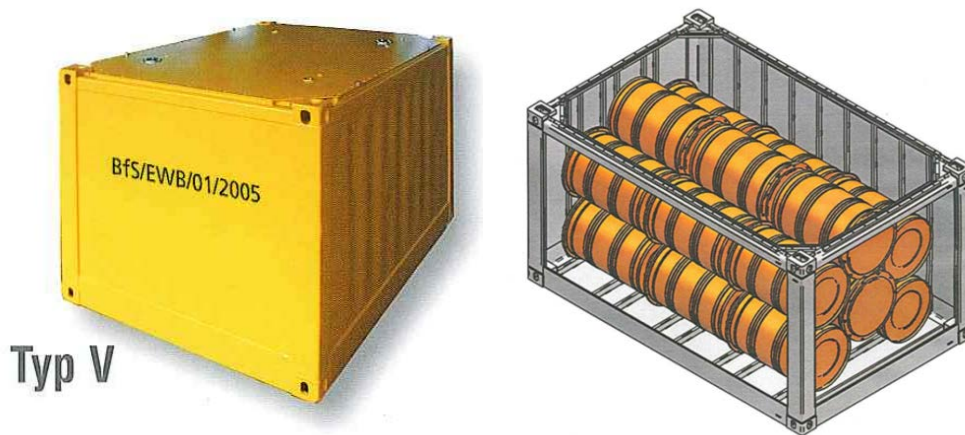


**Figure 2.7.6: Typ V waste container with 10,9 cbm volume**

When the facility was established, limits for gaseous emissions with the upcast ventilation were set for the following nuclide groups:

- H-3:  $1,5 \times 10^{13}$  Bq/a
- **C-14:**  $3,7 \times 10^{11}$  Bq/a
- I-129:  $7,4 \times 10^6$  Bq/a
- Rn-222:  $1,9 \times 10^{12}$  Bq/a
- a-aerosols:  $7,4 \times 10^7$  Bq/a
- b/ $\gamma$ -aerosols:  $3,7 \times 10^6$  Bq/a

The 'Guarantee Values ( $A_G$ )' per waste package are calculated according to the following formula:

$$A_G = \frac{G}{n * (f_0 * w_0 + f_a * w_a)}$$

With:

- $A_G$  guarantee value per waste package
- $n$  max. number of stored waste packages per year ( $\sim 10^4$ )
- $f_0$  release rate from the waste in open storage compartments
- $f_a$  release rate from the waste in closed storage compartments
- $w_0$  Weighting factors to characterize the contributions to the release of open storage compartments normalized to the release from the waste in the first year
- $w_a$  Weighting factors to characterize the contributions to the release of closed storage compartments normalized to the release from the waste in the first year.
- $G$  Values for the release of radioactive substances with the upcast air

With the assumed values for ventilation rates, the number of annually inserted containers, converging rates of the geological layer, open drifts during operation etc., guarantee values have been derived for  $^{14}\text{C}$  and are as presented in Table 2.7.2. With reference to the categories noted in this table, i-graphite falls into ‘other waste product groups’ and is classified in three different classes according to the volatility of the  $^{14}\text{C}$  in the waste matrix. The challenge is to show that i-graphite fulfils the 1% volatility requirement, because otherwise the maximum activity per waste package will be lowered from  $1,8 \cdot 10^{10}$  Bq down to  $1,8 \cdot 10^9$  Bq per package, i.e. 10-times more waste packages to accommodate the same  $^{14}\text{C}$  activity. Assuming a linear release of  $^{14}\text{C}$  over the 40 years operational period it means with some safety margins that the annual releases will be limited to an annual release fraction for i-graphite of about some  $10^{-4}$ /year. This is a challenging analytical requirement as it has to be shown and guaranteed that not more than 1 Bq  $^{14}\text{C}$  out of e.g. 10 kBq/g is released per year as a gas (the gaseous radioactive discharge of the KONRAD repository is the critical limit). Thus, it is no surprise that currently most of  $^{14}\text{C}$ -labelled waste in Germany falls into the ‘unspecified’ category. Leak-tight containers do not really help, as it is assumed that they are damaged by the convergence of the geological formations around the disposal drifts, once the drift has been closed.

Further requirements for the waste containers are derived from the following accident scenarios:

1. Free fall from 3 m height during handling above ground

2. Free fall from 5 m height during underground handling
3. Fire during underground transport with a temperature transient from 30-800°C within 0-5 minutes and a temperature plateau at 800°C over 1 hour, then cool-down to 30°C

In case 3, the following release mechanisms need to be studied

1. Release by pyrolysis of the waste product
2. Release by oxidation of the waste product
3. Release by boiling of water in the waste product
4. Release by sublimation or boiling of radioactive compounds

The released fractions need to be determined for the following groups of radionuclides:

- Halogens and  $^{14}\text{C}$  in volatile form,
- Tritium (as HTO),
- Further radionuclides.

### **2.7.3 I-Graphite disposal in the ASSE test repository**

161 steel drums of 200 liters volume with about 70000 of irradiated moderator and absorber elements (see Figure 2.7.3) have been disposed in the ASSE experimental underground disposal facility, which also contains various other radioactive and  $^{14}\text{C}$ -labelled waste, from different origin. The observed cumulative releases of tritium and radiocarbon in ASSE have been discussed in the German Committee of Radioactive Waste Management (ESK). A public report (in German) is available on the ESK homepage<sup>6</sup> summarizing the inventories and related releases, especially from chamber 12/750, which also contains 42 of the above mentioned drums containing i-graphite from AVR. According to this report (page 27/28), the overall  $^{14}\text{C}$  annual release fraction via the liquid phase (salt brine) is assessed to be in the order of  $7,4 \times 10^{-7}$ . The  $^{14}\text{C}$  activity of this chamber is judged to be about 50% of the overall

---

<sup>6</sup> <http://www.entsorgungskommission.de/downloads/unterlagenzurinventardiskussion.pdf>

$^{14}\text{C}$  activity in the whole ASSE repository, due to the presence of the i-graphite in chamber 12/750.

The cumulative  $^{14}\text{C}$  releases via the upcast ventilation of ASSE in the years 2001-2008 was 0,01 % of the whole inventory, which is near to the 1%  $^{14}\text{C}$  volatility requirement for KONRAD, as explained above. It is recommended by the ESK to determine the chemical speciation of the gaseous  $^{14}\text{C}$  releases, in more detail. The investigations are still going on and may be of interest for the CAST project and other national research activities, in this field. It is currently under discussion to retrieve the radioactive waste from ASSE and to dispose it in another repository, after reconditioning.

#### **2.7.4 Review of CARBOWASTE and CarboDISP**

Within CARBOWASTE, R&D activities in the research centre of Juelich concentrated on the characterization and treatment of i-graphite from MTR and HTR. Samples from UNGG and Magnox were subsequently included. The findings on treatment of irradiated MERLIN and AVR samples have been confirmed with the recent tests of RFR samples, performed in the CAST project. Most treatment experiments performed under inert gas and temperatures between 960 and 1300°C show a pronounced relative release of  $^{14}\text{C}$  with rather small mass losses (< 1%). The mass losses have been calculated by gas analysis and checked by weighing, after the completion of the tests. The treatments have been carried out over more than 10 hours and terminated when the adsorbed oxygen was practically consumed. Rather high  $^{14}\text{C}$  releases in a relative ratio of 20:1 – 10:1 have been observed under these conditions, for MTR i-graphite (See Figure 2.7.7 below). A ratio of 1:1 can be interpreted as a non-selective oxidation of graphite where the  $^{14}\text{C}$  fraction is released proportional to the  $^{12/13}\text{C}$  fraction. The experiments also indicate that treatment of i-graphite powder (MP – Merlin Powder) is less efficient with respect to  $^{14}\text{C}$  removal as compared to cylindrical samples (MM – Merlin Massive) with a diameter of 6-10 mm and some cm length. Treatment by steam appears to be less efficient (10:1 – 5:1 ratios).

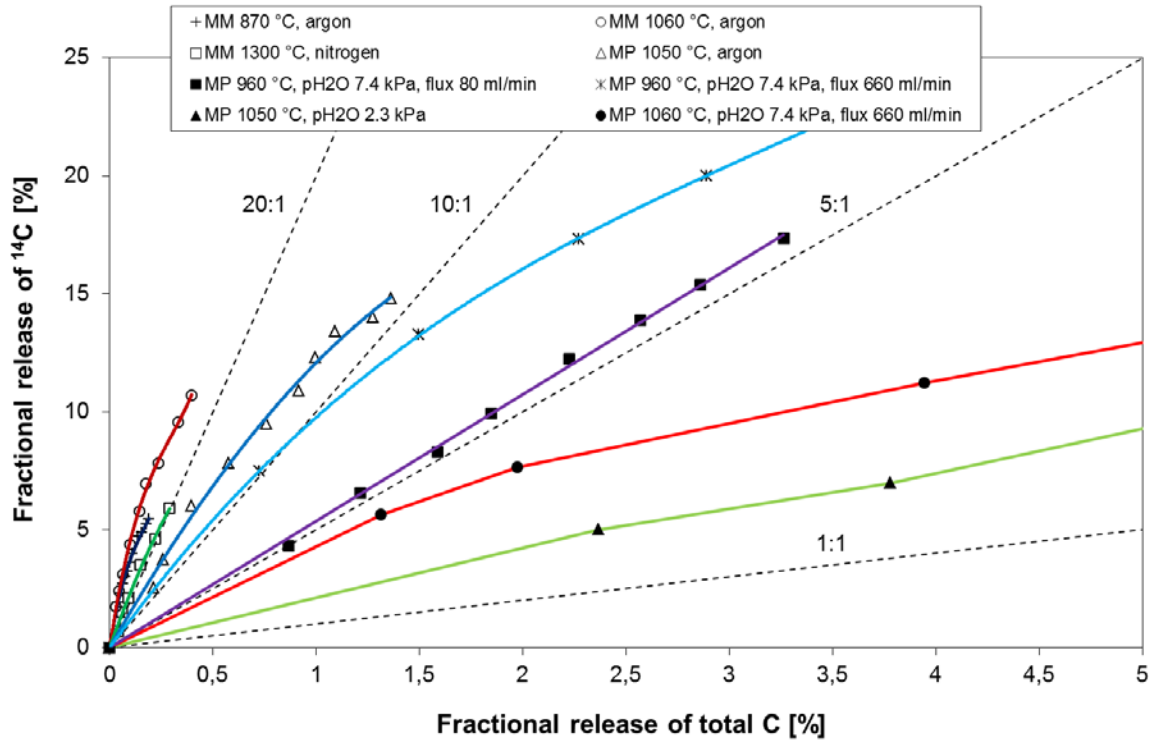


**Figure 2.7.7  $^{14}\text{C}$  fractional releases versus total C fractional releases for MTR i-graphite**

The treatment experiments can also be used as an analytical tool, for proving the existence of releasable or volatile  $^{14}\text{C}$  species at the macroscopic surfaces and within the accessible pore surfaces. These findings still have to be correlated with leach tests, as part of the CAST project and ongoing PhD theses.

The thermal treatment tests are also used to assess potential  $^{14}\text{C}$  releases during accident scenarios, as defined for KONRAD. Weight losses have been determined by thermo gravimetric analyses (TGA) simulation of the accident conditions (i.e. 1 hour at 800°C under air and steam) and can be compared to the related  $^{14}\text{C}$  releases in the figure, above. As a general observation, it can be stated from thermal treatment tests that  $^{14}\text{C}$  releases only occur in conjunction with oxidation / corrosion processes and associated mass losses (no mass loss – no release).

It has been discovered during the CARBOWASTE project that treatment processes under constant process parameters (temperature, pressure, treatment agent etc.) may lead to rather lengthy treatment times, which are not compatible with industrial requirements. The reason is that low temperatures and/or inert / non-aggressive gas environments appear to provide the best decontamination results but they need a long exposure time under these conditions. Higher temperatures only attack the macroscopic surfaces and remove surface contamination in a shorter time. However, a new patented process (see Figure 2.7.8) can overcome these restrictions by separating the insertion of reactive gases at lower temperatures and higher pressure, reacting at higher temperatures for removing  $^{14}\text{C}$  also within the bulk of the i-graphite waste and removing the reaction products under lower pressure. Before stopping the iterative treatment process, further reactions can be undertaken to improve the disposal characteristics (e.g. by hydrophobisation, surface coating etc.).

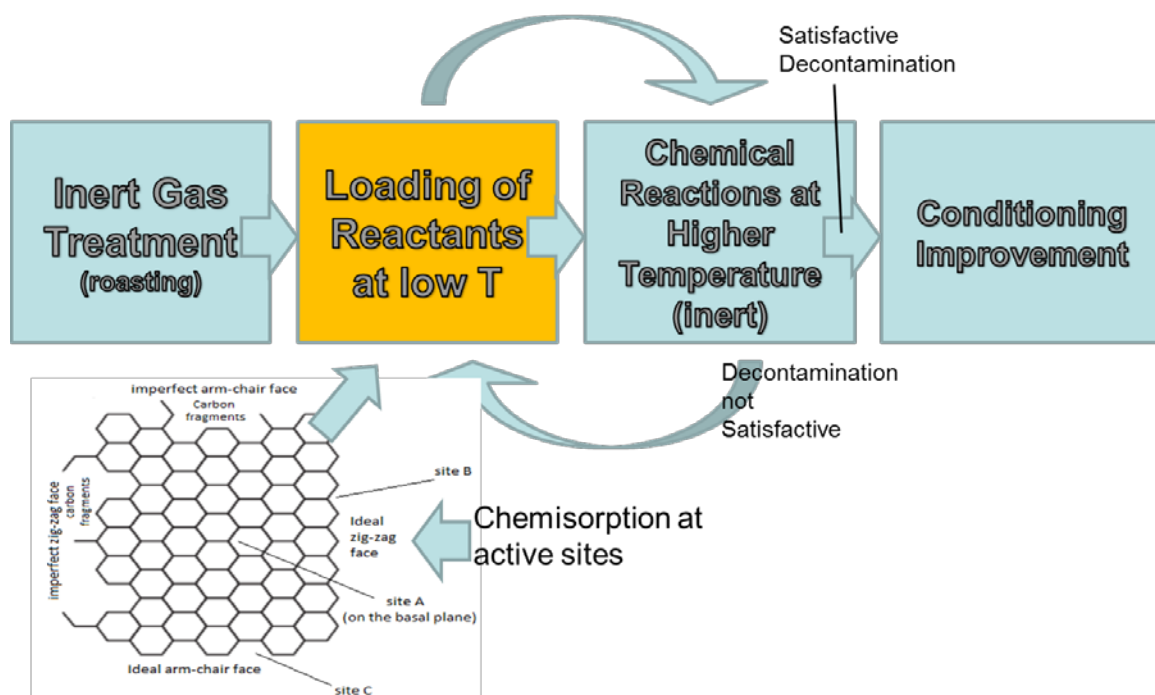


**Figure 2.7.8** New patented process for removing  $^{14}\text{C}$  from bulk i-graphite waste

In CarboDISP, leach tests have been performed with German i-graphite grades under KONRAD conditions in an integral approach, by investigating the  $^{14}\text{C}$  speciation within the

liquid leachate and the gaseous phase. This will be continued under CAST by inclusion of leach tests with pre-treated samples.

Embedding of i-graphite into geopolymers has also been investigated in CarboDISP. The aluminosilicate material is capable to form an inorganic polymer by 3-D-crosslinked structures with

- higher mechanical / chemical stability
- higher leach resistance
- long-term durability
- favorable in processing (thixotropic)
- prolonged hardening by vibration as ideal backfilling material

A 5-years research programme has been defined within the ‘Project-oriented Funding (PoF)’ of the Juelich research centre. It is intended to perform systematic investigations to better understand and quantify the correlations to the parameters affecting the behaviour of i-graphite, as shown in the following Figure 2.7.9.

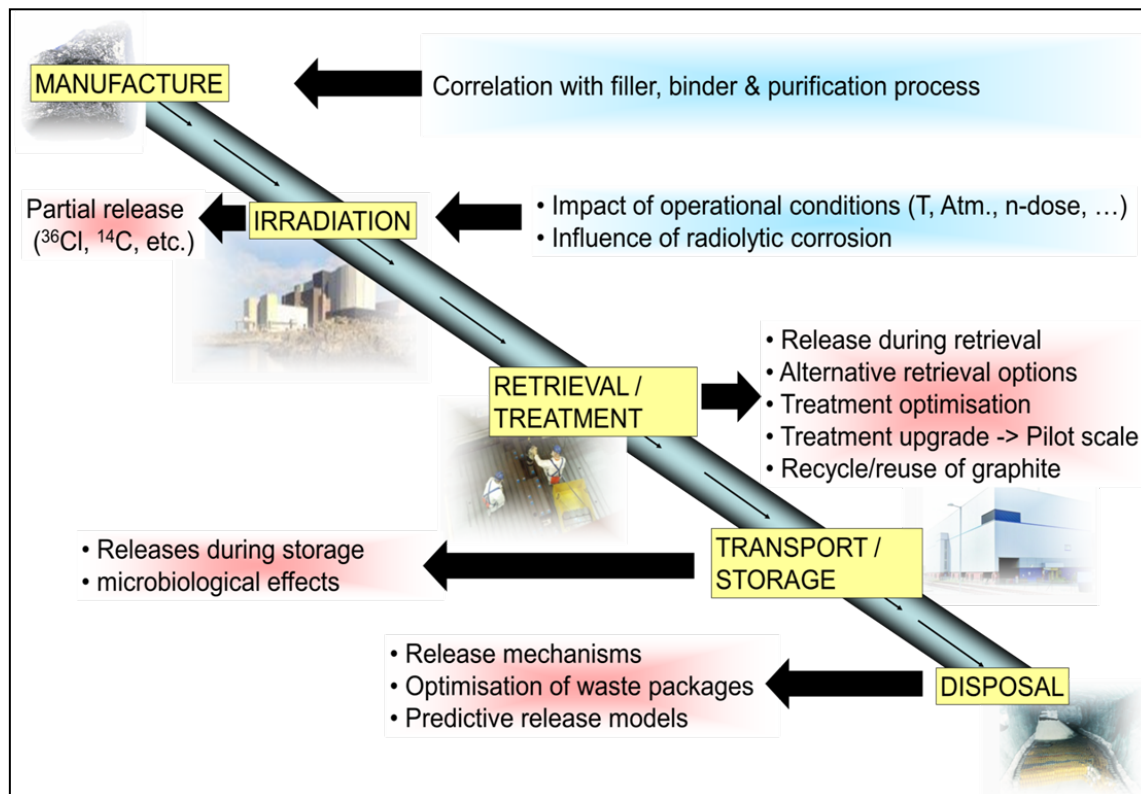


**Figure 2.7.9 Illustration of 5-year research programme for the Juelich research centre**

It is intended to model the surface reactions of functional groups to better understand the release mechanisms and speciation of released compounds. This will be supported by investigations of model substances and separate effect tests as shown in the following Figure 2.7.10.

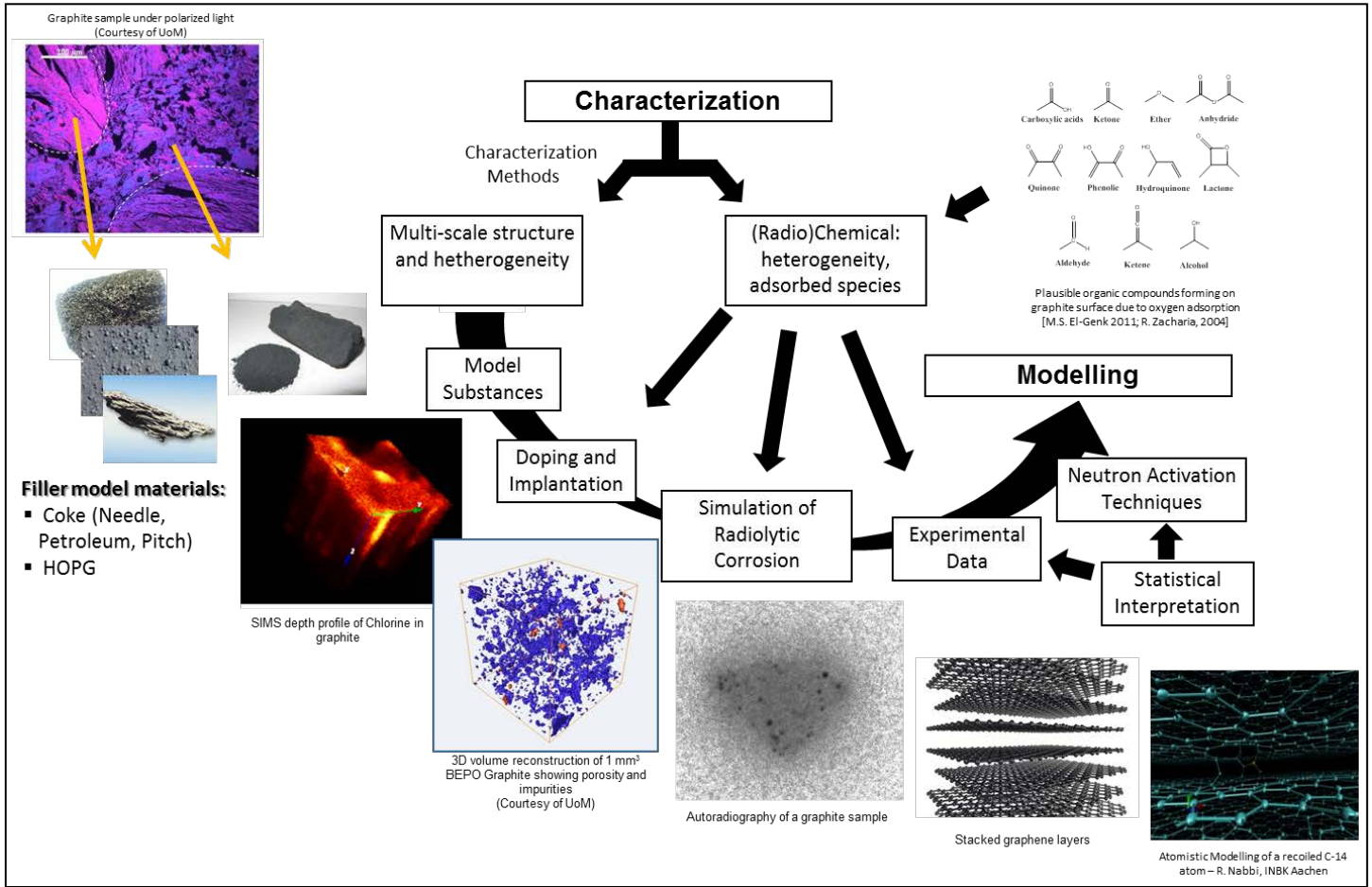


**Figure 2.7.10** Supportive by investigations of model substances and separate effect tests to be undertaken as part of 5-year research programme for the Juelich research centre

## 2.8 Centro de Investigaciones Energéticas Medioambientales y Tecnológicas (CIEMAT)

The section utilises information drawn from the following CARBOWASTE reports :

- Piña, G., Jones, A., Vulpius, D., Comte, J., Narkunas, E. and von Lensa, W. CARBOWASTE D-3.0.0 Summary Report on Work Package 3, 2013.
- Piña, G., Rodriguez, M., Gascón, J.L., Magro, E. and Lara, E. CARBOWASTE D.3.1.5-CWRRT Final Report on Statistical Evaluation & Conclusions, 2013.
- Piña, G., Rodriguez, M., Vulpius, D., Comte, J., Brennetot, R., Dodaro, A., Duskeas, G., Brune, C., Visser – Tynova, E., Van Hecke, K., Landesman, C. and Jones, A. CARBOWASTE T-3.1.6 Topical Report on Characterization Methods, 2013.
- Cobos, J., Gutiérrez, L., Rodríguez, N., Iglesias, E., Piña, G. and Magro, E. CARBOWASTE T3.2.4 Irradiated graphite samples bulk analyses at CIEMAT, 2008.
- Vulpius, D., von Lensa, W., Jones, A., Guy, C., Comte, J., Piña, G., Dodaro, A., Duškesas, G. and Iordache, M. CARBOWASTE D-3.3.1 First Radionuclide Inventory Data on Untreated Graphite /Evaluation for Direct Disposal, 2010.
- Piña, G. et al. CARBOWASTE T-3.5.1 Topical Report with the characteristics of the legacy irradiated graphite, 2013.
- Piña, G., Arsene, C., Capone, M., Gascón, J. L., Jones, A., McDermott, L., Vulpius, D. CARBOWASTE D-4.3.5 Decontamination Factors by Decontamination Agents under Normal Pressure, 2013.
- Gascón, J.L. et al. CARBOWASTE T-4.3.5-d Report on decontamination of irradiated graphite by chemical treatment with liquid agents. 2013.

The i-graphite waste in Spain arises from the Vandellós 1 NPP, which is a UNGG reactor of the French design. A very comprehensive analysis of the issues relating to its disposal has been undertaken. Relevant parameters are as follows:

- 460 MW(e); 56000 GWh (from 05/06/72 to 10/19/89)
- Licensee: 1971 – 1998HIFRENESA
- Operation:1971 – 1989

- Dismantling: 1998 –...ENRESA
- Shutdown Oct 1989
- Decommissioning Level 2 1998 – 2003
- Safe Enclosure: for 25 years

The graphite moderator and reflector comprise 2680 tonnes of Pechiney graphite, whilst a total of 186000 graphite sleeves (~1000 tonnes) were used.

Estimates of overall activity in the fuel sleeves and the moderator have been made from a sampling programme, with the data normalised to 1<sup>st</sup> January 2000 and are shown in Tables 2.8.1 and 2.8.2 respectively. Note that the sleeves have absorbed activity from the fuel storage pond in addition to that generated directly in the graphite (notably <sup>137</sup>Cs).

**Table 2.8.1 Mean radioisotope data for Vandellós graphite sleeves at 01/01/2000**

Isotope	Proportion of Total Activity (%)	Mean Activity (Bq/g)
<sup>3</sup> H	38.44	8.93E+04
<sup>14</sup> C	5.81	1.35E+04
<sup>55</sup> Fe	11.62	2.70E+04
<sup>60</sup> Co	17.22	4.00E+04
<sup>59</sup> Ni	0.27	6.25E+02
<sup>63</sup> Ni	25.31	5.88E+04
<sup>137</sup> Cs	0.16	3.79E+02
<sup>154</sup> Eu	0.19	4.35E+02
<sup>241</sup> Pu	0.29	6.82E+02
Total	99.31	-

The graphite pile will remain inside the reactor building in a safe enclosure for 25 years. The sleeves were extracted as described below and temporarily stored on site in 220 cubic containers of 6 m<sup>3</sup> with the crushed graphite obtained from the standard separation process carried out in Vandellós 1. The total mass of graphite waste is 3500 tonnes: there are 98 cylindrical containers with the wires of the sleeves comprising 22 tonnes.

**Table 2.8.2 Mean radioisotope data for Vandellós graphite moderator at 01/01/2000**

Isotope	Content (%)	Mean Activity (Bq/g)
<sup>3</sup> H	74.97	2.75E+05
<sup>14</sup> C	15.32	5.62E+04
<sup>55</sup> Fe	2.50	9.15E+03
<sup>60</sup> Co	3.65	1.34E+04
<sup>63</sup> Ni	2.39	8.77E+03
<sup>241</sup> Pu	0.19	6.89E+02
Total	99.02	-

One of the issues causing most concern with the *i*-graphite of Vandellós 1, in relation to the waste-acceptance criteria at El Cabril, is the <sup>14</sup>C and <sup>3</sup>H activities, which exceed the total acceptable inventory of the El Cabril repository by factors of eight and two respectively.

The presently estimated activities of principal isotopes in the graphite, compared with the licensed capacity of El Cabril and the content of the wastes already disposed there, is shown in Table 2.8.3.

**Table 2.8.3 Inventory analysis for El Cabril for the four principal graphite-derived isotopes**

Isotope	Permitted Radiological Inventory of El Cabril MBq	Activity Disposed At El Cabril At 14/10/2011 MBq	Extent of Permitted Inventory Currently Used %	Estimated Graphite Activity MBq	Ratio of Graphite Activity to Permitted Inventory %
<sup>3</sup> H	2.0 E+08	3.10 E+06	1.57	4.22 E+08	211
<sup>14</sup> C	2.0 E+07	2.84 E+06	14.2	1.65 E+08	825
<sup>60</sup> Co	2.0 E+10	2.64 E+08	1.32	1.57 E+07	0.08
<sup>63</sup> Ni	2.0 E+09	9.13 E+07	4.57	5.41 E+07	2.7

It is established that the third dismantling stage of Vandellos 1 NPP will begin in 2028 and, before that date, the following issues has to be defined with regard to *i*-graphite:

- Retrieval of the core graphite (methodology);
- Decontamination of graphite from  $^{14}\text{C}$  and  $^3\text{H}$  in order to have available the possibility of disposing of *i*-graphite in the El Cabril repository. The percentage of decontamination for  $^{14}\text{C}$  would need to be 88%, approximately;
- The option to create an impermeable cover, by using a specific glass, of the pore system of graphite to minimise or make negligible the release of volatile or soluble content;
- The possibility of increasing the  $^{14}\text{C}$  radiological capacity of the El Cabril inventory;
- Volume optimisation of the crushed graphite. The current amount of the Vandellos 1 graphite, if it undergoes a crushed pre-treatment, would fill more than 800 concrete containers in the El Cabril Repository.

CIEMAT is involved in the study of *i*-graphite from the earliest '90 when Vandellos I (UNGG reactor) was shutting down.

From that moment to the execution of CARBOWASTE several investigations have been performed in order to know the nuclide vector of *i*-radiated graphite, characterise the physic-chemical behaviour and the structural properties to complete the necessary knowledge for fulfil the waste acceptance criteria for the disposal conditions to be decided.

Here is described briefly the characterisation and treatment methods described under IP-CARBOWASTE as the present applied developments

### 2.8.1 Samples investigate at CIEMAT

URBMA/DFN/DE (Unidad de Residuos de Baja y Media Actividad/División de Fisión Nuclear/Departamento de Energía) of CIEMAT has investigated graphite samples from three type of reactors [Piña, G. et al. CARBOWASTE D-3.0.0 Summary Report on Work Package, 2013]:

- MTR reactors: Samples from JEN-1 (Spain) and samples from Triga (Romania)
- UNGG reactor: Samples from Vandellos-1 (Spain) and from SLA-2 (France)
- Magnox reactor: Samples supplied from Magnox Limited

## 2.8.2 Characterisation Methods developed and applied at CIEMAT

### 2.8.2.1 Sample preparation

The samples were prepared as graphite powder which was obtained by filing the graphite block surface with a grater coupled with a plastic box to collect the powdered graphite in a portable glovebox placed at a fume hood (Figure 2.8.1 and 2.8.2).



Figure 2.8.1: Portable glove box and Grater with plastic box

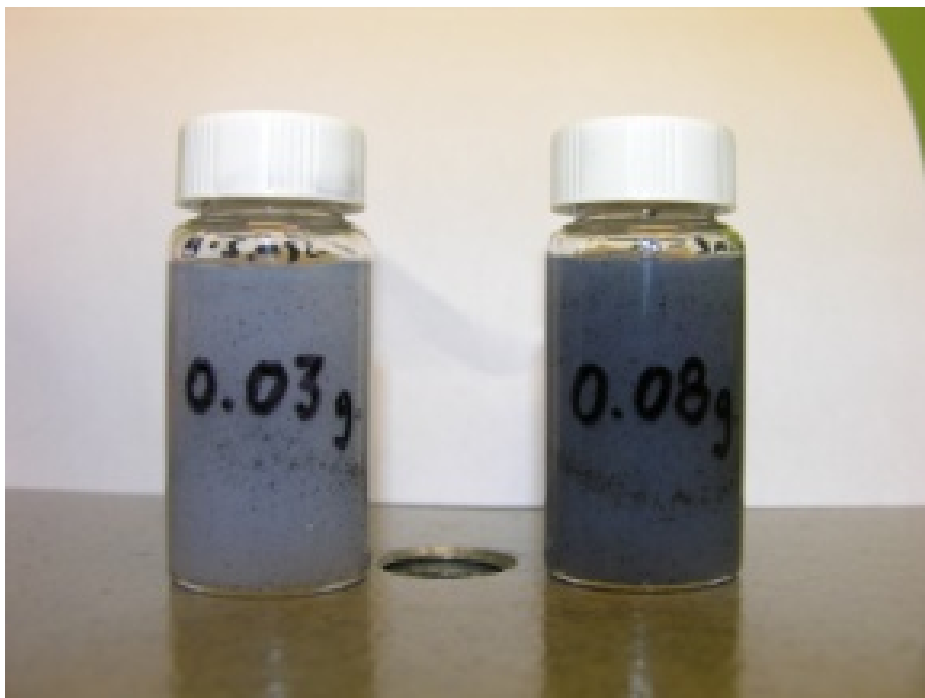


Figure 2.8.2 Samples

### 2.8.2.2 Gamma Spectrometry

In order to characterize the high energy (>60keV) gamma emitting nuclides in powder samples of graphite an experimental efficiency calibration of germanium detectors was made and, by means of using the LABSOCS Geometry Composer V5.0 by CANBERRA program, a mathematical calibration was additionally performed.

The mathematical calibration is used as a way to verify the results obtained using the experimental calibration curve, and moreover, because it makes possible the analysis of a sample quantity 25 times greater and therefore more representative of the material to be analysed.

The experimental calibration was made by mixing in a scintillation glass vial a certain quantity of radioactive standard solution, liquid scintillation cocktail, distilled water and powder graphite. In order to determine the proportion of each component several tests were made on the basis of the following criteria:

- 1 Reasonable counting times;
- 2 Solid suspension in the media enough to perform a precise measurement;
- 3 Amount in the range 0.03 to 0.1 g were used to calibrate the system and obviously to measure sample Time (Figure 2.8.3)

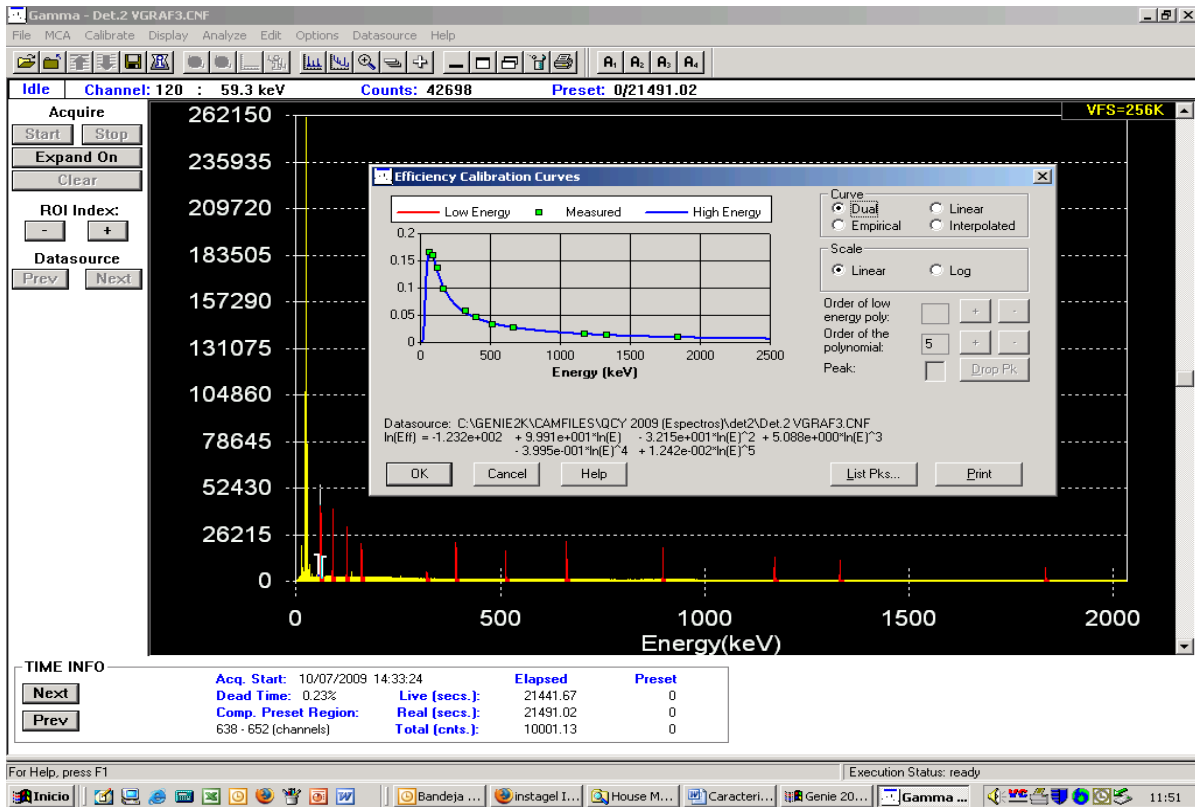


**Figure 2.8.3 Experimental calibration curve.**

The measuring geometry selected to perform mathematical calibration was a scintillation glass vial with 2 g of powder graphite placed 158 mm away from the detector. In order to avoid dead time a device to separate the sample from the detector had to be implemented inside the detector shielding (Figure 2.8.4).



**Figure 2.8.4. Sample set-up**

Several design tests were performed to define the measure geometry considering the following aspects:

- Apparent density of powder graphite from 0.39 g/ml to 0.70 g/ml.
- Sample height in the vial from 5 mm to 15 mm.
- The source-detector distance has been chosen depending on the dead time values.

### **2.8.2.3 Tritium and radiocarbon determination**

The determinations of  $^3\text{H}$  and  $^{14}\text{C}$  activity in the powdered graphite samples were made in a catalytic oxidizer oven. The samples were combusted in a stream of oxygen gas at 900 °C. The bulk of the material is converted to carbon dioxide and water steam and the combustion products then passed through a series of catalysts at 680 °C and then traps the  $^{14}\text{C}$  dioxide and/or tritiated water directly in the scintillation vials, which contain trapping solution. This procedure is illustrated in the flow diagram in Figure 2.8.5.

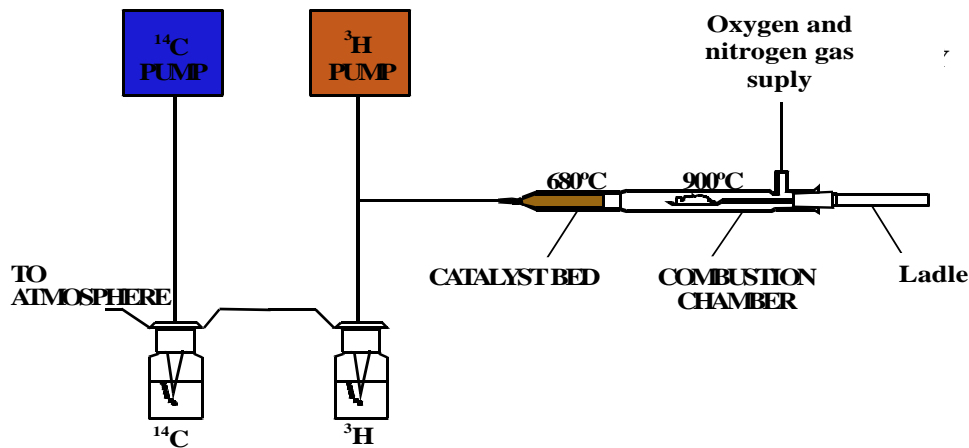


**Figure 2.8.5 Catalytic oxidizer furnace.**

To determine the  $^3\text{H}$  and  $^{14}\text{C}$  activity in graphite, the same sample was burned 3 times during 3 minutes to be sure that any activity remains in the combustion chamber. The activity collected by this form was the 99.9 %.

#### 2.8.2.4 Gross alpha determination

Graphite powder is distributed over a disk of paper on a ribbed planchet adding  $^{241}\text{Am}$  (for Gross alpha calibration) to determine the efficiency in function of the mass of graphite added throughout an auto-absorption curve (Figure 2.8.6).

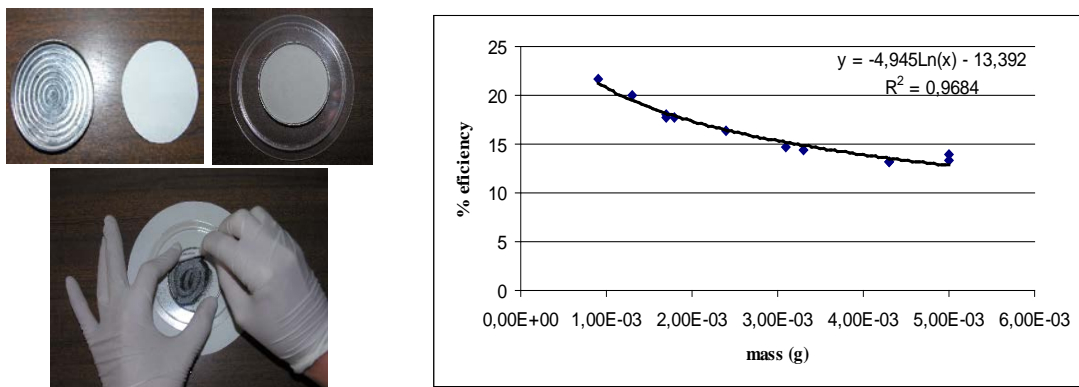


**Figure 2.8.6 Procedure to prepare graphite samples and auto-absorption curve**

### 2.8.2.5 Dissolution methods

To solubilise powder graphite using microwave systems an acidic mixture of concentrated H<sub>2</sub>SO<sub>4</sub> and HNO<sub>3</sub> in 4/1 ratio v/v at 260°C in 30 minutes is used. The temperature slope is 3 minutes to reach 150°C, 3 minutes to reach 230°C and 3 minutes to reach 260°C, finally it is necessary 30 minutes at 260°C to get a complete dissolution of non-volatile material and I and Tc from a mass of graphite under 0.25 g.

An alternative method to dissolve the non-volatile radionuclides one aliquot of the original graphite powder sample was dissolved by an acid treatment with H<sub>2</sub>SO<sub>4</sub>, HNO<sub>3</sub> and HClO<sub>4</sub> acid in a reflux system, obtaining a final solution that was prepared in order to obtain the solution in 4M HCl.

Specific method for dissolution of graphite and recovery of chlorine has been development based on reflux dissolution of graphite powder and trapping in an alkaline media the chlorine as chloride.

### 2.8.2.6 Determination of Pure $\beta$ and $\beta$ - $\gamma$ emitters

**Niobium-93m/94.** The radiochemical separation procedure of niobium is based on its selective precipitation as Nb<sub>2</sub>O<sub>5</sub> in 4M HCl medium after addition of known amounts of stable Nb(V) as carrier. The precipitate Nb<sub>2</sub>O<sub>5</sub> is dissolved by HF forming the stable complex NbOF<sub>5</sub><sup>2-</sup>. The chemical yield of the separation process is obtained by spectrophotometric measurements of the stable purple complex Nb-PAR (where PAR is 4-(2-pyridylazo)resorcinol). Then <sup>94</sup>Nb and <sup>93m</sup>Nb were measured by high-energy and low-energy  $\gamma$ -spectrometry respectively.

**Iron-55/59.** Ferric ions are precipitated as hydroxides by ammonia after addition of known amounts of stable iron as carrier. The precipitate is dissolved in concentrated nitric acid. The final solution obtained is 0.5M HNO<sub>3</sub>. The measurement is carried out once the possible gamma interferences are checked by gamma spectrometry. <sup>55</sup>Fe is determined by liquid scintillation counting by the measured of Auger electrons which are consequence of radioactive decay by electron capture. <sup>59</sup>Fe is measured by gamma ray spectrometry. The chemical yield is determined by spectrophotometry from the initial iron added as carrier.

**Nickel-59/63.** Nickel is precipitated with dimethylglyoxime, after addition of known amounts of stable nickel as carrier for determination of the chemical yield by spectrophotometry. A liquid extraction of nickel with chloroform and re extraction with 0.5M HCl is carried out. The final solution obtained is 0.2M HCl.  $^{63}\text{Ni}$  is determined by the measured of its beta emission by liquid scintillation counting once the possible gamma interferences are checked by gamma spectrometry.  $^{59}\text{Ni}$  is measured by X ray spectrometry with a planar Ge detector.

**Strontium-89/90.** Strontium is separated by adsorption on an Eichrom Sr Resin column after addition of known amounts of stable strontium as carrier and after conversion of the solution to the nitrate form. The resins are prepared (activated for Sr selective absorption) with 8M  $\text{HNO}_3$ , 8M  $\text{HNO}_3$  0.5M oxalic acid and 8M  $\text{HNO}_3$ . The elution of strontium is carried out with 0.05M  $\text{HNO}_3$ . The solution obtained is evaporated to dryness, then  $\text{HNO}_3$  is added and again evaporated to dryness in order to be sure that all sample is in the nitrate form. Finally the residue is weighed and the weigh corresponding to  $\text{Sr}(\text{NO}_3)_2$  form is obtained in order to determine recovery of carrier.  $^{89/90}\text{Sr}$  is determined by the measured of its beta emission by liquid scintillation counting once the possible gamma interferences are checked by gamma spectrometry. Two counting are made, one immediately after the separation and the other one with a minimum time interval of 8-10 days to correct ingrowth of  $^{90}\text{Y}$  and to allow  $^{89}\text{Sr}$  some small decay. In the first counting it is considered the contribution of  $^{90}\text{Sr}$ , a small quantity of  $^{90}\text{Y}$  and  $^{89}\text{Sr}$ . In the second counting it is considered the same contribution of  $^{90}\text{Sr}$ , more  $^{90}\text{Y}$  and less quantity of  $^{89}\text{Sr}$ . In this way it is possible to have two equations to obtain the  $^{89}\text{Sr}$  and  $^{90}\text{Sr}$  activities..

**Calcium-41/45.** Calcium separation is based on selective precipitation reactions by hydroxides, carbonates and chromates after addition of known amounts of stable calcium. At the end of the radiochemical separation procedure the calcium carrier, together with the radionuclides of calcium, is precipitated as calcium carbonate, which is dried and weighed to determine recovery of carrier. Next, the precipitate is dissolved in hydrochloric medium in order to measure the Auger electron emissions, which are consequence of radioactive decay by electron capture, from  $^{41}\text{Ca}$  and the beta emissions from  $^{45}\text{Ca}$ . The measurement is

performed once the possible gamma interferences are checked by gamma spectrometry, by dual label measurement in a liquid scintillation counter.

### 2.8.2.7 Determination of Volatile Pure $\beta$ and $\beta$ - $\gamma$ emitters

**Chlorine-36.** Chlorine separation is based in an oxidation technique performed on the graphite powder sample. The graphite sample is dissolved with concentrated acids  $\text{HNO}_3$ ,  $\text{HClO}_4$  and  $\text{H}_2\text{SO}_4$ . The gases formed during the dissolution pass through a series of  $\text{NaOH}$  bottles where chlorine ( $^{36}\text{Cl}$ ) and carbon dioxide ( $^{14}\text{C}$ ) are trapped. The basic solution obtained is neutralised in order to measure the  $^{36}\text{Cl}$  beta emissions by liquid scintillation counting. The measured is carried out by the dual label technique.

**Technetium-99.** The method developed for  $^{99}\text{Tc}$  considered that the medium for starting dissolution is 1:1  $\text{H}_2\text{SO}_4$  : water.

The methodology consists to extract by solvent extraction with a specific crown-ether as extractant solved in a mixture of toluene/di-methyl-ketone (Figure 2.8.7).

The oxidation state of Tc is VII ( $[\text{TcO}_4]^-$ ), due to oxidising conditions, but it has to be IV in order to ensure the effectiveness of the separation process by extraction (to obtain a distribution coefficient that recover the maximum amount of Tc from dissolution). The way to reduce the Tc and fix in oxidation state IV is adding ascorbic acid after the crown ether (to avoid the decomposition of ascorbic acid by 1:1  $\text{H}_2\text{SO}_4$  of the media) that reduces the  $[\text{TcO}_4]^-$ .

The obtained results shown that Tc is extracted with a chemical yield of 93 % and all interfering radionuclides, except for  $^3\text{H}$ , are quantitatively eliminated.

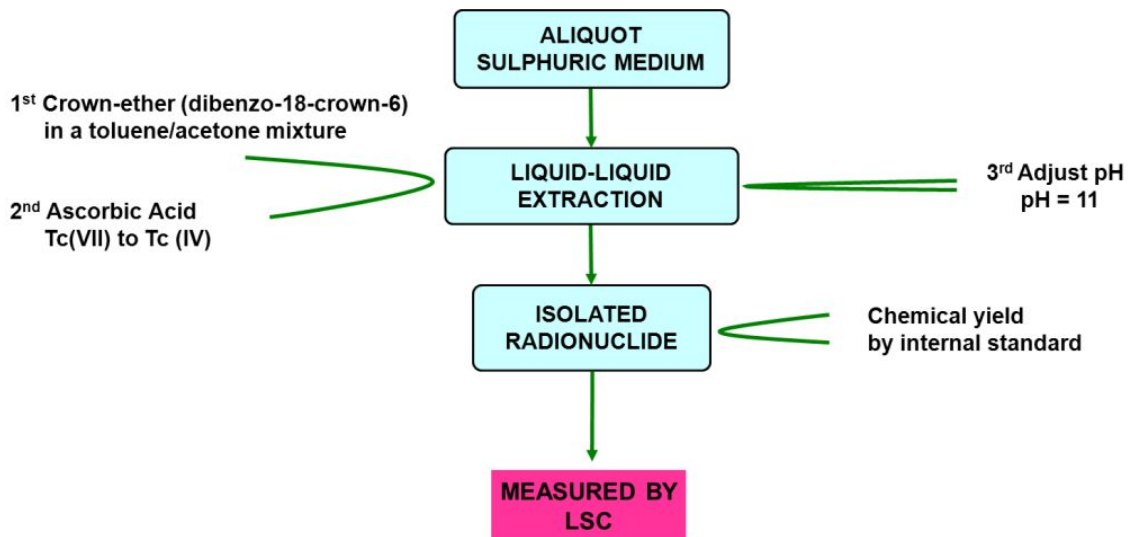


**Figure 2.8.7 Flow Chart of technetium separation**

Interference with  $^3\text{H}$  is avoided in the measurement because, as in the case of  $^{36}\text{Cl}$ , the final refineate is analysed by dual label LSC technique, since the energy ratio between  $^3\text{H}$  and  $^{99}\text{Tc}$  higher than 2 (a calibration method that takes into account the signal of H-3 in Tc-99 spectra can be applied due to the energy resolution of the LSC system; this allows the spectra of both nuclides to be evaluated independently).

**Iodine-129.** The methodology to separate iodine had to be adapted to the matrix effects and to the 1:1  $\text{H}_2\text{SO}_4$  media from the graphite dissolution. The method developed is applied in 2 steps:

1st step.- A dissolution with carriers of Fe(III), Co(II) y Zr(II) is added to the graphite dissolution. These cations forms a hydroxide precipitate at  $\text{pH} > 8$  and so that the interference of these cations is removed by co-precipitation and the main  $\alpha\beta\gamma$  emitters are decontaminated from the sample except for alkaline metals as Cs.

2nd step.- Caesium is precipitated at  $\text{pH} < 4$  with phosphowolframic acid in nitric acid media with addition of stable Cs(I) as carrier.

After performing the analyses of four samples of virgin graphite traced with  $^{129}\text{I}$  standard, the average chemical yield is 70 %.

The measurements are performed in a low energy germanium detector (LEGe) and the uncertainty associated with the determinations ranging within 10-12 %.

### 2.8.2.8 Determination of $\alpha$ -emitters

The determination by alpha spectrometry requires the separation of the  $\alpha$ -emitters from fission products, rare-earth and other elements that interfere in the preparation of the radioactive source and its measurement. All alpha emitters sources are prepared by electro-deposition and measured by a 450 mm<sup>2</sup> ion implanted silicon detector

**Plutonium.** The separation of plutonium is performed by anion exchange chromatography. Fission products and rare-earth are eliminated washing the column with nitric-methanol. Americium and curium are eluted with HNO<sub>3</sub> and finally, the column is rinsed with HCl solution and plutonium is eluted with HCl/HI solution. To calculate the chemical recovery, <sup>242</sup>Pu is used as tracer.

**Americium and Curium.** The solution of americium and curium, obtained in the separation of plutonium, are extracted with 0.45M Di(2 ethylhexyl)phosphoric acid in n heptane. Americium and curium are re-extracted with HCl. Finally, americium and curium are purified by anion exchange chromatography. To calculate the chemical recovery, <sup>243</sup>Am is used as tracer.

**Uranium.** The separation of uranium from plutonium, americium, curium, rare earth and fission products is carried out by liquid-liquid extraction with TBP-n heptane. Uranium is extracted and purified by anion exchange chromatography. To calculate the chemical recovery <sup>232</sup>U is used as tracer.

### 2.8.2.9 Results

All results of CARBOWASTE Project on inventory are collected in the DATA BASE performed in WP3.

Here we show some determinations performed in the samples of Vandellos 1 Pile.

In the characterisation of some high energy gamma emitters determined by direct  $\gamma$  spectrometry all values collected for  $^{24}\text{Na}$ ,  $^{54}\text{Mn}$ ,  $^{58}\text{Co}$ ,  $^{59}\text{Fe}$ ,  $^{65}\text{Zn}$ ,  $^{95}\text{Zr}$ ,  $^{106}\text{Ru}$ ,  $^{108\text{m}}\text{Ag}$ ,  $^{110\text{m}}\text{Ag}$ ,  $^{125}\text{Sb}$ ,  $^{144}\text{Ce}$  and  $^{152}\text{Eu}$  are under minimum detectable activity (MDA).

Specific activity variation in function of coordinates in the moderator (height and radius) is calculated for  $^3\text{H}$ ,  $^{14}\text{C}$ ,  $^{60}\text{Co}$  and  $^{137}\text{Cs}$  (case of  $^{14}\text{C}$  is represented in the Figure 2.8.8).

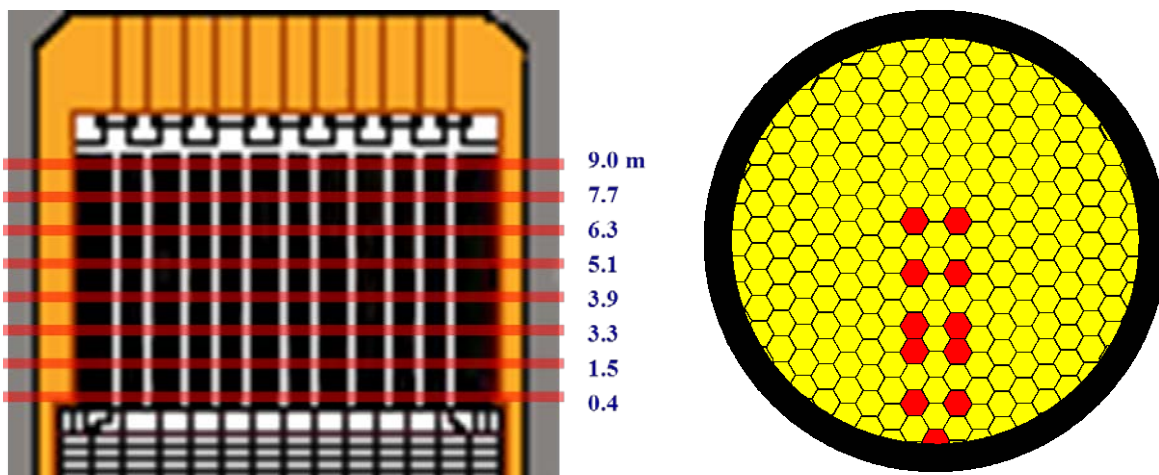


**Figure 2.8.8  $^{14}\text{C}$  representation - specific activity variation in function of coordinates in the moderator.**

Relative activity of alpha, pure beta and beta-gamma emitters are plotted in bar diagrams as are shown in Figure 2.8.9. The relative specific activity per nuclide is calculated as the ratio between activity of each sample and average activity of the six samples in order to get comparable activities values to study the tendency.

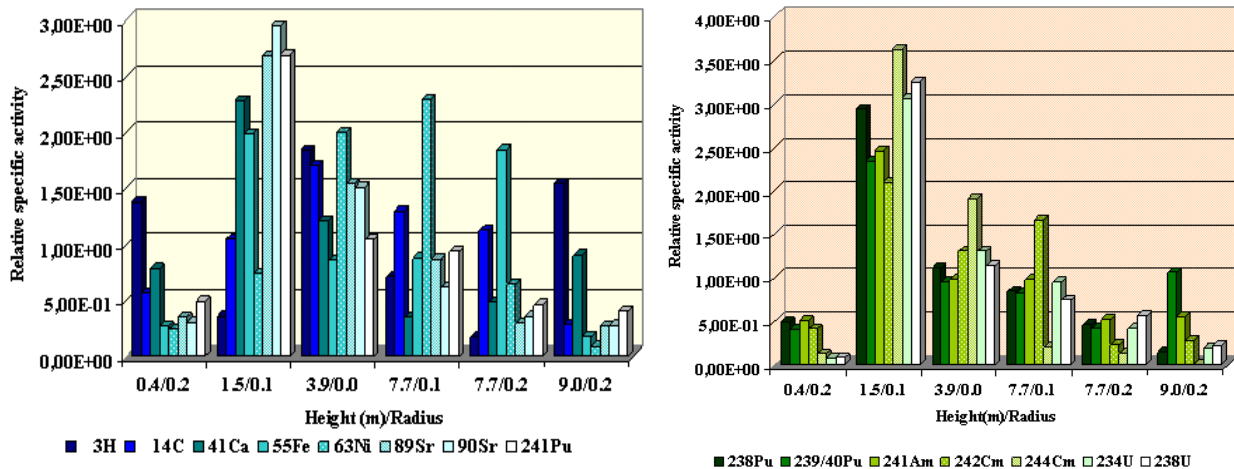


**Figure 2.8.9 Data for beta nuclides (left) and alpha nuclides (right) of UNGG Moderator samples**

### 2.8.2.10 Validation and reference methods

In IP-CARBOWASTE a proficiency test on radiological characterization of i-graphite were performed among the members of WP3 with analytical abilities used in routine.

CIEMAT organised the proficiency test called CW-Round Robin Test and evaluate the data supplied by 11 labs (Fz Jülich (D), CIEMAT (S),CEA-CADARACHE (F), CEA-SACLAY (F), ENEA(IT), FTMC (LI), INR (RO), NRG (NL), SCK•CEN (B), SUBATECH (F) and UoM (UK).

The CW-RRT aimed to identify the stronger and the weaker points in order to establish the continuous improvement lines of every lab and to establish new analytical procedures for i-graphite characterisation. Another additional objective is the harmonisation of inventory determination within EU in order to increase the confidence in the nuclides determination in the whole life cycle of i-graphite from retrieval to final disposal.

The results are presented and discussed by nuclide and by Lab along the five nuclides studied: H-3, C-14, Cl-36, Co-60, Ni-63 and Sr-90 based on the analytical methodologies described in the “CW-Cook-Book”<sup>7</sup>, in Figure 2.8.10 the whole flow-chart with the summary of <sup>14</sup>C methodologies is plotted and the quote in the statistical evaluation.

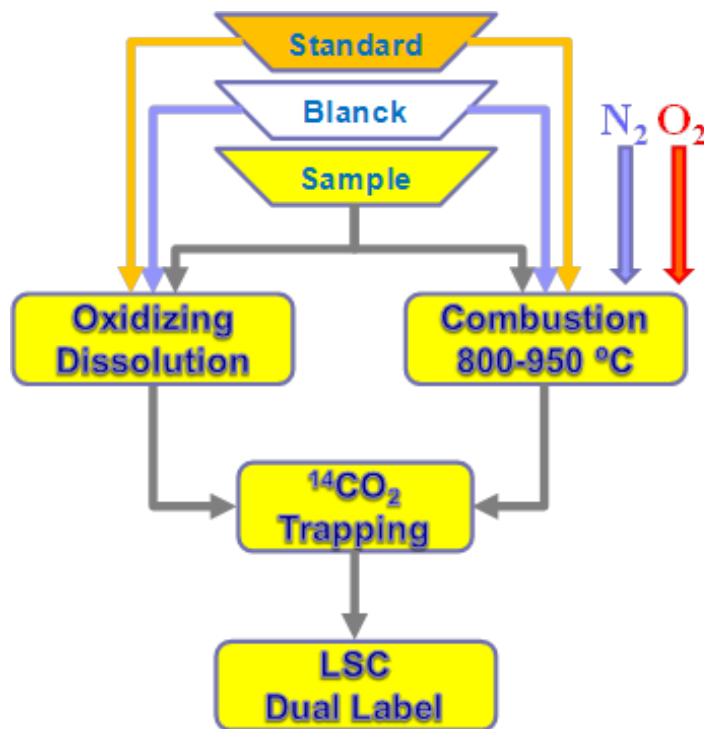


**Figure 2.8.10 Flow-chart of methods for <sup>14</sup>C determination**

The results of C-14 were the ones in the Figure 2.8.11 and the q-score evaluation (relative difference vs reference values and u-score (statistical evaluation regarding t-student distribution) are in Figure 2.8.12.

<sup>7</sup> Piña, G., Rodriguez, M., Vulpius, D., Comte, J., Brennetot, R., Dodaro, A., Duskeas, G., Brune, C., Visser – Tynova, E., Van Hecke, K., Landesman, C. and Jones, A. CARBOWASTE T-3.1.6 Topical Report on Characterization Methods, 2013.

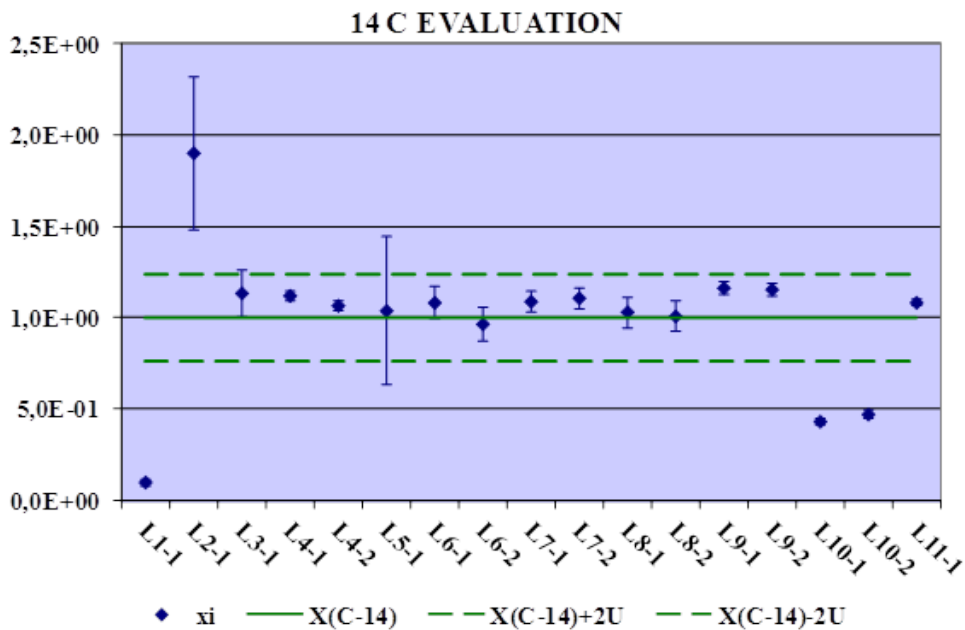


Figure 2.8.11 Results of <sup>14</sup>C determination

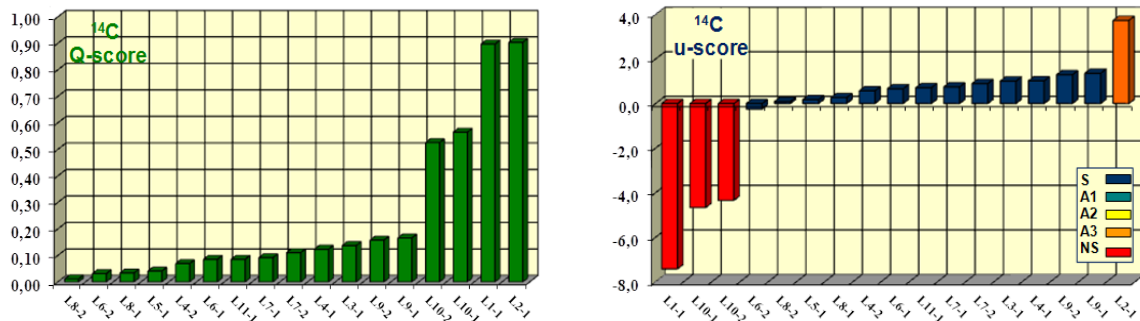


Figure 2.8.12 Statistical evaluation of <sup>14</sup>C determinations by q-score(left) and u-score (right)

### 2.8.3 Structural Characterization on i-graphite

X-ray diffraction, diffraction laser and physisorption techniques were used to obtain the structure in crystals and also microstructural information of the material (Cobos et al., 2013).

The broadening of diffraction lines occurs for three categories:

1. **Intrinsic profile** The intrinsic profile results of the absorption of a photon in a perfect crystal.
2. **Instrumental contribution** depends on the instrumental arrangement
  - a. The “parafocusing condition” (out of focus) in the Bragg-Brentano geometry. The usually arrangements use a flat specimen tangent to the focusing circle. This produces a small asymmetry in the profile.
  - b. Sample Transparency. Causes an asymmetry in the profile, particularly at the lowest angles.
3. **Physical sample effects** can be divided into crystallite size (diffraction order independent) and micro strain (diffraction order dependent).

A crystallite size is a domain of solid-state matter that has the same structure as a single crystal. The information about the crystallite sizes and or micro strain is extracted by the analysis of profile parameters in X-ray patterns.

Size analysis using profile gives the crystallite size which is not directly comparable with results from other techniques. Method such as laser granulometry, BET or Electron Microscopy (SEM) determine particle size, a parameter not directly related to crystallite size. A particle can be made of several crystallites. The analysis of crystallite size of graphite samples was the target of this work.

Methods were applied to domestic irradiated graphite samples and samples from abroad.

### 2.8.3.1 X-ray Diffraction (XRD)

The XRD analyses were performed after system pre-calibration procedure, as followed:  $2\theta$  are calibrated using 11 peaks from the external standard material Silicon (Ref. ICDD 27-1402). The peak positions of the internal standard phase were compared to their theoretical values and a polynomial curve is calculated which describes the aberrations in  $2\theta$ .

This allows correcting graphite samples diffractions patterns for angular aberrations as sample transparency or displacement of specimen surface against the reference surface of the diffractometer. Microstructural characterizations of the materials involve among other the amount of the phases in the sample, crystallographic parameters, the crystalline size and

stress. An observed diffraction line is the result of the convolution of a number of independent factors, some symmetric and some asymmetric.

Crystallite size is a measure of the size of a coherently diffracting domain. The analysis of crystallite size is based on the integral breadth of the diffraction lines, and gives the apparent dimension in the direction parallel to the diffraction vector. The structural broadening of the sample needs the elimination of instrumental broadening effects, recording a standard specimen.

The standard specimen to obtain the instrumental resolution function used to evaluate the instrumental resolution function using the optical instrumental arrangement. This material should not present micro-strain or size broadening.

Graphite crystallites have a large a-direction, and a small c-direction one. The c-direction size can be obtained from (0 0 1) peak. However, a-lattice size is obtained from an (h k 0) peak.

At lower - upper symmetric angle the space is higher due the system geometry. This reason makes that at upper angles is necessary to increase the measurement time in order to get enough data to increase the statistical data accuracy. Considering crystal system for the graphite case:

- Crystal system:Hexagonal
- Space group:P63/mmc
- Space group number:194

In Table 2.8.4 is shown Crystallographic Parameters performed with correction of the internal Si standard and samples The crystal size has been calculated from the Scherrer equation using the (004) to Lc and (110) to La. The crystal system for graphite is shown in Figure 2.8.13; original spectra of SLA2-65 and 634-2-4-3 are shown in Figure 2.8.14.

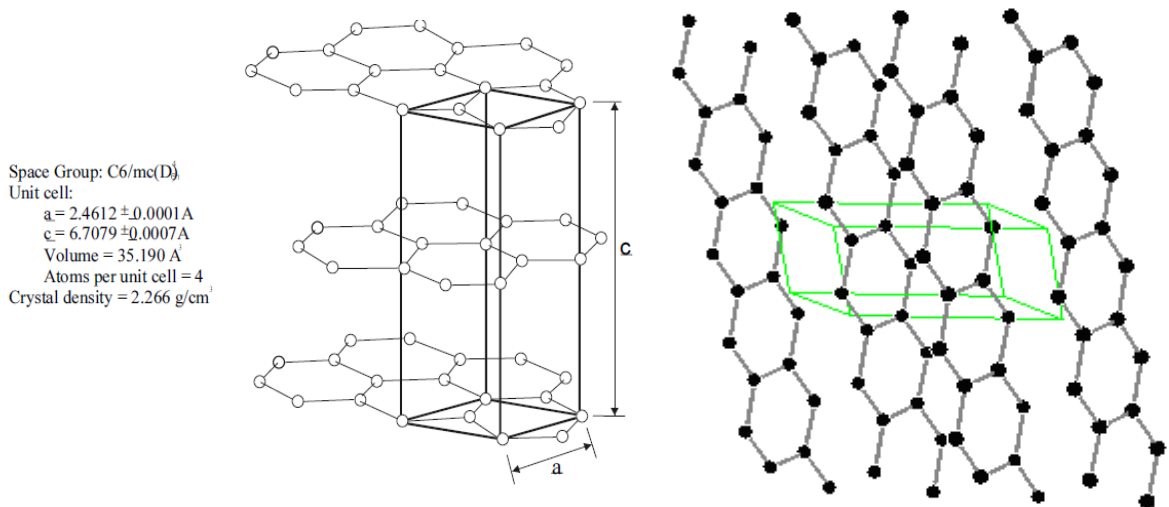


**Figure 2.8.13 Crystal system for the graphite**

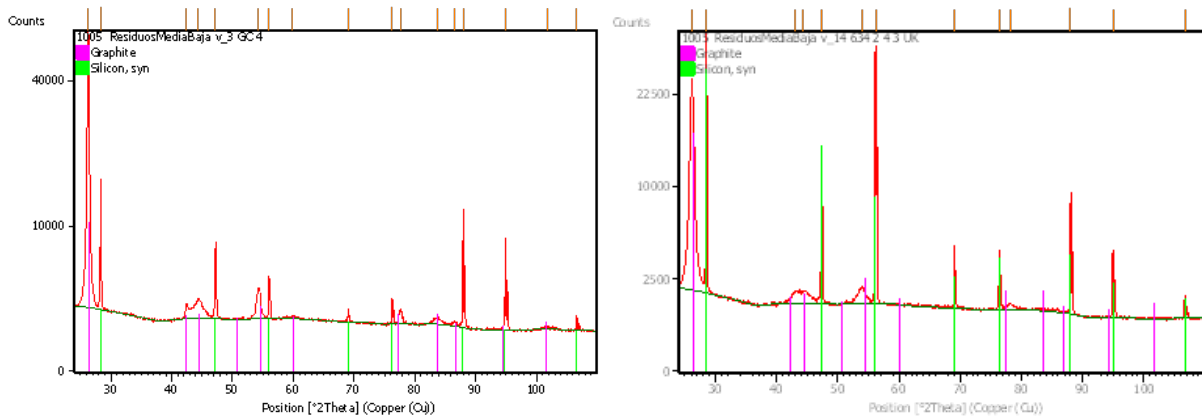


**Figure 2.8.14 XRD result of UNGG sample (left) and Magnox sample (right) (internal Si standard) Graphite Crystallographic parameters**

**Table 2.8.4 Crystallographic parameters over 15 samples.**

Ref. Sample	Nº	a=b [Å]	c [Å]	V [Å <sup>3</sup> ]	r <sup>2</sup>	L <sub>c</sub> (004) [Å]	L <sub>a</sub> (110) [Å]
Virgen V-1 1	1	2.4613	6.7288	35.305	1.00	182.3	506.8
Virgen V-1 2	2	2.4614	6.7226	35.291	0.99	220.9	568.9
GC-4 (grano fino)	3	2.4572	6.7461	35.275	0.98	119.5	213.3
Virgen INR	4	2.4609	6.7222	35.267	0.99	371.5	1062.1
i-INR	5	2.4610	6.7260	35.280	0.99	282.0	650.1
SLA2-63	6	2.4586	6.7404	35.287	0.98	119.5	213.3
SLA2-65	7	2.4581	6.7426	35.284	0.98	116.9	193.3
SLA2-71	8	2.4584	6.7547	35.356	0.99	99.4	118.1
SLA2-76	9	2.4540	6.75476	35.230	0.98	97.6	164.3
SLA2-79	10	2.4606	6.7338	35.309	0.99	178.1	461.4
Virgen JEN-1	11	2.4613	6.7219	35.268	1.00	352.1	857.7
JEN-1	12	2.4619	6.7285	35.317	0.99	210.0	648.0
634-2-4-2	13	2.4483	6.8052	35.327	0.98	53.8	82.2
634-2-4-3	14	2.4469	6.8112	35.320	0.98	73.6	49.6
676-4-1	15	2.4477	6.8027	35.299	0.98	55.3	59.4

### Particle size distribution

The diffraction laser equipment is a MALVERN series 2600. Particle size distribution has been obtained by suspending the powder in ethanol. The lens used for the analysis is a 63mm one (allows characterizing 1-150 μm particle sizes). The number of measurements done for each of the samples was fixed up to 15,000 interactions<sup>8</sup>. Five replications were carried out.

<sup>8</sup> The laser beam interferes in the sample 15000 times per measurement in order to extract the distribution of the particle size in the replicant.

### **2.8.3.2 Specific surface analysis**

Physisorption equipment is an ASAP-2020 from Micromeritics. All of the samples were pre-treated with a previous measurement thermal program (up to 150°C) to clean the pores to facilitate the adsorption process. After the heating and evacuation processes, pores are ready to be characterized. The evacuation rate was 10 mm Hg's<sup>-1</sup> for 30 minutes, before the heating phase, with a temperature ramp from 10 to 100°C for 60 min. The pressure was 100 mm Hg during the pre-treatment. The adsorbate was N<sub>2</sub> (following ISO 12800E). The complete isotherm is reduced to an isotherm piece (between 0.05 and 0.3 P/P<sub>0</sub>) indicated for the BET surface area measurement.

### **2.8.3.3 Discussion of Results**

Due to the very high transparency of the samples, the use of silicon as an internal standard, to correct the deviations of the diffraction patterns due to the transparency of the graphite, improves the results obtained in relation to the use of Bragg Bretano geometry for calculations of structural parameters. Therefore the method used (internal silicon standard) is the suggested mode for the optimum diffraction analysis for irradiated graphite.

Taking into account the results aforementioned it is possible to plot a dependence of the specific surface area versus the particle size distribution of each sample (Figure 2.8.15). The samples show a different specific surface area values for similar particle size. Probably this behaviour could be related to different parameter, like as: lattice size, thermal treatment, fracture behaviour (cleavage) related to irradiation history.

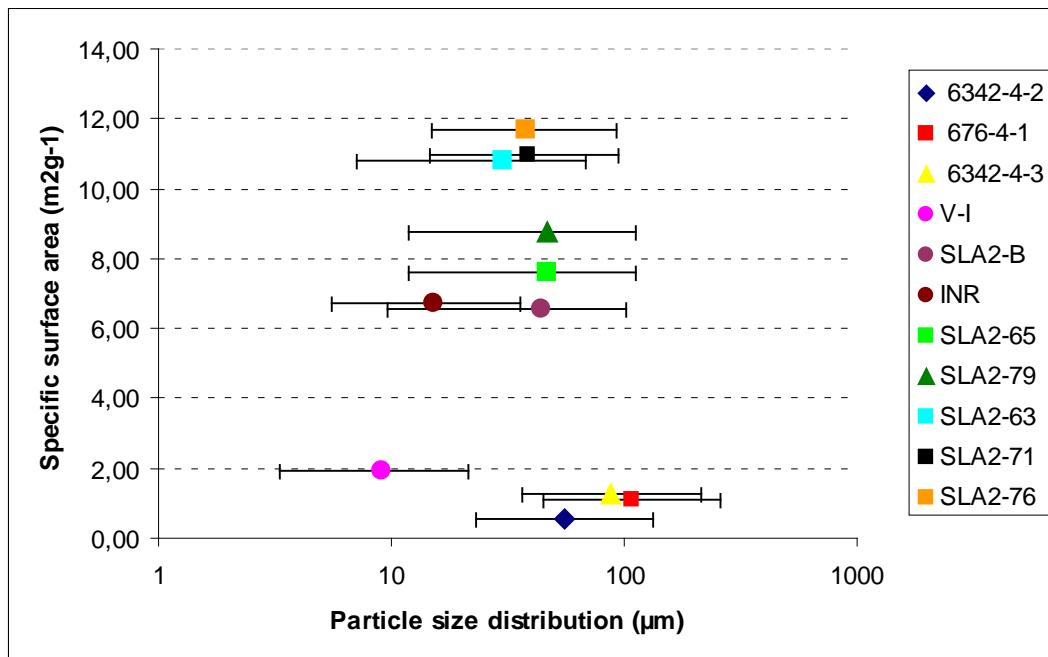


**Figure 2.8.15** Dependence of the specific surface area versus the particle size distribution of each sample.

## 2.8.4 Organic Molecules contents

An earlier study on speciation of virgin graphite was performed using different thermal and analytical techniques [Piña, G. et al. CARBOWASTE T-3.5.1, 2013]; this presents a basic understanding of the techniques to be used in CAST.

Hydrogen in graphite can be found in three forms as water, as gaseous H<sub>2</sub> or as heteroatom bounded to the graphite structure, possibly as a part of hydrocarbon. To determine the content and the location of these three forms two procedures were used: Thermal decomposition and solvent extraction.

### 2.8.4.1 Thermal decomposition extraction

In general terms this procedure is based on heating in a determined sequence the graphite in inert or oxidizing atmospheres in order to break or decompose the lighter structures in it. The decomposition products can be detected by different techniques.

When atmosphere is oxidizing the carbons react to form CO<sub>2</sub> and CO and hydrogen is oxidized to H<sub>2</sub>O, breaking some chemical structures by oxidation effect. When the atmosphere is inert the free molecules at treatment temperature are released without transformation or reacting with the molecules chemisorbed in the surface. In oxidizing atmosphere from 450° C the combustion starts and the graphite is corroded.

The thermal decomposition and the analysis of the reaction products were carried out by different methods

### **Thermo gravimetry and DSC**

Twenty grams of reflector graphite powder (60-100 µm) was used for thermal treatment in the holder of a CI Instruments thermo-balance. In N<sub>2</sub> atmosphere (60 ml/min) the graphite was heated in 20°C steps to 900°C, and then maintained for 1 hour. The gases were measured connecting the thermo-balance to a Gas Chromatograph –MS VG quadrupole.

In the detection of volatile materials by thermo-balance connecting to a GC-MS for a ≈0.35 g of graphite, the mass lost detected during the heating process was ≈7E-4 g. This mass from volatile materials during 20 minutes of experiment duration gives a weak signal which was not possible to evaluate. However it was possible to determine in function of the desorption temperature in the thermo-balance and similar results were obtained by Differential Scan Calorimetry (DSC)

### **Mass Lost by heating**

The mass lost by heating was performed heating in N<sub>2</sub> atmosphere. Taking into account that the hydrogen content of graphite must be very small, the first assay performed was the mass loss of relatively large amount of graphite by volatile material release when it is heating. Additionally the sample must be as a powder in order to facilitate the volatile release.

Two samples (2.5 g of powder (60-100 µm) sample of graphite from reflector and 2.5 g of powder (60-100 µm) graphite from sleeves) were placed for heating in an horizontal tube furnace at 900 °C during 3 hours in a N<sub>2</sub> flux of 80 l/min and a heating rate of 10° C/min.

After cooling to 100° C inside the furnace, the samples were placed in a desiccator until they had cooled to room temperature. In this condition the mass loss is determined.

A small amount of mass loss in the order of 0.20 % in graphite from reflector and 0.18 % in graphite from sleeve was detected.

### **Controlled Thermal Desorption-IR spectrometry analysis**

The controlled thermal decomposition were carried out on powder samples in a furnace LECO that allows to maintain a pre-programmed slope of heating between room temperature and 1500°C. The released gases are analyzed by IR spectrometry that allows determining the CO<sub>2</sub> and H<sub>2</sub>O generated in the treatment. The furnace can be maintained at different atmospheres inert (N<sub>2</sub>) and oxidizing (O<sub>2</sub>). When the atmosphere is inert only the water content and the CO<sub>2</sub> absorbed in the graphite (probably some amounts from the reaction of the O<sub>2</sub> absorbed with the carbon of the structure) are measured. When the atmosphere is oxidizing CO<sub>2</sub> and H<sub>2</sub>O resulted from the oxidation of the extracted molecules is also measured.

By this procedure is detected:

- In inert atmosphere to 1000°C, CO<sub>2</sub> and H<sub>2</sub>O absorbed as gasses.
- In oxygen atmosphere to 450°C, hydrocarbon compounds
- In oxygen atmosphere >450°C, free H<sub>2</sub> or undefined bounded (probably bonded in a hydrocarbon molecule).

The analysis in inert atmosphere (N<sub>2</sub>) shows that the absorbed water is released between 20 and 150°C, being lower and constant for higher temperatures.

Coincidence detection in the simultaneous analysis of water and CO<sub>2</sub> was registered that can be attributed to the chemisorbed CO<sub>2</sub> or chemisorbed O<sub>2</sub> that reacts with the available carbon present.

The CO<sub>2</sub>/H<sub>2</sub>O mass ratios in the first two temperature regions are lower than hydrocarbon compounds (Table 2.8.5); this could be caused by the existence of adsorbed H<sub>2</sub>O. In the

third temperature region (130-450°C) the CO<sub>2</sub>/H<sub>2</sub>O ratio increases to about one, which corresponds to saturated hydrocarbon compounds with 2-4 C atoms. However, desorption temperatures are higher than boiling points of these substances that could be caused by the vapour pressure increment by pore system location of these compounds. On the other hand it is possible that another hydrocarbon compounds with higher CO<sub>2</sub>/H<sub>2</sub>O ratio were released and the signal was hiding below the low CO<sub>2</sub>/H<sub>2</sub>O signal.

**Table 2.8.5 C/H ratio in the products released by Thermal Desorption**

Temperature Range	CO <sub>2</sub> /H <sub>2</sub> O mass ratio	
	Sleeve Graphite	Reflector Graphite
0-100	0.030	0.02
100-130	0.110	0.20
130-450	1.003	0.98

It is observed, analysing in detail that there are specific desorptions at 130-133°C, 200-230°C and 300-330°C. It was also observed that carbon content in the hydrocarbon compounds desorption increases when the temperature is higher than 330°C.

It is deduced the existence of light hydrocarbon molecules that are released in a wide temperature range depending on the pore size and possible existence of heavier hydrocarbon compounds which are released at temperatures higher than 300°C.

### Flash Pyrolysis

Very high heating rate experiments (Flash Pyrolysis) were performed. In an inert atmosphere, approximately 2 mg of graphite from reflector was introduced in a Pyro-probe 1000, which allows heating the sample, by means of a platinum probe, to 900°C in a rapid way (20°C/ms); gas is observed practically instantly. The composition and the amount of hydrocarbon molecules were determined by gas chromatography with flame detector.

Flash pyrolysis was performed in order to concentrate the volatile material output. The analysis of the produced gases is expressed in weight% in Table 2.8.3. The expected uncertainty values are high due to the experimental set-up.

**Table 2.8.6 Hydrocarbons detected in the reflector graphite flash pyrolysis by Gas Chromatography**

Hydrocarbon Compound	Detected weight %
Methane	0.028
Ethylene/Acetylene	0.0055
Ethane	0.0052
Propylene	0.0043
Propane	0.0014
2-methy-propane	0.0033
Butylene/Butene	0.0027
<b>TOTAL</b>	<b>0.05</b>

The presence of light hydrocarbon compounds is remarkable, especially methane that is about double the %weight concentration of the other detected compounds combined. The molecular concentration in the gas release will be higher as the molecular weight is lower. The total fraction of released hydrocarbon compounds is calculated to be around 0.05 wt%.

#### **Controlled Thermal Desorption- GC-MS**

This procedure was used for determined the compounds released under 300° C.

An ATD-400 Perkin-Elmer apparatus with a desorption time of 5 minutes at 300° C was used. The extracted products are analysed quantitatively by Gas-Chromatography with a FID detector and MS in a 30-300 Da<sup>9</sup> range.

---

<sup>9</sup> Atomic mass unit(u) = Dalton (Da)

The attempt to identify the desorbed products by GC\_MS of the gases produced in the controlled thermal desorption (till 300°C) of powder Vandellós 1 virgin graphite detecting similar products than in the pyrolysis assay.

### **Thermo-gravimetry (TG) and Differential Scan Calorimetry (DSC)-IR Spectrometry**

A quantitative study by TG was performed on samples after they had been analysed by DSC-IR, to check for the presence of volatile hydrogenated. Samples used were standard powder (0.63 and 0.100 mm) and 8x6x4 mm blocks standardized from virgin sleeves of Vandellós 1.

### **Solvent Extraction**

Extractions with S<sub>2</sub>C were performed in a Soxhlet system during 24 hours from 20 g of graphite powder sample (60-120 µm) and the extraction products were analysed in a Gas Chromatograph system. Some samples were exposed at ambient before extraction in order to check the adsorption of volatile organic compounds.

By extracting the organic compounds with S<sub>2</sub>C, heavier molecules are detected than in the other methods (Table 2.8.7) because it is not an aggressive treatment and avoids bonds breaking.

**Table 2.8.7 Hydrocarbons detected by Gas Chromatography after extraction with S<sub>2</sub>C**

<b>Hydrocarbon Compound</b>	<b>% relative</b>
1-3 dimethyl nonane Benzene,	2.93
1-phenyl Ethanone	10.4
2-methyl Benzaldehyde	25.62
4-methyl Benzenemethanol	2.67
1-ethyl-4-(1-methylethyl) Benzene	5.91
1-3 dimethyl-5-(1-methylethyl) Benzene	10.14
1-4 dimethyl-2-(1-methylethyl) Benzene	14.69

## 2.8.5 Chemical Treatment by Inorganic Agents

The decontamination of graphite by chemical treatment with liquids agents depends on several factors like chemical composition of the leachant, temperature or the state of the graphite (block or powder).

### 2.8.5.1 Samples

CIEMAT studied the influence of several factors on the decontamination of i-graphite powder from sleeves of a UNGG reactor by chemical treatment with liquid agents and then the decontamination of i-graphite block.

Initial activity was characterised in a homogeneous sample of sleeve powder, the inventory of which is shown in Table 2.8.8.

**Table 2.8.8 Specific activity of UNGG samples used for leaching experiments**

<b>A<sub>0</sub> (Bq/g)</b>							
<sup>239/40</sup> Pu	<sup>241</sup> Am	<sup>94</sup> Nb	<sup>137</sup> Cs	<sup>154</sup> Eu	<sup>14</sup> C	<sup>60</sup> Co	<sup>3</sup> H
4.50E01	6.69E01	8.76E01	1.50e02	2.25e02	2.07e04	2.30e04	7.10e04

### 2.8.5.2 Leaching of <sup>3</sup>H and <sup>14</sup>C

The study of the decontamination of <sup>14</sup>C and <sup>3</sup>H in irradiated graphite powder was carried out with several leachants: 0.1M sodium hydroxide, 0.1M sodium hydroxide with hydrogen peroxide, 3M nitric acid and mixtures of nitric, hydrochloric and sulphuric acids. In all the experiments a mixture of 0.15 g of graphite powder and 5ml of solution was used (Figure 2.8.16).

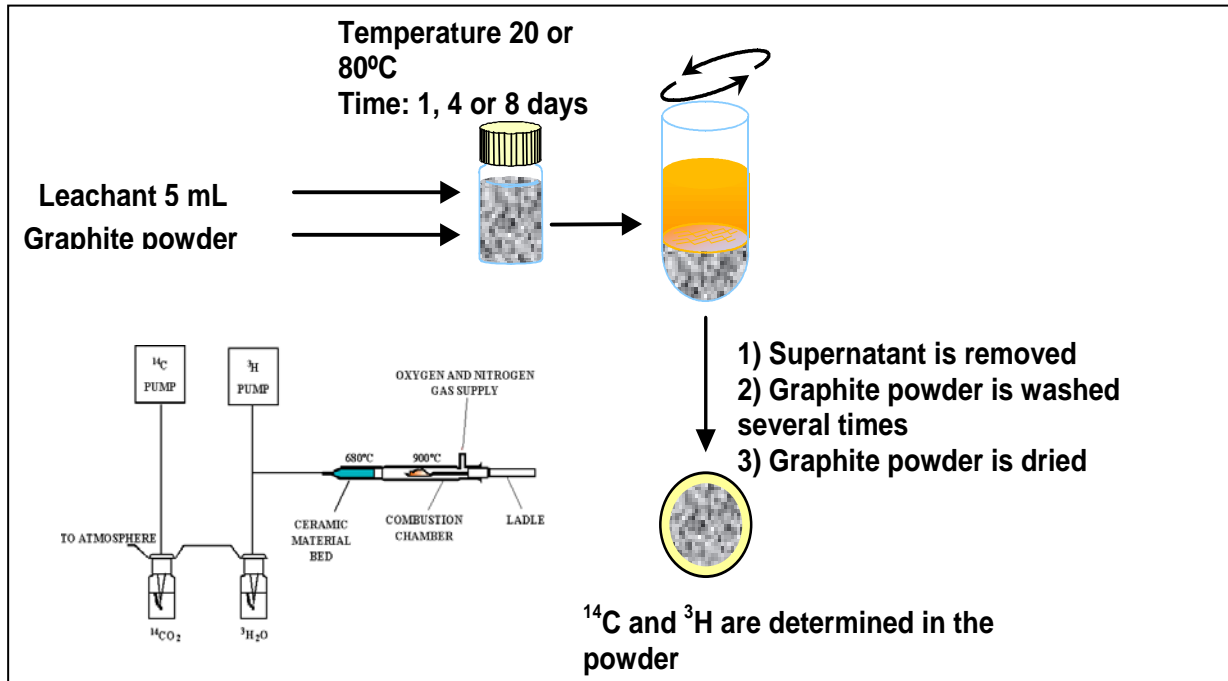


**Figure 2.8.16 Procedure for UNGG graphite sleeves leaching experiment**

The results are shown on Figure 2.8.17 and expressed as a % of the activity leached.

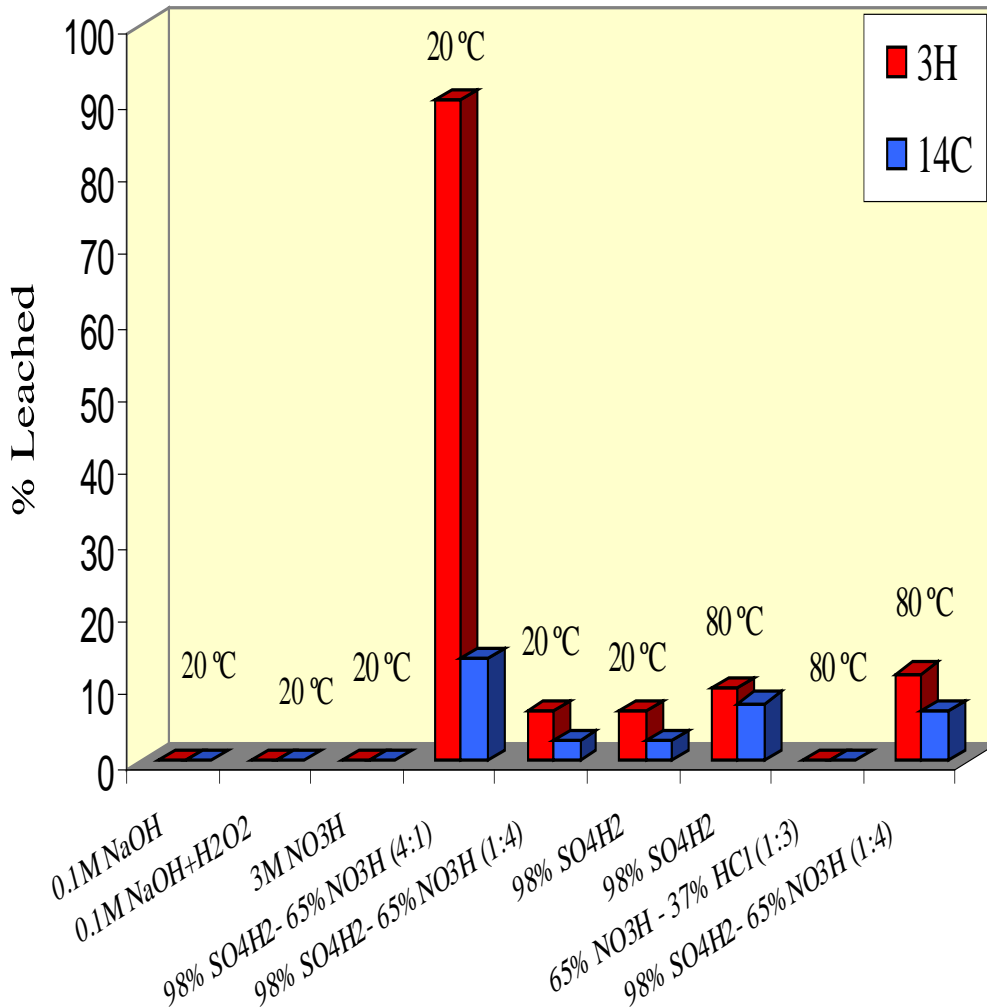


**Figure 2.8.17 Decontamination factors for UNGG graphite sleeves for <sup>3</sup>H & <sup>14</sup>C**

Neither <sup>14</sup>C nor <sup>3</sup>H are leached at all with 0.1M sodium hydroxide or a mixture of 0.1M sodium hydroxide and hydrogen peroxide at 20°C during 24 hours. The mixture H<sub>2</sub>SO<sub>4</sub> 98%-HNO<sub>3</sub> 65% (4:1) at 80°C dissolved the powder of graphite. The best results were obtained with the mixture H<sub>2</sub>SO<sub>4</sub> 98%-HNO<sub>3</sub> 65% (4:1) at 20 °C. This mixture leached both 90% of <sup>3</sup>H and 14 % of <sup>14</sup>C. Also, with this mixture the influence of the leaching time was studied. This study was carried out in the same conditions as before but with two different leaching time: 4 or 8 days. The results are shown on Figure 2.8.18.

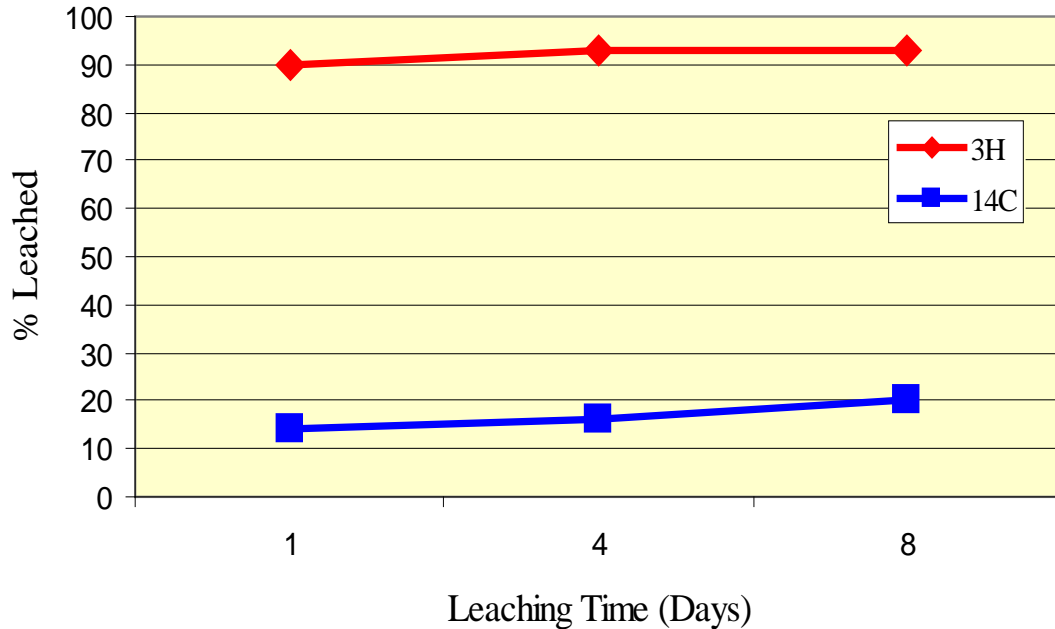


**Figure 2.8.18 Results obtained for the decontamination <sup>3</sup>H and <sup>14</sup>C in i-graphite powder (UNGG sleeves) at different leaching time in H<sub>2</sub>SO<sub>4</sub>/HNO<sub>3</sub> at 20 °C**

The results are similar to the ones obtained when the leaching time was one day. When the same procedure of leaching with H<sub>2</sub>SO<sub>4</sub>-HNO<sub>3</sub> (4:1) was applied six times repeatedly on the same graphite powder the decontamination for <sup>14</sup>C was 50% and 99% for <sup>3</sup>H but only 10 % of the graphite powder was recovered.

Finally, the stability of virgin graphite under the same conditions as the previous ones used for the leaching of irradiated graphite has been studied. The virgin graphite was dissolved with the mixture H<sub>2</sub>SO<sub>4</sub> 98%-HNO<sub>3</sub> 65% (4:1) at 80 °C while it was stable when it was treated with the mixture H<sub>2</sub>SO<sub>4</sub> 98%-HNO<sub>3</sub> 65% (4:1) at 20 °C. So the virgin graphite has the same behaviour as the irradiated graphite.

### 2.8.5.3 Leaching of beta-gamma emitters

Although beta-gamma emitters present in irradiated graphite are not really relevant to the behaviour of <sup>14</sup>C, studying them can provide additional information about the behaviour of this material. The decontamination of irradiated graphite powder has been studied with

several leachants: nitric, hydrochloric, phosphoric, sulphuric acids at different concentrations and their mixtures with citric and oxalic acids. In all the experiments a mixture of 0.15g of graphite powder and a solution volume of 5 mL was put into a vial and was shaken for 24 hours. Then, the mixture was centrifuged and the supernatant was removed and passed through a 0.20  $\mu\text{m}$  filter. The leaching procedure was carried out at three different temperatures 20, 60 and 80  $^{\circ}\text{C}$  and using different solutions. In all cases the filtrate was measured by high resolution gamma spectrometry. The results are shown in Figure 2.8.19.

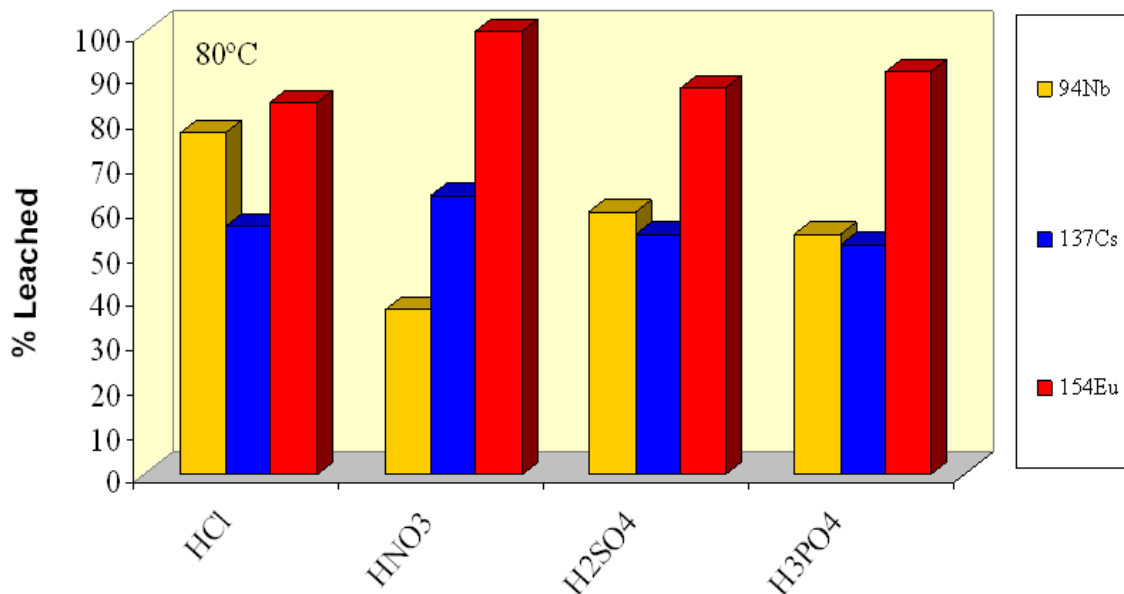


**Figure 2.8.19 Extraction of  $\beta$ - $\gamma$  emitters at difference acidic media**

For  $^{60}\text{Co}$ , the decontamination using either an acid dissolution of hydrochloric or nitric acid increases when the temperature does and the highest leaching, around 96%, is when the leachant is 3M hydrochloric acid solution and the temperature is 80 $^{\circ}\text{C}$ .

For Nb, Co and Cs the percentage of leaching decreases when the leachant is oxalic acid alone or a mixture with another acid. The highest leaching for Nb is about 77% when 3 M chlorhidric acid at 80  $^{\circ}\text{C}$  is used. For Cs the leaching is between 52 and 63 % for any acid medium at 80  $^{\circ}\text{C}$  and the percentage decreases to 40 % in presence of oxalic acid.

The highest percentage of leaching for Eu is using either dissolution of 3M nitric acid at 80 °C, dissolution of 0.5M citric acid or a mixture of 0.5M citric acid with any acid at 20 °C.

Another study has been carried out using either 0.5 M citric acid, 0.5 M oxalic acid or their mixtures with 3M nitric, hydrochloric, phosphoric and sulfuric acids.

The decontamination of Co increases when either 0.5M oxalic acid or 0.5M citric acid is added to any 3M acid solution at 20°C. The highest percentage of leaching for Co, 32%, is when the leachant is a mixture of 0.5M oxalic and 3M chlorhidric acid at 20 °C.

For Nb the percentage of leaching decreases when the leachant is either oxalic, citric acid or their mixture with another acid. In the case of Cs the decontamination is less influenced by the presence of either oxalic or citric acid.

#### 2.8.5.4 Alpha Emitters

Studies on alpha emitters are undertaken by CIEMAT because of the relevance for the management of low and intermediate level waste in a near surface repository. Experimental conditions for performing a leaching test for alpha emitters decontamination are already explained in the method of CIEMAT for beta-gamma decontamination process, being the measurement in the case of alpha emitting nuclides by alpha spectrometry.

The leaching of Am and Pu with any acid solution increases when the concentration decreases. On the other hand, the leaching of both increases when the temperature does within the range of temperatures and concentrations studied. The best conditions for the leaching of Am, 100%, are with any 3M acid solution at 80 °C. The best result for the decontamination of Pu, 94%, is when the leaching is carried out with 3M H<sub>2</sub>SO<sub>4</sub> at 80 °C.

Results obtained for the decontamination of <sup>239,40</sup>Pu using as leachant either 0.5 M citric acid, 0.5 M oxalic acid or their mixtures with 3M nitric, hydrochloric, phosphoric and sulphuric acids at 20°C shows in Figure 2.8.20, demonstrate that the decontamination of Pu increases when 0.5M oxalic acid is added to any 3M acid solution at 20°C. The highest percentage of leaching for Pu, 84%, is when the leachant is a mixture of 0.5M oxalic and 3M phosphoric acid at 20 °C.

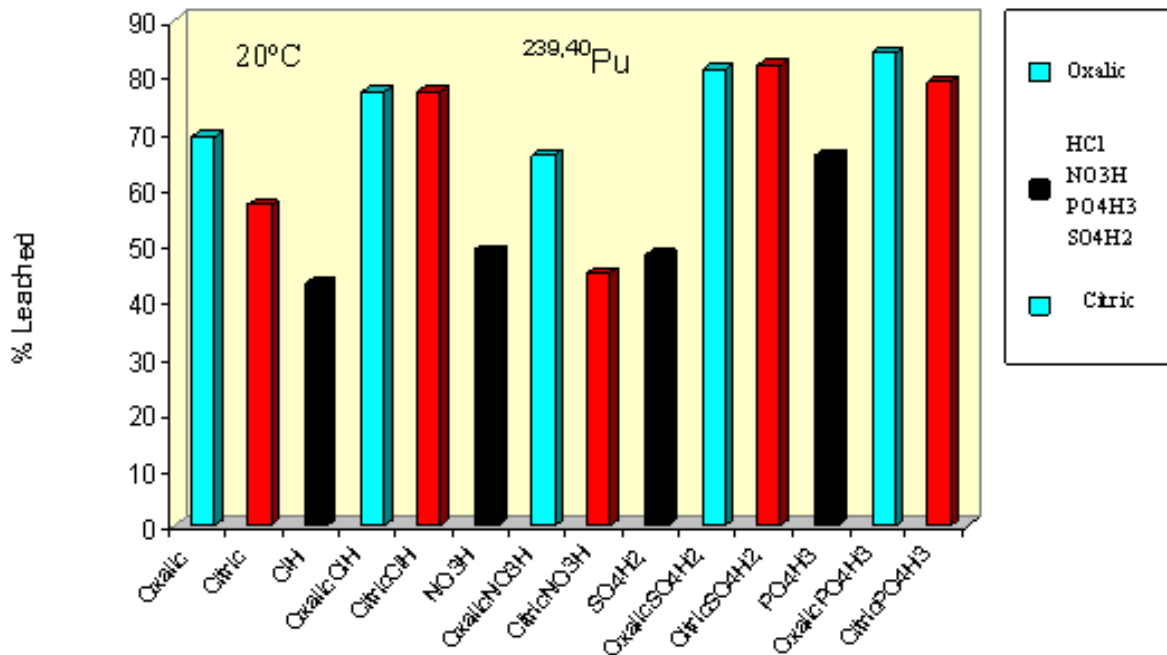


Figure 2.8.20 Extraction of  $^{239,40}\text{Pu}$  emitters in oxalic and citric acids and their mixture with different inorganic acids

### 2.8.5.5 Intercalation process

An experiment was carried out to study the leaching of a virgin graphite block with a solution of  $\text{H}_2\text{SO}_4:\text{HNO}_3$  (4:1). When a 0.7 g virgin graphite block was put into a vial with 5 mL of a mixture of  $\text{H}_2\text{SO}_4:\text{HNO}_3$  (4:1) the block broke down into powder. In Figure 2.8.21 is shown the virgin graphite block and graphite powder obtained after the treatment with the mixture  $\text{H}_2\text{SO}_4:\text{HNO}_3$  (4:1).



**Figure 2.8.21 Graphite block before (left) and after (right) treatment**

The powder was washed with water until both sulphuric and nitric acids were removed. After several washings the water was analysed by ion exchange chromatography in order to check the presence of sulphate or nitrate. The recovery of graphite powder was about 98 %. An examination of the structure for both the virgin graphite block and the virgin graphite powder was carried out by SEM. The images are shown on Figure 2.8.22

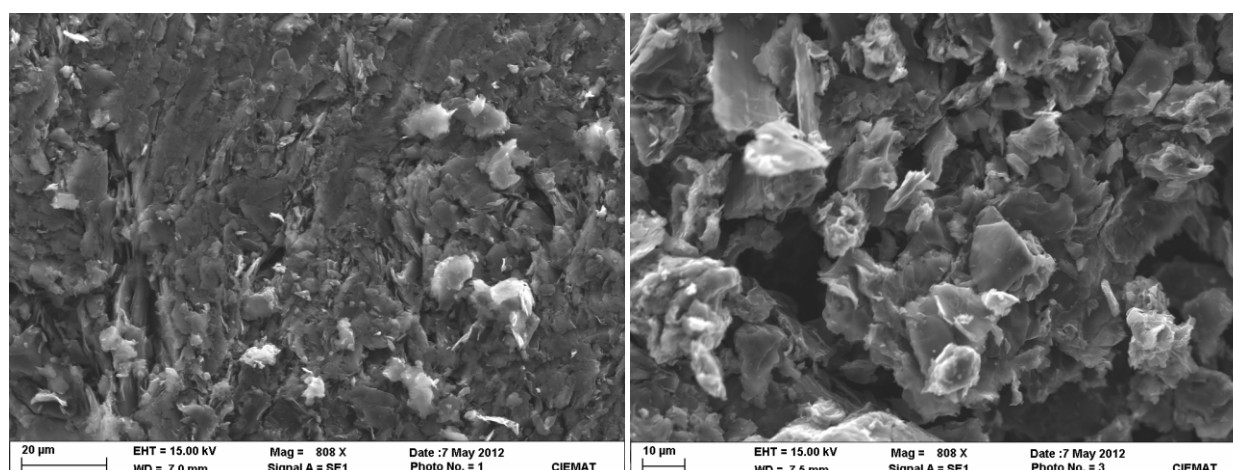


**Figure 2.8.22 SEM images of a virgin graphite block (left) and its powder after treatment (right)**

## **2.9 Radioactive Waste Management (RWM) summary**

### **2.9.1 Introduction**

RWM has been carrying out a range of research and assessment studies to improve the understanding of carbon-14 behaviour in a geological disposal facility (GDF), specifically the likelihood of a free (bulk) gas phase forming and its consequences for calculated risks. The findings of those ongoing studies are summarised elsewhere [NDA, 2010a; NDA 2012].

Carbon-14 is present in many of the waste materials that will be emplaced in a GDF, particularly irradiated graphite, irradiated metals and spent fuel. The half-life of carbon-14 is 5,730 years, which is much less than some other radionuclides. If it is contained within a multi-barrier disposal system for a sufficiently long time (e.g. by a long-lived high integrity container), then it will decay and cause no significant radiological risk within the timescales considered in safety assessments.

Work performed as part of the UK research programme on geological disposal over several years has shown carbon-14 to be a key radionuclide in the long-term safety assessment for a GDF. In particular, the consequences of a carbon-14 bearing gaseous phase forming in a GDF were recognised in the generic disposal system safety case (DSSC) [NDA, 2010b]. Free gas (bubbles) if formed in sufficient quantity have the potential to escape rapidly from the water-saturated near-field of a GDF, migrate through the geosphere and be released to the accessible environment. Therefore, trace gases containing carbon-14 could, for example, be transported in a bulk hydrogen gas phase formed from metal corrosion. This may potentially occur much faster than dissolved species can be transported the same distance in groundwater, and before decay can significantly reduce the concentration of carbon-14. As discussed below, irradiated graphite is the major contributor to the inventory of carbon-14 that may be disposed to a GDF in the UK.

## **2.9.2 The Inventory of Carbon-14 in irradiated graphite in the UK Radioactive Waste inventory**

The current best estimate total inventory of carbon-14 likely to be disposed to a GDF in the UK is 17,770 TBq (Table 2.9.1), based on the derived 2013 UK Radioactive Waste Inventory (UKRWI) that includes wastes from a potential new build programme of reactors in the UK [ADEOGUN, 2014]. Irradiated graphite contributes about 40% of this total inventory of carbon-14.

Most carbon-14 is produced by the  $^{13}\text{C}(n,\gamma)^{14}\text{C}$  and  $^{14}\text{N}(n,p)^{14}\text{C}$  reactions in the graphite cores of Magnox reactors and Advanced Gas-cooled Reactors (AGRs). About 60% of the carbon-14 generated is produced by interaction with the nitrogen impurities and 40% by interaction with the carbon-13 in the graphite [NDA, 2012]. The graphite cores of research and prototype reactors at Sellafield and Harwell, as well as graphite from the dismantling of Magnox and AGR fuel elements give rise to much smaller quantities of carbon-14.

Core graphite remains in the reactor during care and maintenance, and will arise as waste during final reactor decommissioning. There are five types of graphite used in nuclear reactors in the UK:

- a) Piles Grade A (PGA) and Piles Grade B (PGB): which are produced from the same raw materials by essentially the same process, but small differences in manufacturing conditions result in PGB having a lower density. PGA graphite is used for the Magnox moderator graphite and PGB is used for Magnox reflector graphite.
- b) Gilsocarbon: which is used in AGR cores, and is manufactured from artificial graphite made from Gilsonite coke.
- c) VFT and Nittetsu: which are used in AGR fuel element sleeves and struts pre-1990 and post-1993 respectively.

Characterisation of radioactive graphite waste is complicated because there are many variables affecting nuclear plant design and operational conditions. The wastes contributing

to carbon-14 in graphite in the 2013 UK Derived Radioactive Waste Inventory [ADEOGUN, 2014] are grouped as follows:

- a) ILW core graphite (Magnox, AGR, Sellafield, Harwell);
- b) ILW AGR fuel assembly graphite;
- c) ILW Magnox fuel element graphite; and
- d) Other wastes LLW core graphite.

Table 2.9.1 shows the contribution of these irradiated graphites to the total UK inventory of carbon-14 expected to be consigned to a GDF in the UK.

Core graphite in both AGR and Magnox reactors lose mass due to oxidation during reactor operating lifetimes. The extent of the loss depends on the reactor design and operating conditions including lifetime power output. Graphite weight loss will be less in Magnox reactor cores compared to AGR cores.

The loss of graphite affects the carbon-14 content in two ways. First, any carbon-14 associated with graphite is lost to the gas coolant when that portion of the graphite core is oxidised. Second, the precursor nitrogen is also lost, so the bulk carbon-14 generation rate is progressively reduced over time. Carbon-14 lost to gas coolant by graphite corrosion is assumed to be discharged relatively quickly as a result of coolant leakage or blowdowns.

Calculations of the carbon-14 activity reported in the 2013 UKRWI take no account of the loss of graphite by corrosion. The impact on the total carbon-14 inventory would be broadly proportionate to the amount of graphite lost by corrosion, which could vary from as little as 5% to more than 20% of mass. The Office of Nuclear Regulation (ONR) has set regulatory limits on graphite loss for UK AGRs that range from 8 % (Dungeness B) to 17 % (Hartlepool) [EDFE, 2014].

**Table 2.9.1: UK Carbon-14 Inventory in the 2013 Derived Inventory**

Category – Waste stream group	Carbon-14 Activity at 2200 (TBq)
<i>Magnox ILW core graphite</i>	4,210
<i>AGR ILW core graphite</i>	2,490
<i>Sellafield ILW core graphite</i>	174
<i>Harwell ILW core graphite</i>	7
<i>ILW AGR fuel assembly graphite</i>	45
<i>ILW Magnox fuel element graphite</i>	2
<i>LLW core graphite</i>	2
Graphite total	6,930
Steels	7,080
Reactive metals	114
Spent fuel	3,290
Other wastes	307
Total carbon-14 inventory (to 3SF)	17,700

## 2.9.3 Leaching studies of carbon-14 release from irradiated graphites

### 2.9.3.1 Introduction

Although leaching studies of irradiated graphite have been undertaken for over 30 years, a comprehensive analysis methodology has yet to be developed that would enable discrimination and quantification of both inorganic and organic carbon-14 releases to both gas and solution phases. Some identification and differentiation of the carbon-14 species produced has been achieved (as for example:  $^{14}\text{CO}$ ,  $^{14}\text{CO}_2$ ,  $^{14}\text{C}$ -carbonate, volatile  $^{14}\text{C}$ -hydrocarbons/organic compounds or soluble  $^{14}\text{C}$ -organic compounds).

Carbon-14 releases to the gas phase are dependent on the water chemistry, and increase significantly as the pH is lowered. Under near-neutral and acidic conditions, a significant fraction of any carbon-14 released as  $^{14}\text{CO}_2$  may partition into the gas phase. In contrast, under high-pH conditions, carbon-14 releases to the gas phase would be significantly smaller and thus require more sensitive and accurate methods to be applied to capture and then measure the carbon-14 released. Under high-pH conditions, the majority of any  $^{14}\text{CO}_2$  released would be expected to remain in solution as carbonate or to precipitate (e.g. as calcium carbonate).

The scope of published experimental studies on graphite leaching is summarised in Table 2.9.2.

The UK understanding of the release of carbon-14 from irradiated graphite has been developed from experiments carried out as part of the RWM research programme and from work carried out elsewhere. This is discussed in the remainder of this section.

**Table 2.9.2: Summary of Irradiated Graphite Leaching Experiments for Measurement of Carbon-14 Release to Solution and /or Gas**

Study	Graphite	Form of sample (no. of tests)	Conditions	Durations	Solution analysis	Gas phase analysis
WHITE et al, 1984	Magnox (reactor unspecified)	Monolith (4)	Oxic, near-neutral pH	150 days	Discrimination unclear	None
GRAY & MORGAN, 1988	Hanford C	Monolith (5)	Oxic, near-neutral pH, T=25, 50, 90°C	56 days	Total C-14 <sub>(aq)</sub>	None
GRAY & MORGAN, 1989	Marcoule G2 (UNGG)	Monolith (3)	Oxic, near-neutral pH	91 days	Total C-14 <sub>(aq)</sub>	None
TAKAHASHI et al, 2001	Tokai (Magnox)	Unclear (6)	Alkaline, redox conditions unclear	720 days	Discrimination unclear	None
ISOBE et al, 2007, 2008a,b, 2009	Tokai (Magnox)	Powder (5)	Anoxic, alkaline	1460 days	<sup>14</sup> CO <sub>3</sub> <sup>2-</sup> <sub>(aq)</sub> , <sup>14</sup> C-organics <sub>(aq)</sub>	None
BASTON et al 2006	WAGR	Powder (1)	Oxic, Ca(OH) <sub>2</sub> solution	14 days	None	Total C-14 <sub>(g)</sub>
HANDY, 2006	WAGR	Monolith (1), Powder (1)	Oxic, Ca(OH) <sub>2</sub> solution	127 days	Total C-14 <sub>(aq)</sub>	<sup>14</sup> CO <sub>2(g)</sub> , ( <sup>14</sup> CO+ <sup>14</sup> C-organics) (g)

**Table 2.9.2: Summary of Irradiated Graphite Leaching Experiments for Measurement of Carbon-14 Release to Solution and /or Gas**

Study	Graphite	Form of sample (no. of tests)	Conditions	Durations	Solution analysis	Gas phase analysis
MARSHALL et al, 2011	BEP0	Monolith (1)	Oxic, pH 13	431 days	For final sampling only: total C-14 <sub>(aq)</sub> and possible 14C-organic <sub>(aq)</sub>	( <sup>14</sup> CO+ <sup>14</sup> CO <sub>2</sub> ) <sub>(g)</sub> , <sup>14</sup> C-organics <sub>(g)</sub>
McDERMOTT, 2011	BEP0	Powder (multiple), Monolith (6)	Oxic, pH 13, water, oxidants and acids	85 days and 190 days	Total C-14 <sub>(aq)</sub>	None
	Wylfa (Magnox)	Granulated (8)	Oxic, pH 13, water, oxidants and acids	190 days		
BASTON et al., 2014	Oldbury (Magnox)	Monolith (6)	Anoxic, pH 13 (1)	372 days	Total C-14 <sub>(aq)</sub>	<sup>14</sup> CO <sub>2(g)</sub> , <sup>14</sup> CO <sub>(g)</sub> , <sup>14</sup> C-organics <sub>(g)</sub>
			Anoxic, pH 13 (2)	366 days	Total C-14 <sub>(aq)</sub> for final sampling only	
			Anoxic, pH 7 (1), Anoxic, pH 13, 50°C (1) Oxic, pH 13 (1)	91 days	None	
		Powder (1)	91 days	Total C-14 <sub>(aq)</sub> for final sampling only		

**Table 2.9.2: Summary of Irradiated Graphite Leaching Experiments for Measurement of Carbon-14 Release to Solution and /or Gas**

Study	Graphite	Form of sample (no. of tests)	Conditions	Durations	Solution analysis	Gas phase analysis
VENDÉ, 2012	St Laurent A2 (UNGG)	Powder (6) [0.35 to 1.5g]	Anoxic, pH 13 (2)	821 days	Total C-14 <sub>(aq)</sub> only	None
			Anoxic, pH 13 (3); Anoxic, pH 13, 50°C (1)	680 (3) days 438 (1) days	Total C-14 <sub>(aq)</sub> and for final sampling <sup>14</sup> C-organic <sub>(aq)</sub>	For final sampling only: <sup>14</sup> CO <sub>2(g)</sub> , ( <sup>14</sup> CO+ <sup>14</sup> C-organics) (g)
	Powder (2) [15 & 30g]	Anoxic, pH 13	512 or 280 days	Total C-14 <sub>(aq)</sub> and <sup>14</sup> C-organic <sub>(aq)</sub>	<sup>14</sup> CO <sub>2(g)</sub> , ( <sup>14</sup> CO+ <sup>14</sup> C-organics) (g)	
	Marcoule G2 (UNGG)	Powder (1) [50g]	Anoxic, pH 13	180 days	Total C-14 <sub>(aq)</sub> and <sup>14</sup> C-organic <sub>(aq)</sub>	<sup>14</sup> CO <sub>2(g)</sub> , ( <sup>14</sup> CO+ <sup>14</sup> C-organics) (g)

Experiments undertaken at ambient laboratory temperature except where stated

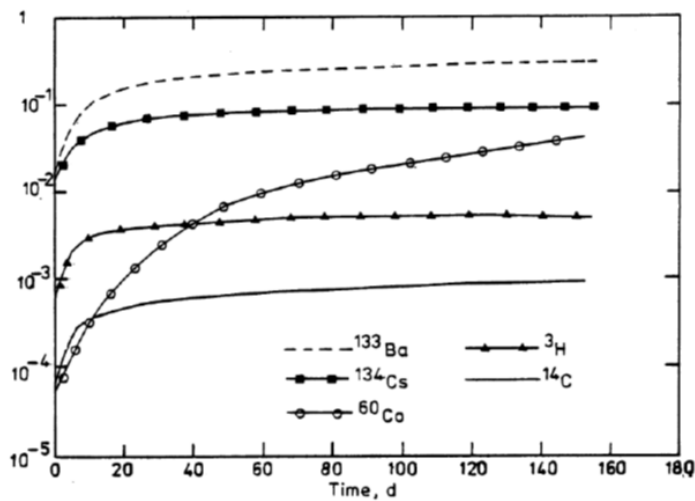
#### **2.9.4 Early UK graphite leaching experiments**

In the 1980s a study of graphite leaching in the UK [WHITE et al., 1984] was performed on small samples that had been irradiated in the core of an unspecified UK Magnox reactor for about 13 years at about 16,000 MWd/t, then stored for about three years post-irradiation.

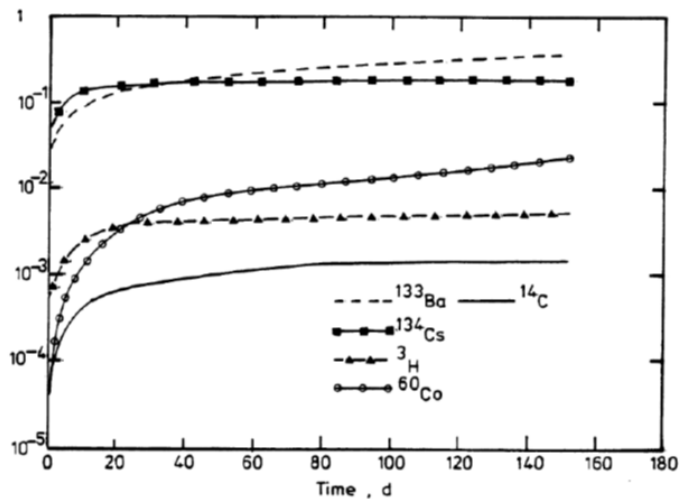
To minimise possible interferences from surface contaminants the samples were machined to remove their surface layer before use in dynamic leaching tests. In most cases, the samples were hollow cylinders. Duplicate samples were leached in demineralised water, a simulated argillaceous groundwater or simulated sea water at ambient temperature under aerobic conditions; a further pair of samples was leached in simulated sea water at  $2.5 \pm 0.7^\circ\text{C}$  and a pressure of 450 bar to simulate conditions at a depth of 4000m.

The cumulative fractions of leachable radionuclides from the irradiated graphite with time in water and the simulated groundwater are shown in Figure 2.9.1. Similar results were obtained under all conditions studied. In each case (with the exception of cobalt-60), there is a sharp initial rise in cumulative radionuclide release over the first 10 days of the tests, before the rate of release drops and the radionuclide concentrations approach plateau values. It is notable that each radionuclide shows a different leachability and, in particular, that carbon 14 shows the lowest cumulative release ( $\sim 0.1\%$ ) and the lowest incremental rate of release after 100 days ( $\sim 1 \times 10^{-6} \text{ cm day}^{-1}$ ).

The leaching behaviour shown in Figure 2.9.1 is typical of the results presented in the literature for radionuclide releases to solution from irradiated graphite [BASTON et al., 2014; VENDÉ, 2012, GRAY & MORGAN, 1988; 1989; YAMASHITA, 2012a]. In general, under all conditions studied, a decrease in the total carbon-14 release rate to solution is observed over a period of 10 to 100 days. The results suggest a fast initial release of surface species that are readily mobilised on contact with water, followed by a slower long-term release that may be controlled by the rate of out-diffusion of carbon-14 from the porosity of the graphite. Total fractional releases (i.e. the total release as a fraction of the sample C-14 inventory) seen in the laboratory can vary by up to between two to three orders of magnitude reflecting the different sources, irradiation histories and irradiation conditions of the graphites, as well as differences in the geometries of leached samples.



a)



b)

**Figure 2.9.1: Cumulative Fraction of Activity Leached from Irradiated Magnox Graphite at Ambient Temperature a) in Demineralised Water, b) in a Simulated Argillaceous Groundwater [WHITE et al., 1984].**

Few leaching studies have yielded information on the speciation of the carbon-14 released to gas or solution. The most relevant published studies relate to experiments performed on moderator and reflector graphites from the Tokai (Magnox) reactors in Japan, graphites

from the Oldbury Magnox reactor in the UK, and a recent study on French graphite reactors. The results of these studies are summarised below.

### 2.9.5 Japanese Tokai graphite leaching studies

Recent leaching studies of moderator and reflector graphites from the Tokai (Magnox) reactors in Japan [ISOBE et al., 2007; 2008a,b; 2009; YAMASHITA, 2012a,b] included separation of the organic carbon 14 species in solution from  $^{14}\text{C}$ -carbonate, with attempts to identify the nature of these organic species.

The leaching experiments ran for up to 4 years. It was found that about 0.1% of the total carbon-14 inventory of the graphite samples was released to solution over three years, with the majority of the release occurring in the first month, as shown in Figure 2.9.2.

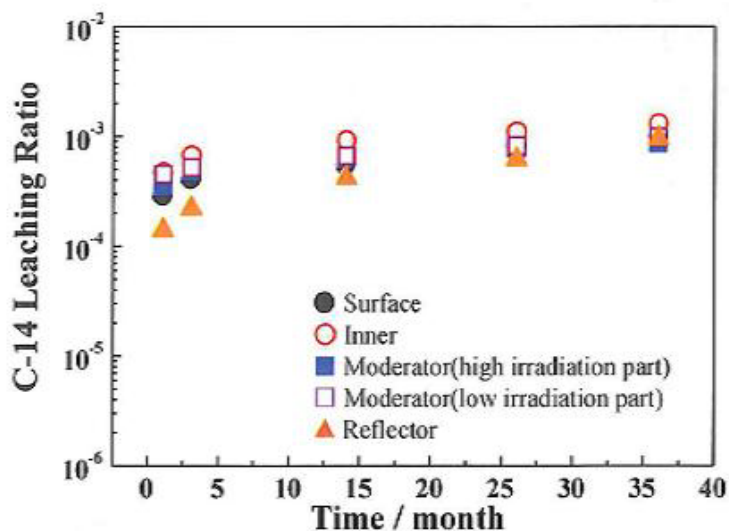


**Figure 2.9.2: Cumulative Fraction of Carbon-14 Leached into Alkaline Solution from Irradiated Tokai Graphites under Ambient, Anaerobic Conditions [YAMASHITA, 2012a].**

It was reported that about 80% of the carbon-14 released was in organic form with only 20% as carbonate [YAMASHITA, 2012b]. Although an attempt was made to identify the dissolved  $^{14}\text{C}$ -organic compounds by High Performance Liquid Chromatography (HPLC), the results were not conclusive. However, this does not affect the important observation

from these studies that a significant proportion of the carbon-14 released to solution is as organic molecules.

### 2.9.6 UK Leaching studies of irradiated graphites

Work funded under the RWM research programme has focused on measurements of gas-phase carbon-14 releases from leaching in high-pH solutions.

An initial exploratory study found that some carbon-14 was released to the gas phase by static leaching of a sample of irradiated graphite taken from the Windscale Advanced Gas-cooled Reactor (WAGR) in alkaline solution under aerobic conditions at room temperature [BASTON et al., 2006].

Further series of leaching experiments on the WAGR graphite and on irradiated graphite from British Experimental Pile 0 (BEP0) followed [HANDY, 2006; MARSHALL et al., 2011; BASTON et al., 2012]. These studies measured gaseous carbon-14 release with leaching time under similar conditions to those of the initial exploratory study (i.e. high pH aerobic conditions at ambient temperature). However, in contrast to the initial exploratory study, the gas analyses discriminated between organic/hydrocarbon and inorganic gaseous forms of carbon-14 released from the reaction vessel. The results confirmed the observation from the exploratory study that some carbon-14 was released as gaseous species during leaching of irradiated graphite at high pH and also identified that these could include inorganic species (assumed to be  $^{14}\text{CO}$  because  $^{14}\text{CO}_2$  should be retained in the alkaline leachant in the reaction vessel) as well as hydrocarbon/organic species.

In the case of BEP0 graphite it was found that about 0.1% of the carbon-14 inventory was released to the solution phase and that 0.005% of carbon-14 was released to the gas phase over a period of 14 months. In the gas phase 80% was as inorganic species (assumed to be  $^{14}\text{CO}^{10}$ ) and 20% as hydrocarbon/organic species (assumed to be  $^{14}\text{CH}_4$ ) [MARSHALL et al., 2011]. There was some evidence from the residual carbon-14 activity in solution

---

<sup>10</sup> Ongoing work suggests that oxygen-containing organic species (e.g. ketones, aldehydes) could be oxidised under the same conditions used to oxidise  $^{14}\text{CO}$  in the experimental methodology and would be included the resulting  $^{14}\text{CO}_2$  trapped for analysis.

samples after acidification that a fraction of the carbon-14 in solution ( $\leq 20\%$ ) was present as organic species. The rate of gas phase release decreased with time.

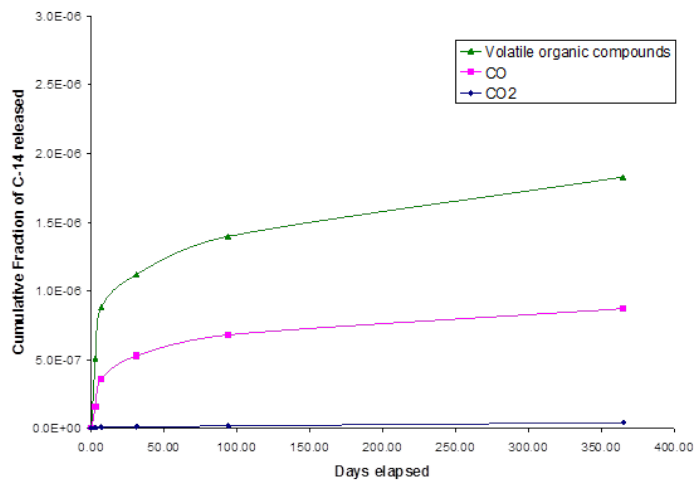
The most recent study, on carrier graphite from one of the Oldbury Magnox reactors in the UK, has investigated the effect of experimental conditions on the speciation of carbon-14 and its release to the gas phase [BASTON et al., 2012, BASTON et al., 2014]. The study investigated:

- a) the effect of anaerobic conditions compared to aerobic conditions;
- b) leaching under neutral conditions compared to highly alkaline conditions;
- c) leaching at 50°C rather than at ambient room temperature; and
- d) the effect of crushing the graphite compared to leaching a single piece.

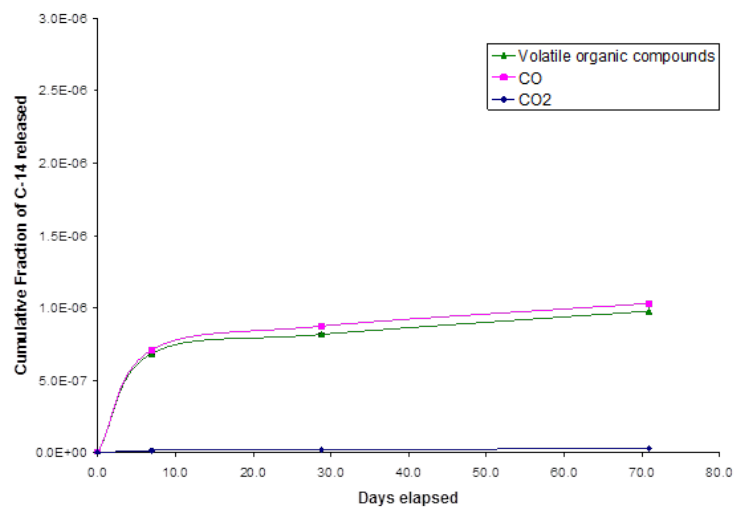
In common with the previous BEP0 study [MARSHALL et al., 2011], measurements of carbon-14 releases to the solution phase were only made at the end of the experiments to avoid the potential of compromising the gas phase sampling. However, a parallel experiment under anaerobic high-pH conditions was set up with periodic sampling to measure solution-phase releases only.

Figure 2.9.3 compares the gas-phase release measured from an intact sample of Oldbury Magnox graphite at pH 13 and ambient temperature under anaerobic conditions with the equivalent experiment under oxic conditions. Under aerobic conditions the ratio of  $^{14}\text{C}$ -hydrocarbon/organic compounds to  $^{14}\text{CO}$  was about 1:1, under anaerobic conditions it was closer to 2:1.

A comparison of the total fractional gas and solution-phase releases of carbon-14 from Oldbury graphite under anaerobic high-pH conditions is shown in Figure 2.9.4. Releases to both solution and gas phases show an initial rapid release followed by a slower release over longer timescales. The ratio of solution phase to gaseous release was of the order of 100:1 at most sampling points but had increased slightly to between 200:1 to 300:1 for samples taken after one year. In comparison, a lower ratio of about 20:1 was measured on termination of the BEP0 experiment after 431 days [MARSHALL et al., 2011].



a)



b)

**Figure 2.9.3: Fractional Release of Gaseous Carbon-14 from Leaching of Irradiated Oldbury Graphite at pH 13 and Ambient Room Temperature a) Under Anaerobic Conditions, b) Under Oxic Conditions [BASTON et al., 2014].**

An important feature of these results is that release of carbon-14 was observed to both gas and solution phases during the final sampling period, which lasted from 3 to 12 months, i.e. carbon-14 releases were continuing, albeit at a slow rate.

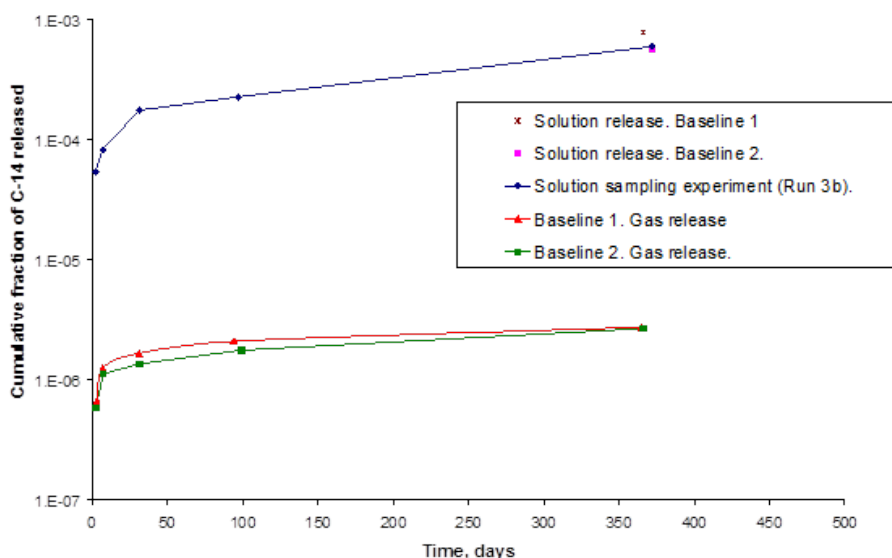


**Figure 2.9.4: Comparison of Cumulative Fractional Releases of Carbon-14 to both solution and gas from Leaching of Irradiated Oldbury Graphite at pH 13 and Ambient Room Temperature under Anaerobic Conditions [BASTON et al., 2014]**

The results of all six Oldbury graphite experiments in terms of the total gaseous phase carbon 14 releases as a fraction of the sample inventory are compared in Figure 2.9.5 (the Figure also includes the BEP0 [MARSHALL et al., 2011] and WAGR [BASTON et al., 2006] results). In all cases, after an initial period of faster release, the rate of carbon-14 release decreases and is continuing at a slower rate at the end of the experiments.

The highest initial rate of gaseous carbon-14 release from Magnox graphite was measured in the experiment at 50°C but this release rate decreased more rapidly over time (up to 94 days). In the experiment at pH 7 the gaseous releases were dominated by  $^{14}\text{CO}_2$  because of the lower solubility of  $\text{CO}_2$  as carbonate at this lower pH. The gas phase releases of  $^{14}\text{CO}_2$  in this case were about 15 times higher than those of  $^{14}\text{CO}$  and  $^{14}\text{C}$ -hydrocarbon/organics combined at the same time, both of which were released at similar rates and in a similar ratio as at pH 13.

The gas-phase releases from the sample of powdered graphite were less than those measured from the single piece samples, however, the total carbon-14 release to the solution phase over the three-month duration of the experiment increased by about 65%. It is possible that

some of the more labile carbon-14 was released during crushing (similar behaviour has been reported elsewhere [GIRKE et al., 2011]). However, the overall increase in carbon-14 release to solution with increase in geometric surface area of the graphite is consistent with other studies.

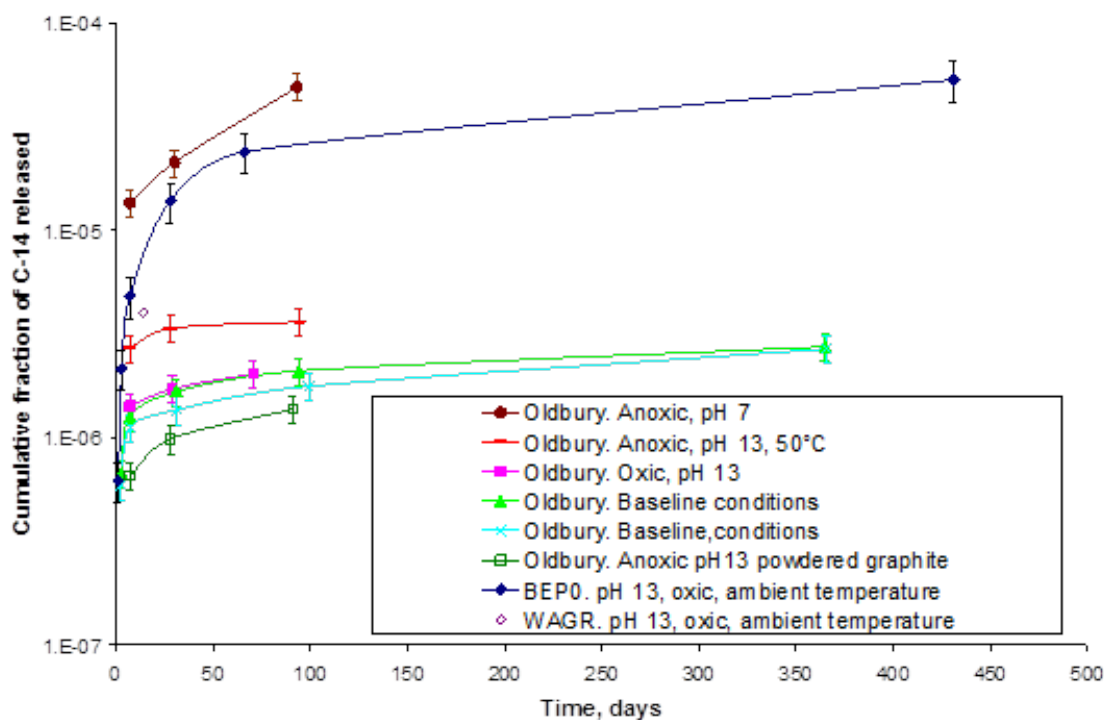


**Figure 2.9.5: Total Cumulative Releases of Carbon-14 from Irradiated Oldbury Graphite to Gas Compared to BEP0 and WAGR graphites [BASTON et al., 2014]**

The fractional release to the gas phase was found to be about one order of magnitude lower for the Oldbury Magnox graphite than for the BEP0 graphite under oxidic conditions. However, a higher proportion of carbon-14 was released as  $^{14}\text{C}$ -hydrocarbon/organics even under aerobic conditions. The ratios of the  $^{14}\text{C}$ -hydrocarbon/organics to  $^{14}\text{CO}$  in the gas phase during the Oldbury and BEP0 graphite experiments are compared in Figure 2.9.6. Both the cumulative ratios and the ratios measured at each sampling point (which show greater variability) are shown in this graph (the closed symbols joined by full lines are cumulative ratios; the open symbols joined by dashed lines are the ratios measured at each sampling point and the lines joining the points are included to aid the eye). In all of the anaerobic Oldbury Magnox experiments, the ratio of  $^{14}\text{C}$ -hydrocarbon/organics to  $^{14}\text{CO}$  was

about 2 on average; whereas a ratio of about 1 was measured in the oxidic experiment. In comparison, the gas phase  $^{14}\text{C}$ -hydrocarbon/organics to  $^{14}\text{CO}$  ratio measured for the BEP0 graphite under oxidic conditions was lower, and cumulatively was about 0.25 at the end of the experiment.

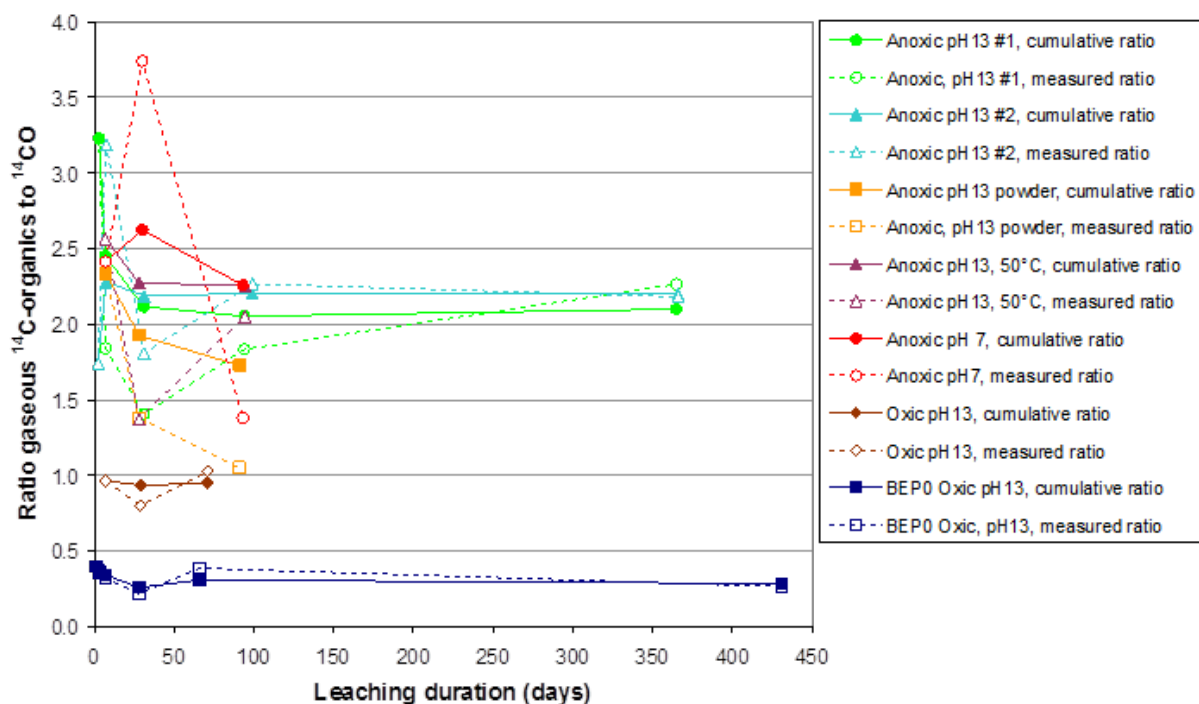


**Figure 2.9.6: Comparison of Ratios of Gaseous Carbon-14 Releases as Organic/Hydrocarbon Species to  $^{14}\text{CO}$  from Irradiated Oldbury and BEP0 Graphites**

Only total carbon-14 releases to the solution phase were measured for the Oldbury samples [BASTON et al., 2014]. These data are compared with a number of datasets from the literature [GRAY & MORGAN, 1988, 1989; WHITE et al., 1984] in Figure 2.9.7. These datasets were acquired by leaching intact monolithic samples of irradiated graphites (from different reactors with differing irradiation histories) of varying dimensions, under a variety of experimental leaching conditions (solution composition, pH, redox and temperature). As a result there is a wide variation in both the rates and the extent of carbon-14 releases over the experimental timescales. Owing to the relative short total duration of most of the early experiments, they provide only limited information on longer-term leaching behaviour. The largest variation in leach rates is observed between different sources of irradiated graphite.

The Oldbury data are comparable in magnitude with the Tokai data illustrated in Figure 2.9.2.

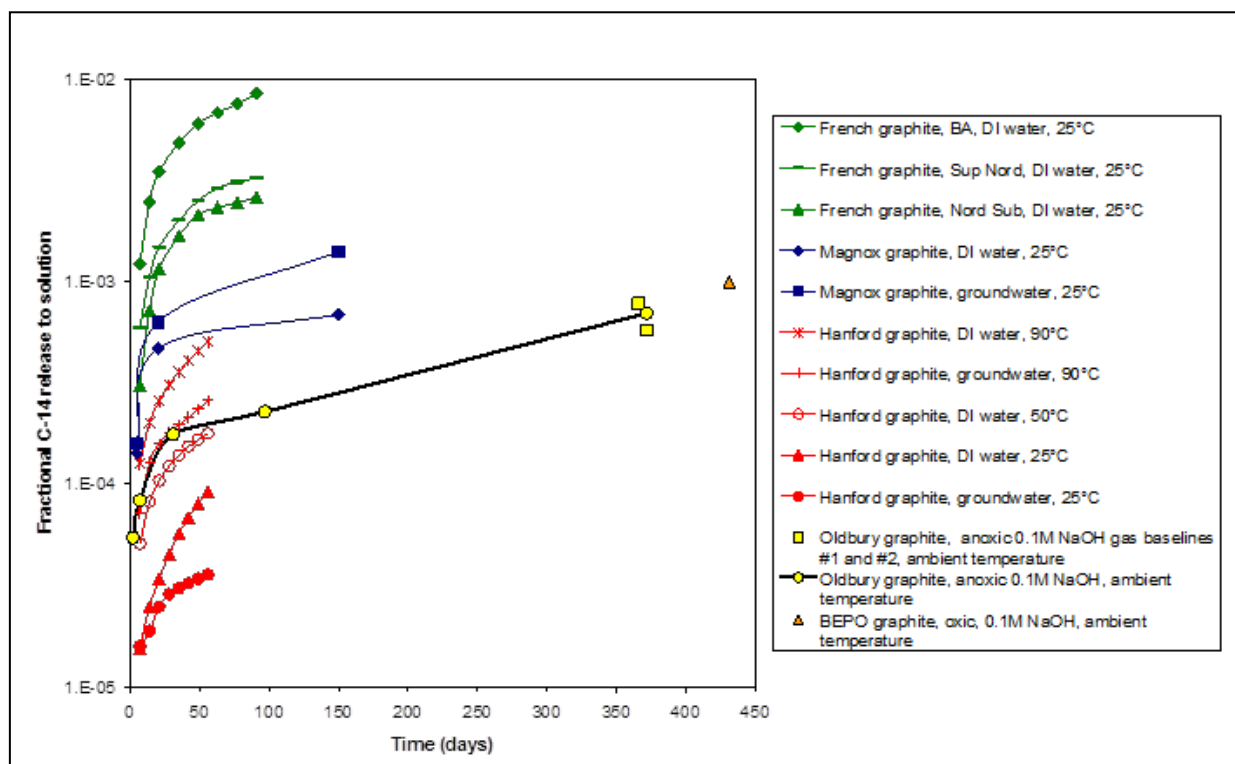


**Figure 2.9.7: Comparison of Carbon-14 Releases to Solution from Oldbury Graphite with Published Values for Monolithic Samples of Other Graphites [GRAY & MORGAN 1988, 1989; WHITE et al., 1984], values for Magnox graphite were estimated from plots given in WHITE et al. (lines joining points are included to aid visualisation)**

### 2.9.7 French leaching studies of irradiated graphites

A study on the leaching behaviour of graphites from two French UNGG (Uranium Naturel Graphite Gaz)-type reactors [VENDÉ, 2012] has been performed as part of the European CARBOWASTE project. That study included measurements of both gas phase releases and quantification of the fraction of carbon-14 released to solution as organic species.

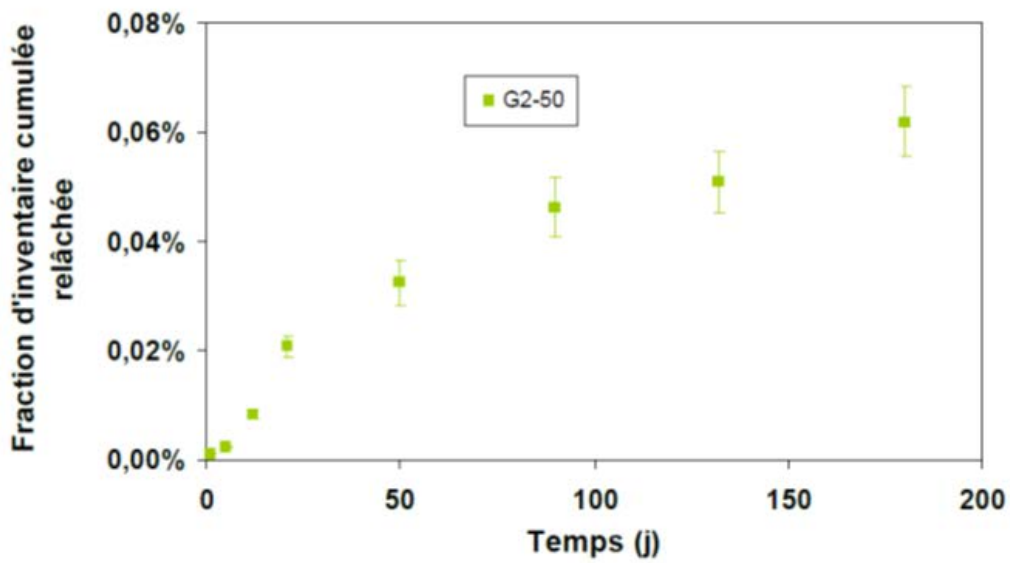
Nine graphite leaching experiments were undertaken under anaerobic, high-pH (0.1 mol dm<sup>-3</sup> NaOH solution) conditions over durations ranging from 180 to 821 days:

eight on samples from the St. Laurent des Eaux A2 (SLA2) reactor and one on graphite from the G2 reactor at Marcoule. Apart from one experiment on SLA2 graphite, conducted at 50°C, the experiments were performed at ambient temperature ( $22 \pm 2^\circ\text{C}$ ). Varying quantities of powdered graphite with a range of particle size distributions were used. The experiments were stirred continuously but, as a result, comminution of the powder was increasingly apparent during the experiments.

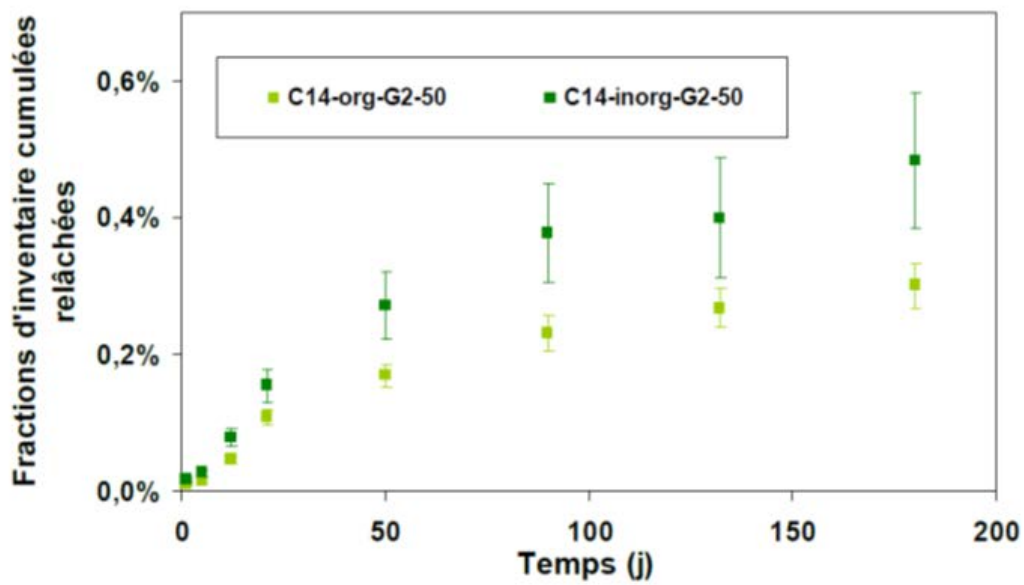
In three experiments containing larger quantities of graphite, carbon-14 was detected in the gas phase as well as in the solution, and the dissolved carbon-14 was distributed between organic and inorganic species. The results are shown in Figure 2.9.8 for G2 graphite, for which fractional releases to the gas phase were about an order of magnitude lower than total carbon 14 releases to solution. This compares to a ratio of gas to total solution phase releases of about 1:30 for two SLA2 samples.

The predominant form of carbon-14 in solution was carbonate for samples of both SLA2 and G2 graphites. The proportion of organic carbon-14 species in solution varied between  $18 \pm 4\%$  and  $38 \pm 7\%$  at the termination of the experiments. Releases of organic carbon-containing species were also detected by TOC measurements and followed the same trend as the  $^{14}\text{C}$ -organic releases. However, while the extent of TOC release was similar for the two graphites (around 0.02% after 150 days), the ratio of  $^{14}\text{C}$ -organic fractional release to TOC fractional release was higher for the G2 sample (about 15) compared to the SLA2 sample (about 1.5).

Evidence for continuing release of carbon-14 over longer timescales was also found. In three cases, after about 51 days of leaching, a steady state seemed to have been reached ( $\sim 0.1\%$  total carbon-14 release). However, when the experiments were resampled after a further 630 days, significant further release was measured, with cumulative releases in the range  $\sim 0.35$  to  $0.45\%$  total carbon-14. In two experiments where the leaching solution was exchanged completely after 241 days, further carbon-14 release was measured in a final sample taken 580 days later.



a)



b)

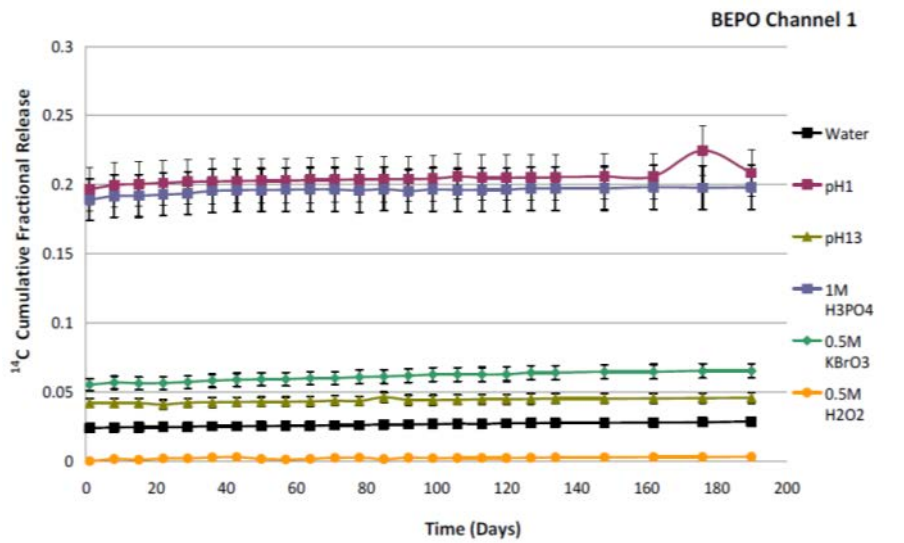
Figure 2.9.8: Fractional Carbon-14 Releases from G2 Graphite leached under anoxic conditions in 0.1 mol dm<sup>-3</sup> NaOH solution a) gas phase release b) solution phase release [VENDÉ, 2012]

### 2.9.8 Leaching of UK graphites as a potential chemical pre-treatment

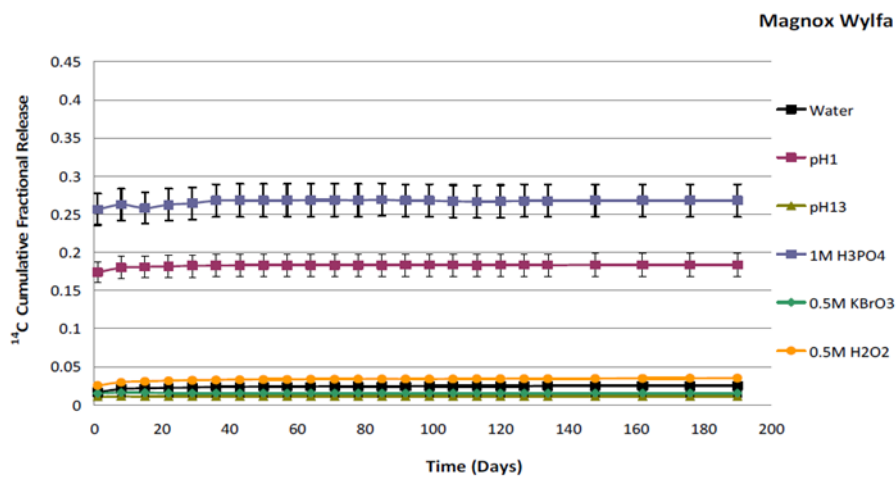
A recent study on chemical leaching of UK irradiated graphite has been undertaken as part of the CARBOWASTE programme [McDERMOTT, 2011]. Although the principal objective of this work was to investigate the potential chemical treatment of irradiated graphite to remove labile carbon-14 and tritium prior to disposal, it provides insight into the potential long-term availability of the carbon-14 content of irradiated graphites under disposal conditions.

Irradiated graphite samples from BEP0 and Wylfa Magnox reactors were leached at room temperature under oxidic conditions on small monolith or powdered samples (0.5g) of irradiated graphites, with sampling and replacement of 10% of the solution volume (50 cm<sup>3</sup> total) every 7 days. A wide range of leachant solutions were used varying from demineralised water and a pH 13 (NaOH/KCl) buffer solution, representative of near-field disposal conditions, to solutions of oxidants (hydrogen peroxide, potassium bromate) at varying concentrations and strong acids (pH 1 buffer solution, 1 mol dm<sup>-3</sup> phosphoric or hydrochloric acids).

The effect of leachant on the carbon 14 release is illustrated in Figure 2.9.9 for powdered BEP0 and granulated Wylfa Magnox graphites. In each case there is a very fast initial release of carbon-14 during the first day of leaching, followed by a much slower release over the remainder of the experiment duration with a steady state apparently being reached under most conditions by day 90. The releases are limited to at most ~6% in water, pH 13 and oxidant solutions (BEP0). However, much higher releases are measured in the more acidic solutions: up to 21% for the BEP0 channel 1 graphite; 25% for BEP0 channel 16 graphite and 27% for the Magnox graphite. This higher release fraction was attributed to intercalation of anion species in the acid into surface material (penetration of interlayer spaces within the graphite structure) allowing the release of loosely-bound carbon-14 species located there.



a)



b)

Figure 2.9.9: Cumulative Fraction of Carbon-14 Leached into Solution from powdered Irradiated Graphites in Different Leachants under ambient, aerobic conditions a) BEPO channel 1 graphite ( $55 \text{ m}^2\text{g}^{-1}$ ) b) Wylfa Magnox graphite ( $32 \text{ m}^2\text{g}^{-1}$ ) [McDERMOTT, 2011]



It should be noted that, because of the low pH of the acid solutions used, carbon and carbon-14 released from the irradiated graphite as CO<sub>2</sub> would be released as gas. Thus (although not discussed in McDermott, 2011) it can be postulated that the carbon-14 measured in the solution phase in the acid experiments would have been in the form of water-soluble organic species. Subsequent thermal analysis of leached samples confirmed that the majority of carbon-14 had remained in the graphite after leaching. It was concluded that, even under harsh acidic conditions, not more than 30% of the carbon-14 was released from these powdered irradiated graphites on leaching. This provides evidence that a significant proportion of the carbon-14 content is part of the graphite matrix and may be unavailable for leaching under disposal conditions.

## **2.9.9 Other relevant information**

### **2.9.9.1 Thermal treatment of graphite and graphite oxidation in the presence of water**

Thermal treatment of graphite has been used to develop an understanding of the mobility of carbon-14 in irradiated graphites [VULPIUS et al., 2013; PODRUZHINA, 2005; CLEAVER et al., 2012] and as a potential method for selective carbon-14 removal. VULPIUS et al., 2013 and PODRUZHINA, 2005 used a combination of:

- a) inert gas (pyrolysis) experiments, to study the diffusion of carbon-14 through the graphite matrix; and
- b) treatments that include a small amount of oxygen or steam, to investigate selective oxidation of the different forms in carbon in the irradiated material.

It has been established that carbon-14 is preferentially released compared to bulk carbon when heating irradiated graphite in the range 870-1300°C, in an inert atmosphere or in steam [PODRUZHINA, 2005]. The highest ratios of carbon-14 to total carbon were obtained in an inert atmosphere; the ratio decreased in steam and at higher temperatures. The high carbon-14 release fraction under an inert gas is explained by oxygen sorbed to the surface of the graphite close to the carbon-14 atoms (detectable by SIMS). At elevated temperatures the oxygen reacts with surrounding carbon atoms, including carbon-14, until

all of the available oxygen is exhausted, at which point no further oxidation will occur. Water vapour can act as an oxidant at higher temperatures but promotes general, as opposed to more localised, oxidation of the graphite. Such results give evidence for elevated concentrations of carbon-14 associated with less-graphitised and surface material.

Similar variations in selectivity of carbon-14 release with temperature were observed in oxidation experiments of irradiated Merlin graphite with 1% oxygen in nitrogen [VULPIUS et al., 2013]. In experiments at 900°C, the enrichment factor of carbon-14 gradually decreased from about two towards one with time, whereas at 700°C there is an enrichment of carbon-14 by a factor of about three throughout the treatment. These findings were interpreted in terms of three different mechanisms of graphite oxidation that are recognised to operate at different temperatures:

- a) uniform oxidation inside the porous material (chemical regime, <500°C) – occurs on all graphite surfaces and is slow;
- b) location-dependent oxidation inside the porous material (in-pore diffusion controlled regime, 500-900°C) – transitional range; and
- c) surface oxidation (boundary layer controlled regime, >900°C) – occurs on the outer surface of graphite and is fast.

Thus, in the experiments at 900°C, carbon-14 was released due to progressive oxidation of the graphite matrix, with some initial enhancement of carbon-14 by release from the surface. At 700°C, carbon-14 release occurs predominantly from the pore surfaces implying that there is a significant enhancement of carbon-14 in these regions.

There has been relatively little work on the reactions and leaching behaviour of inactive graphite at temperatures lower than 400°C. Gray measured the oxidation rate of a graphite powder (and other carbonaceous materials) in the presence of water and air at 200-300°C [GRAY, 1982]. CO, CH<sub>4</sub> and CO<sub>2</sub> were released when graphite samples were then outgassed by heating to 500°C. No hydrogen was detected in any of the experiments and this was taken as evidence that the reaction was with oxygen rather than water although it appeared that water catalysed the oxidation reaction.



Experiments of up to 2 years' duration and at lower temperature (90°C) have been undertaken with unirradiated graphite from a dummy High Temperature Reactor (HTR) fuel element and pyrocarbon coatings from an unirradiated fuel particle [PODRUZHINA, 2005]. Small (1 g) samples of the carbon material of varying particle size and surface area were contacted with an aqueous phase (water, brine) under argon, air or oxygen. At the end of the leaching period the gas phase was sampled. No analyses were performed on the solution phase but in calculations of carbon mass loss, corrections were made for partitioning of CO<sub>2</sub> between solution and gas. Small amounts of CO<sub>2</sub> were detected in the gas phase in all cases after 770 days for leaching experiments in brine under an argon atmosphere, with a correlation between the amount of CO<sub>2</sub> detected and the surface area of the sample. No hydrogen was detected indicating no reduction of water by the graphite. It was hypothesised that the amount of CO<sub>2</sub> released was related to the amount of oxygen sorbed onto the surface of the graphite. In experiments in an air or oxygen atmosphere, the amount of CO<sub>2</sub> detected in the gas phase increased and small amounts of CO were also detected. The amounts of CO<sub>2</sub> produced were about two times higher in an oxygen atmosphere than in air. No observations of methane were reported.

### **2.9.9.2 The location and form of carbon-14 in irradiated graphite**

The nitrogen content of an unirradiated nuclear-grade graphite material has been investigated in a Japanese study [Takahashi et al., 2001]. The overall nitrogen content of a graphite block was measured to be about 44 ppm and was unchanged on heating to 400°C. SIMS profiling of the CN<sup>-</sup> ion with depth into the surface of a graphite block found that the nitrogen was most concentrated on the surface and that the concentration decreased with depth to a background level of about 40 ppm at depths greater than 30 nm.

SIMS profiles of irradiated and unirradiated reflector graphite from a German experimental pebble bed (AVR) reactor also showed concentration of nitrogen near the surface [Vulpius et al., 2013]. It was noted that the only <sup>14</sup>C-containing fragment detectable by SIMS was the single <sup>14</sup>C<sup>-</sup> ion. The predominant fragments of both carbon-12 and carbon-13 detected from irradiated graphite by SIMS were also single carbon ions. This would be consistent with a hypothesis that much of the carbon-14 is bound within the graphite in a similar way to natural carbon, which is present predominantly as matrix graphite.

SIMS area scans of irradiated graphite samples from St Laurent A2 found evidence for the presence of carbon-14 hotspots in the irradiated graphite (the distribution of impurity ions such as  $\text{Cl}^-$ ,  $\text{Na}^+$  and  $\text{Cs}^+$  was also inhomogeneous) [Vulpus et al., 2013]. Inhomogeneous impurities and hotspots have also been observed by autoradiography of irradiated UK graphites [McDermott, 2011].

A comparison of samples of irradiated PGA graphite taken from two different Magnox station reactor cores in the UK has been made using a combination of focused ion beam milling and imaging and Raman spectroscopy [Heard et al., 2014]. Surface deposits of thickness 5 to 20  $\mu\text{m}$  were observed on samples from one of the two reactors. These had a “cauliflower-like” morphology and a different elemental composition (in particular increased oxygen) from both the underlying irradiated graphite and unirradiated PGA graphite. In contrast, although there was evidence that some deposits existed on samples taken from the second Magnox reactor, this was patchy, thin and insignificant compared with that found on samples from the other station. Subsequent work using magnetic sector secondary ion mass spectrometry (MS-SIMS) on samples of irradiated graphite from one of the Oldbury station reactor cores in the UK has found increased concentrations of carbon-14 in deposits on the channel wall faces ( $47 \pm 8\text{ppm}$ ) compared to concentrations below the detection limit (estimated to be 5 to 10 ppm) within the graphite samples [PAYNE et al., 2014]. In comparison to the AVR study discussed above, this study analysed the  $^{12}\text{C}_2^-$  and  $^{14}\text{C}_2^-$  peaks at  $m/z = 24$  and 28 respectively.

The quantity and form of adsorbed oxygen complexes in pre- and post-irradiated graphite have been studied by SIMS and X-ray photoelectron spectroscopy (XPS) at the State University of Idaho [SMITH et al., 2013]. Samples of a nuclear graphite (NGB-18) and a highly porous, high-surface area graphite foam (POCOFoam®) were irradiated in sealed containers. Fragments containing both carbon and oxygen, such as  $\text{CO}$ ,  $\text{CO}_2$ ,  $\text{C}_2\text{O}_2$  and  $\text{C}_2\text{HO}$  were only found in SIMS analysis of irradiated samples although adsorbed oxygen fragments ( $^{16}\text{O}$ ) were detected for both irradiated and unirradiated graphite. XPS indicated multiple bonding structures: peaks attributed to ester- and carboxyl-like structures were predominant on the NGB-18 graphite with a carbonyl-like structure peak also present. A carboxyl-like structure peak was predominant for the POCOfoam®.

## 2.9.10 Discussion

### 2.9.10.1 Location of carbon-14 in irradiated graphite and implications for leaching

Vulpus and co-workers [2013] postulate that carbon-14 originating from nitrogen-14 will be concentrated on surfaces, in near-surface structures and in disordered or amorphous regions of incompletely graphitised binder or filler materials. In contrast, it is postulated that carbon-14 arising from carbon-13 within the graphite matrix (the recoil energy of the  $^{13}\text{C}(n,\gamma)^{14}\text{C}$  reaction energy is high enough to dislocate the  $^{14}\text{C}$  atom from its previous place in the lattice) will either recombine with vacancies in the graphite matrix, remain in place or migrate as an interstitial species between graphene layers [VON LENZA et al. 2011].

This results in a conceptual model for the distribution of carbon-14 in irradiated graphite in which there is a homogeneously distributed part throughout the graphite matrix that arises primarily from the activation of carbon-13 and a heterogeneously distributed part that is enriched in hotspots and on surfaces. The chemical form of carbon-14 is primarily elemental (the homogeneously-distributed part) and is bound covalently in the graphite structure. As a result, removal of the bulk of the carbon-14 would only occur by oxidation of the graphite matrix (i.e. with conversion to either  $^{14}\text{CO}$  or  $^{14}\text{CO}_2$ ).

It is important to note that reactor operating conditions and the reactor lifetime are also important in relation to the inventory and distribution of carbon-14 in irradiated graphite. Radiolytic and general oxidation of graphite will occur during reactor operation. As a result, enhanced release of carbon-14 compared to carbon can be expected to occur from the pore surfaces of the graphite during operation. Oxidation also results in an increase in porosity and the opening up of closed pores within the graphite increasing the accessibility of carbon-14. On the other hand, the greater annealing of graphite that occurs at higher operating temperatures is likely to result in a greater ordering of the graphite structure and re-incorporation of displaced carbon-14 into the graphite matrix, which can be expected to make it less accessible. All this has implications for the leaching behaviour of irradiated graphite and suggests this would be dependent on the source and operating history of the sample under investigation.

The results of the chemical treatment studies of McDermott [2011] suggest that three different forms of carbon-14 may be present that differ in their accessibility and releasability from irradiated graphite on leaching. Thus it may be postulated that:

- a) carbon-14 bound up in the graphite matrix would be least accessible for release and would only be released via oxidation processes of the bulk graphite;
- b) carbon-14 in interstitial positions between graphene layers would potentially be accessible if degradation of the graphite structure occurs, e.g. by intercalation of anions between graphene sheets; and
- c) carbon-14 associated with pore surfaces, edge sites and less ordered regions of the graphite would be the most accessible for potential release.

There is some evidence from leaching studies of irradiated graphites from different reactor types that, in lower temperature reactors (or from lower temperature regions) that have seen less radiolytic oxidation and graphite annealing, a greater proportion of the carbon-14 inventory may be associated with pore surfaces and potentially available for release on immersion in water. This may explain why higher release rates and extents of release have been observed from irradiated graphites from the lower-temperature Marcoule G2 and BEPO reactors compared to Magnox graphites.

#### **2.9.10.2 Long-term release of carbon-14 from graphite**

Whether carbon-14 incorporated into the graphite matrix could potentially be released at significant rates in a GDF post-closure before carbon-14 has decayed away (>60,000 years) depends on the long-term stability of graphite under disposal conditions.

For the carbon-14 to be released, a chemical reaction needs to occur between the graphite matrix and the porewater solution. The relative reaction rates for carbon with oxygen and water at low temperatures are extremely slow and it is difficult to obtain reliable information on the oxidation of graphite at temperatures below 200°C. In effect, those studies that have been performed to study the reactions of graphites with water, oxygen and air at temperatures up to 200°C [e.g. GRAY, 1982; PODRUZHINA, 2005] have strong

similarities to leaching experiments on irradiated materials, in so far as they have studied the reactions of the whole graphite or carbon material assemblage, rather than the stability of the graphitic carbon matrix. Thus, they provide information only on the ‘releasable’ fraction of carbon-14. Studies of the thermal treatment and oxidation behaviour of graphite at elevated temperatures give greater insight into graphite stability and potential release of carbon-14 in the longer term.

To illustrate the high stability of graphite to oxidation it has been noted that [MARSDEN et al., 2002]:

- a) graphite is used in large quantities at very high temperatures, in the steel and other industries;
- b) in its manufacture, temperatures in excess of 1800°C are required to start the carbon-carbon atomic diffusion process, which allows the graphitisation process to take place;
- c) in the presence of air, temperatures well in excess of 300°C are required before appreciable oxidation takes place and oxidation only becomes significant at temperatures around 400°C [IAEA, 2000]; and
- d) air-cooled and graphite-moderated reactors in which the core operated in air at low temperatures (e.g. BEPO 110°C, French G1 ~200°C) operated for many years without significant thermal oxidation of the moderator.

The reaction between graphite and water vapour is highly endothermic and is generally considered to be insignificant below 800°C [IAEA, 2000]. However, in the chemical regime of graphite oxidation (i.e. <500°C), the rate of oxidation can be increased by the presence of even relatively low concentrations of impurities [IAEA, 2000], which reduce the activation energy. According to MARSDEN et al. [2002], typical oxidation rates for unirradiated PGA graphite in air are about  $3.2 \times 10^{-6}$  per hour at 400°C with activation energies of about 170 kJ mol<sup>-1</sup>. However, severely contaminated graphite from Windscale Pile 2 (after the 1957 incident), which might be expected to contain significantly higher concentration of catalytically-active impurities as an extreme example, was reported to have a much higher oxidation rate of 3.4% per hour at 400°C with an activation energy of 125 kJ mol<sup>-1</sup>. In

general, the extent of carbon and carbon-14 release from irradiated graphite on thermal treatment under inert gas appears to be dependent on the amount of oxygen that is present chemisorbed to the graphite surface and once this oxygen is removed, and in the absence of oxygen addition, no further oxidation takes place [VULPIUS et al., 2013; PODRUZHINA, 2005]. Thus in a GDF, which would be expected to become anaerobic after closure as a result of oxygen consumption by metal corrosion processes, any possibility of chemical oxidation of the graphite matrix might be expected to cease once all of the surface oxygen species have been removed. In the absence of alternative graphite degradation processes (e.g. microbial, radiolytic) this would be expected to limit the amount of carbon-14 that would be releasable from the graphite matrix.

### **2.9.11 Summary of current understanding of carbon-14 releases from graphite on immersion in water**

#### **2.9.11.1 Release rates and extent of release**

In general, only a small fraction of the total carbon-14 inventory (up to ~1%) is released on leaching in solution over timescales of up to 3 to 4 years. The total fractional releases and rates of release over experimental timescales are dependent on the source of irradiated graphite. This may be related to different irradiation histories, operating temperatures, nature of graphite and extent of radiolytic oxidation.

Even when harsh acidic conditions are applied, <30% of the carbon-14 inventory is released over experimental timescales. The majority of release occurs to the solution phase; small amounts of gaseous phase releases have been measured. Leaching studies show an initial fast release followed by an approach to a steady state with a very low incremental release rate. Crushing may increase the accessibility of carbon-14 to water but volatile carbon-14 may be lost during crushing. This points to the likelihood that there are two forms of carbon-14 in irradiated graphite: leachable (with the leachability depending on accessibility to leachant) and non-leachable (inaccessible, probably part of graphite matrix).

### **2.9.11.2 Speciation**

There is evidence from separate studies that  $^{14}\text{C}$  is released to the solution phase in organic as well as inorganic ( $^{14}\text{CO}_2$ /carbonate) forms under alkaline conditions. Evidence from French and UK studies show that carbon-14 is released to the gas phase phase under high-pH conditions. Gas phase releases include both volatile  $^{14}\text{C}$ -hydrocarbon/organics (probably  $^{14}\text{CH}_4$ ) and  $^{14}\text{CO}$ .  $^{14}\text{CO}_2$  is also purged from solution at near-neutral pH. The form of gaseous carbon-14 release is affected by redox conditions with a lower redox seeming to favour  $^{14}\text{C}$ -hydrocarbon/organic compounds.

### **2.9.11.3 Location and form of carbon-14**

There is evidence that carbon-14 has homogeneously distributed part throughout the graphite matrix that arises primarily from the activation of carbon-13 and a heterogeneously distributed part that is enriched in hotspots and on surfaces. The distribution of carbon-14 dependent on irradiation and operational history and the extent of radiolytic oxidation that will remove surface carbon and the extent of reordering due to graphite annealing.

The chemical form of carbon-14 is primarily elemental and it is bound covalently in the graphite structure. Thus the removal of the bulk of the carbon-14 would only occur by oxidation with conversion to either  $^{14}\text{CO}$  or  $^{14}\text{CO}_2$  but the graphite matrix is extremely resistant to oxidation at GDF temperatures and is unlikely to undergo oxidation once GDF conditions have become anaerobic after closure.

### **2.9.11.4 Mechanisms of release**

Experimental evidence shows release of carbon from unirradiated graphite is dependent in part on the presence of oxygen; water is required to catalyse the reaction in some way at low temperatures. Release of  $^{14}\text{CO}_2$  as a major product is consistent with a principal mechanism of release being an oxidation process similar to that for graphite at elevated temperatures. The mechanisms of formation of hydrocarbon and/or other VOC species is uncertain but may result from the association of hydrogen with active carbon sites.

### 2.9.12 Conceptual Model for Carbon-14 Release from Irradiated Graphites

Based on the above discussion a conceptual model for the release of carbon-14 from irradiated graphites under cementitious disposal conditions can be proposed as shown in Figure 2.9.10.

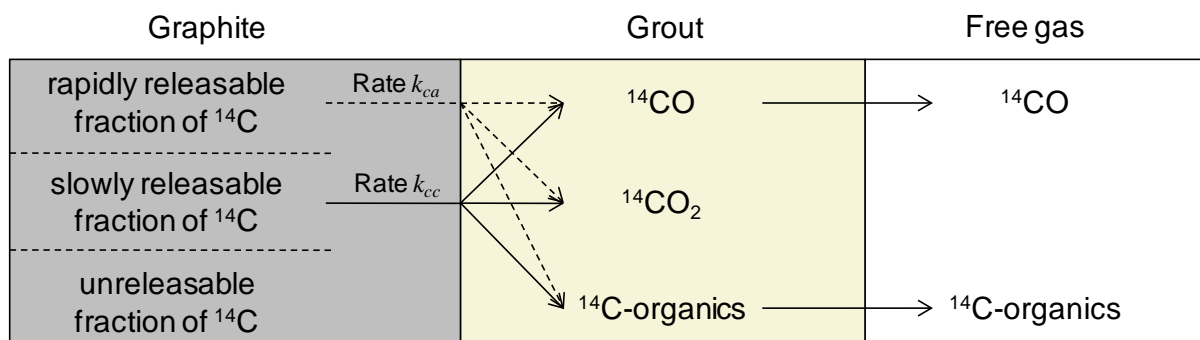


**Figure 2.9.10: Conceptual Model for Release of Carbon-14 from Irradiated Graphite under Cementitious Disposal Conditions**

This conceptual model reflects:

- a) a substantial fraction of the carbon-14 in graphite will not be releasable under disposal conditions;
- b) some carbon-14 will initially be released rapidly, and some will be released more slowly at a rate reducing over time;
- c) carbon-14 can be released to both the gas and aqueous phases and carbon-14 released to the gas phase may exist as a number of different species including organic/hydrocarbon species (e.g.  $\text{CH}_4$ ),  $\text{CO}_2$  and  $\text{CO}$ ;
- d) release rates and speciation of the released carbon-14 may change depending on the conditions (e.g. pH, presence of oxygen).

#### Acknowledgements

This section is based on a review being carried out as part of the RWM generic research programme. Steve Swanton and Bill Miller of Amec Foster Wheeler are thanked for their significant contributions to this text.

## **2.10 Furnaces Nuclear Applications Grenoble (FNAG) summary**

### **2.10.1 Introduction**

The corrosion behaviour of bulk graphite will enable the prediction of C-14 release from that part of C-14 which is fixed in graphite matrix. This is directly related to the bulk graphite corrosion and is slower than the release of loose bound C-14 on surfaces as well as from disturbed structures. Graphite is a stable material in nature which is proven by its natural occurrence. Only strong oxidative environments will lead to measurable graphite corrosion rates. Small quantities of oxygen absorbed on the graphite surface or dissolved in natural waters can be ruled out as oxidation species for several reasons:

- Low ambient temperature
- Preferential oxidation with waste containers which consume the oxygen totally
- Slow reaction kinetic

Therefore only high reactive species, e.g. radicals, will lead to significant corrosion rates. Furthermore these species have to be produced in the near field of the graphite because otherwise they will react with other materials in their surrounding environment. The only source for such species is the radiolysis of water. This review summarises the studies related to graphite corrosion in aquatic phases induced by  $\gamma$ -irradiation. The most detailed investigation was a diploma thesis of T. Rieger [Rieger, 2008].

### **2.10.2 Background**

Graphite is an inert high temperature resistant material which is used in industry for many applications e.g. as crucibles for molten metals, fireproof products, fuel cells or electrodes [Graphit Kropfmühl AG, Wikipedia]. Its long term geological stability is proven by the natural occurrence of graphite formed in the Precambrian age [Crespo, 2004].

Graphite has been widely used in nuclear industry as reflector and moderator. Around 250,000 tons of irradiated graphite (i-graphite) exists worldwide and can be considered as a current waste or future waste stream. The largest national i-graphite inventory is located in

UK (~ 100,000 tons) with significant quantities also in Russia and France [Marsden and Wickham, 2006]. Most of the i-graphite remains in the cores of shutdown nuclear reactors including the MAGNOX type in UK and the UNGG in France. Whilst there are still operational power reactors with graphite cores, such as the Russian RBMKs and the AGRs in UK, all of them will reach their end of life during the next two decades.

Therefore the corrosion behavior of i-graphite under disposal conditions become an important role for management of i-graphite. Only slow corrosion can be induced by high irradiation dose rates due to the formation of aggressive species from water radiolysis. Corrosion rates were observed in the range of  $10^{-5}$  to  $10^{-7}$   $\text{gm}^{-2}\text{d}^{-1}$  [Fachinger, 2008]. However this becomes only relevant if the graphite pore system is filled up with water because geometrical surfaces of graphite blocks are small in comparison to the huge surface area of the pore system. This leads to the conclusion that graphite with a sealed pore system will be also stable under disposal conditions because the pore system is sealed.

### **2.10.3 Behaviour of graphite in aqueous phases at high $\gamma$ -dose rates**

#### **2.10.3.1 Thermodynamic approach**

The thermodynamic approach shows that graphite is not the thermodynamic stable form and will react to carbon dioxide or to methane depending on the expected conditions in the repository. A small stability field of graphite is only given at lower pH values.

However the thermodynamics say nothing about the time scale for this reaction. The oxidation of graphite is kinetically controlled and requires such high activation energy that thermodynamic models cannot be used for the description of the long term evolution of the graphite. This is proven by the natural occurrence of extremely old graphite and coal deposits in nature. Therefore the thermodynamic approach is not discussed in detail.

#### **2.10.3.2 Kinetic approach**

Several experimental studies have been made to understand the corrosion behavior of graphite under disposal conditions [Gray, 1982]. A diploma thesis of Rieger [Rieger, 2008] is a relative unknown work where the relationship of graphite corrosion rate to gamma-dose rates has been studied.

The oxidation of graphite requires an oxidative species. Where could such species come from? First it could be dissolved oxygen in aqueous phases. However this small amount of oxygen will preferentially react with the metal surface of a waste. Therefore the oxygen will be consumed and not be available for graphite oxidation in the long term. It could be expected that reducing conditions are established by the iron corrosion products. The small amounts of oxygen in aqueous phases, which are in contact graphite from the beginning, are not large enough to cause significant graphite oxidations. Furthermore the temperature in a geological disposal side without heat generation waste can be assumed less than 50°C, which is not sufficient to initiate the graphite oxidation by oxygen. This is in accordance with studies from Podruzina [Podruzina, 2005] where graphite corrosion was reported at temperatures of 200°C. Corrosion experiments at room temperature were also performed but not reported because the obtained results show only background values with a wide scatter. The scatter did not allow an estimation of a corrosion rate (even negative corrosion rates, which are impossible, were obtained due to scattering of the background) and therefore these results were not reported in the work of Podruzina [Podruzina, 2005].

A second source of oxidative species is the radiolysis of water. The work of Podruzina [Podruzina, 2005] shows that radiolysis will be a significant source of oxidative species and lead to graphite oxidation. However these experiments were performed with extreme high dose rates not relevant for GDF. More relevant could be a diploma thesis of Rieger [Rieger, 2007]. She investigated the graphite corrosion rate of A3-3 powders with different grain sizes as function of dose rate under argon atmosphere in water and salt brines. The powder was prepared from unirradiated AVR fuel pebbles by lathing and sorted into fractions with different grain size by sieving (Gsf – very fine grainsize <0,05 mm; Gf – fine grainsize 0,05 – 0,08 mm; Gm – medium grainsize 0,6 – 0,15 mm; Gg – coarse grainsize >0,15 mm). The dose rates used in this work were in the same order of magnitude as in the work of Podruzina [Podruzina, 2005] but would allow the estimation of corrosion at low dose rates. Experiments performed in water under an argon atmosphere revealed an increase of the corrosion rate by factor of about 10 by increasing the irradiation dose from 1,9 to 2,3 MGy (Figure 2.10.1). Similar results were obtained by using different dose rates and constant irradiation times (Figure 2.10.2). Also experiments were performed under an air atmosphere. The values with doses of 3.5 MGy, particularly, show extreme scattering. A

further study criterion was the particle size of the powdered material (Figure 2.10.3). The values shown were mean values of three different measurements. These results indicate that corrosion rate decreases with the increasing particle size. The fine powder fraction of the A3-3 material has also a higher content of carbonized binder material. This indicates that the carbonized binder is more reactive in comparison to the graphite grains which is in agreement with measurements of the oxidation behavior at the AVR. However the fine material (Gf and Gsf) shows no dependency on the dose. An explanation could be that a maximum reaction rate has been obtained.

However the measured data indicate that there is a clear dependency of the corrosion on the irradiation dose.

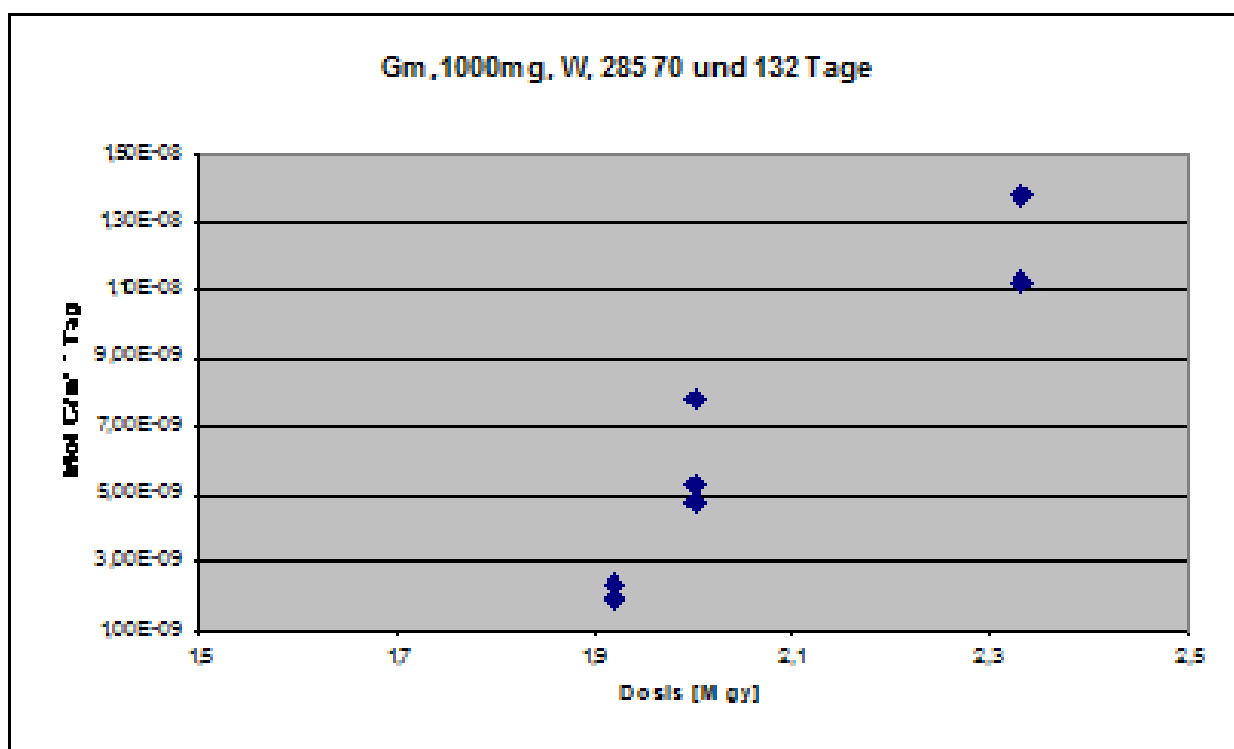


**Figure 2.10.1 Graphite corrosion related to dose rate in water under argon atmosphere (constant dose rate, different irradiation times)**

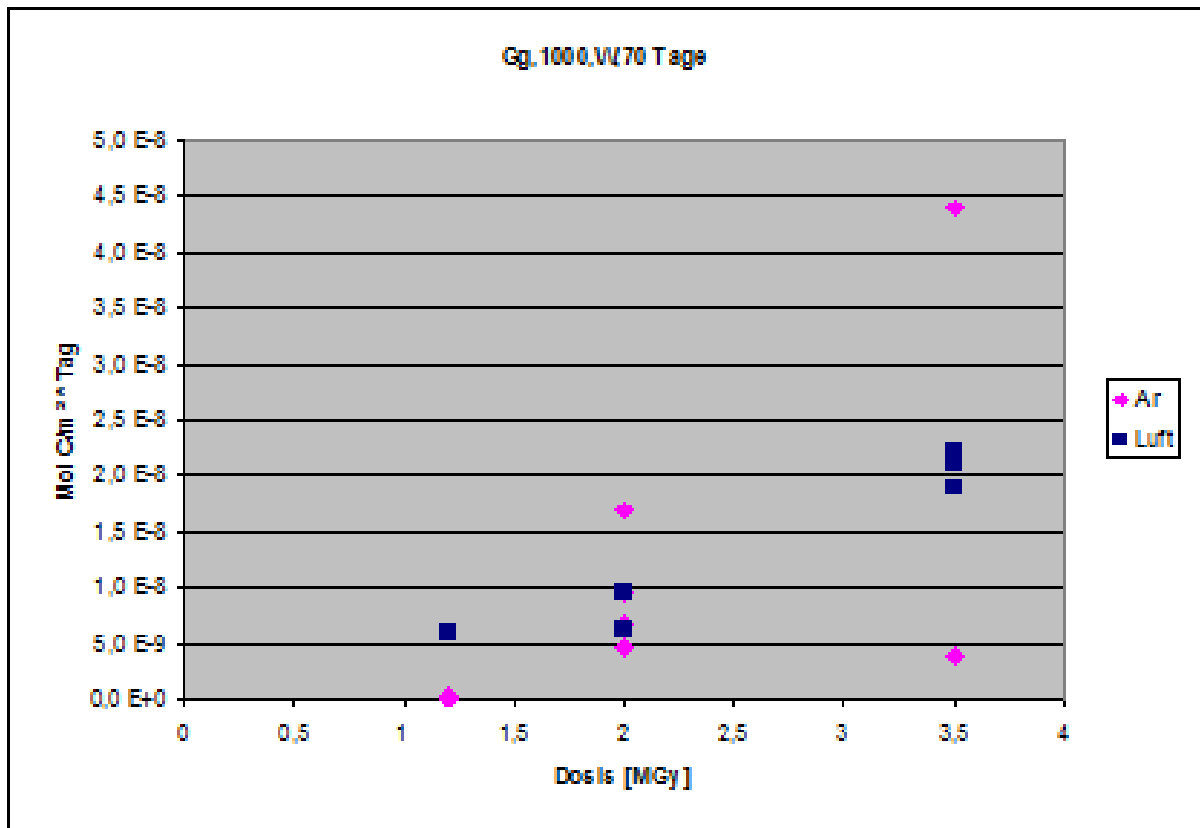


**Figure 2.10.2 Graphite corrosion related to dose rate in water under argon atmosphere (different dose rates, constant irradiation times)**

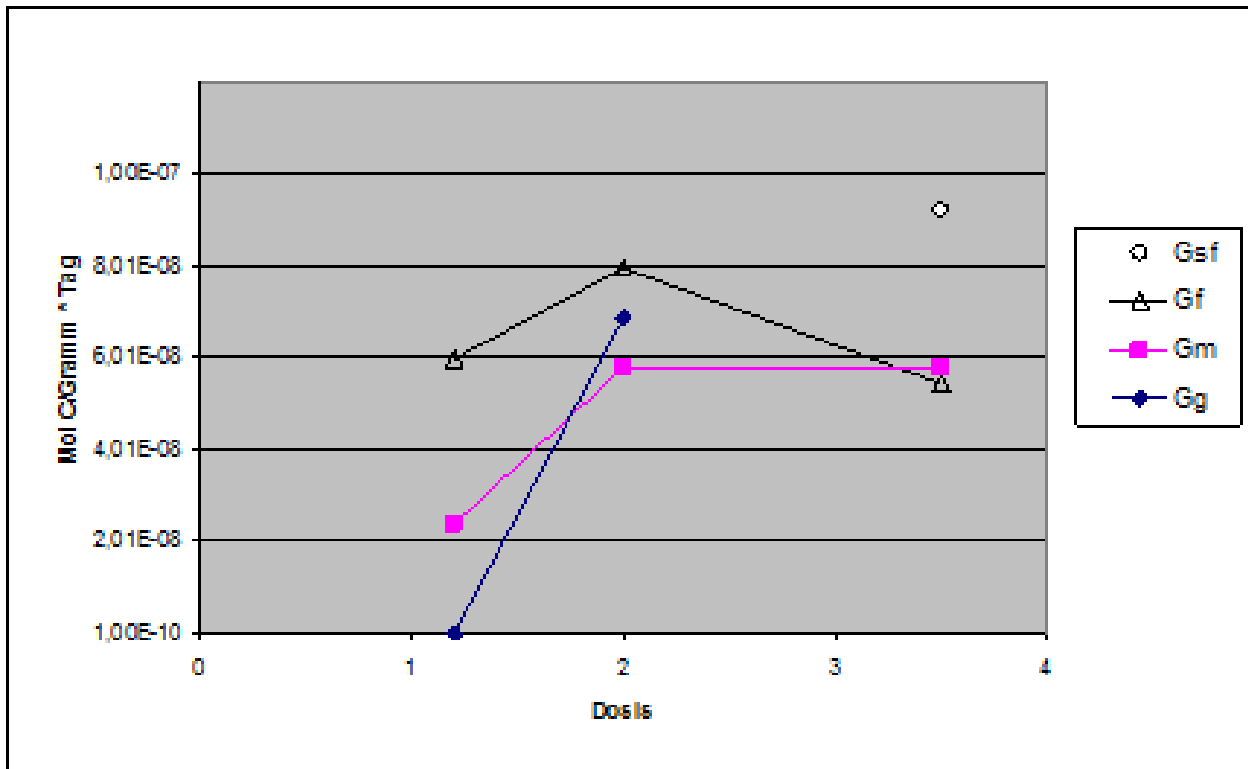


**Figure 2.10.3 Corrosion rate related to grain size (Gsf – very fine grainsize; Gf – fine grainsize; Gm – medium grainsize; Gg – coarse grainsize)**

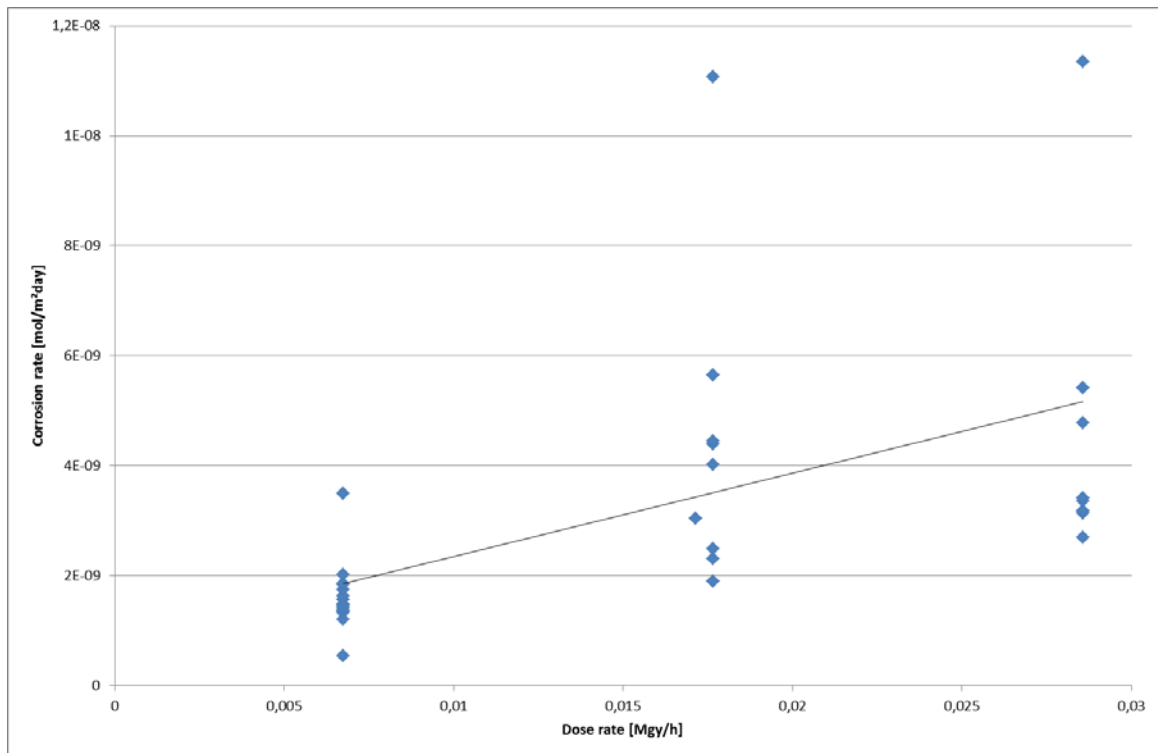


**Figure 2.10.4 Data from Rieger [Rieger, 2008] not sorted by grain size**

The work of Rieger [Rieger, 2008] has no evaluation of measurement errors. Therefore the difference between the results under air and argon could be due to scattering.

Figure 2.10.4 shows the obtained corrosion rates for medium and large graphite grains. The calculated slope of the dose rate dependence is  $2,07e-07 \times DR + 8e-10$ . This shows that graphite corrosion becomes extremely slow at low dose rate, even if the scatter is very large. Figure 2.10.5 shows a simplified calculation of the graphite weight loss for an A3-3 pebble with a diameter of 40 mm. This diagram shows that the graphite will have a life time of about  $10E6$  years even in high gamma-irradiation fields. Please be aware that this calculation is a worst case model which is not realistic because of the following assumptions:

- The dose rate has been assumed as constant for  $1E7$  years and is already larger than expected in the surroundings of the HTR fuel pebbles.

- It is assumed in the model that water is always and everywhere available on any point of the graphite surface. The model did not reflect any reduction of the water by consumption or clogging of pores by precipitates.
- Graphite corrosion products are not taken into account.
- The complete pore volume is filled with water.
- No diffusion processes for water and corrosion products out of and into the pore system were included in the model.
- No surface reduction by the corrosion process over the whole life time.

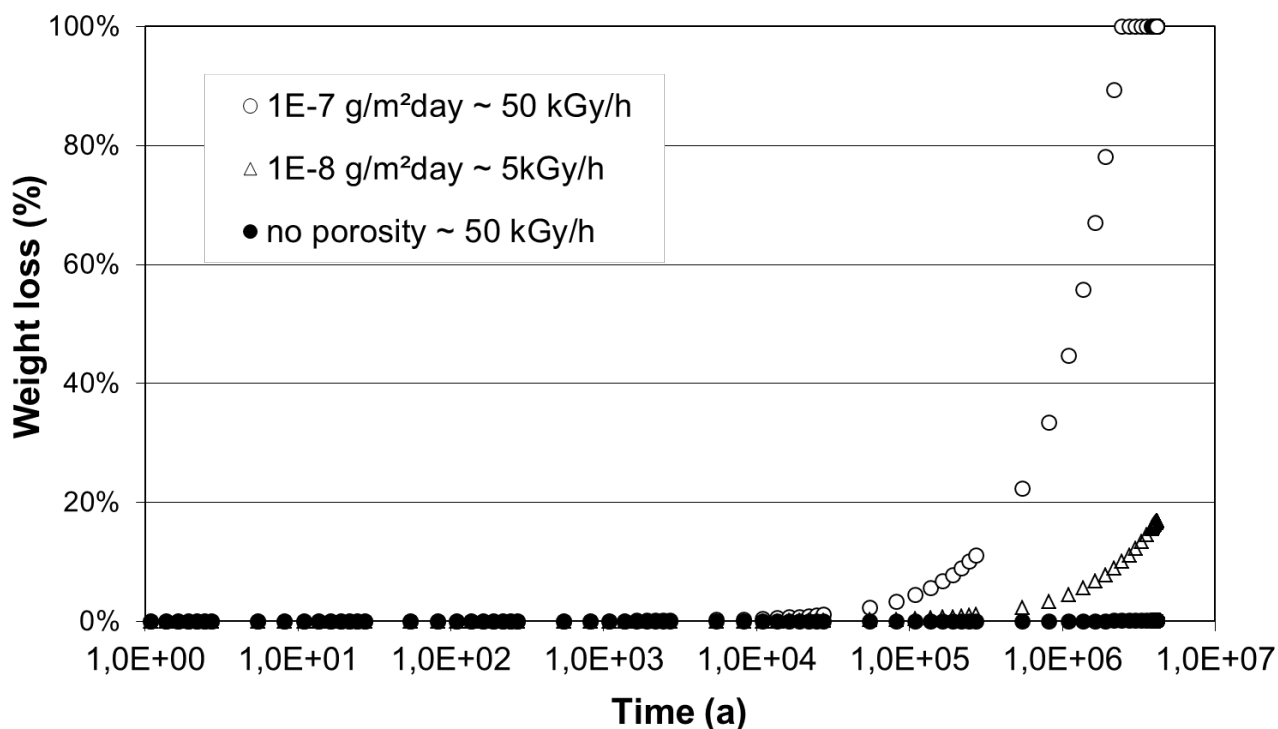


**Figure 2.10.5 Estimation of graphite weight loss from a 40 mm A3-3 pebble based on corrosion data from Rieger [Rieger, 2008]**

### 2.10.4 Oxidation products of graphite corrosion

The reactive species are different when produced by water radiolysis in comparison to oxidation in presence of oxygen. A wide variation of different radicals can react with the graphite.  $O_2^-$ ,  $e^-$  as well as  $HO_2^-$  species become dominant at high pH values.

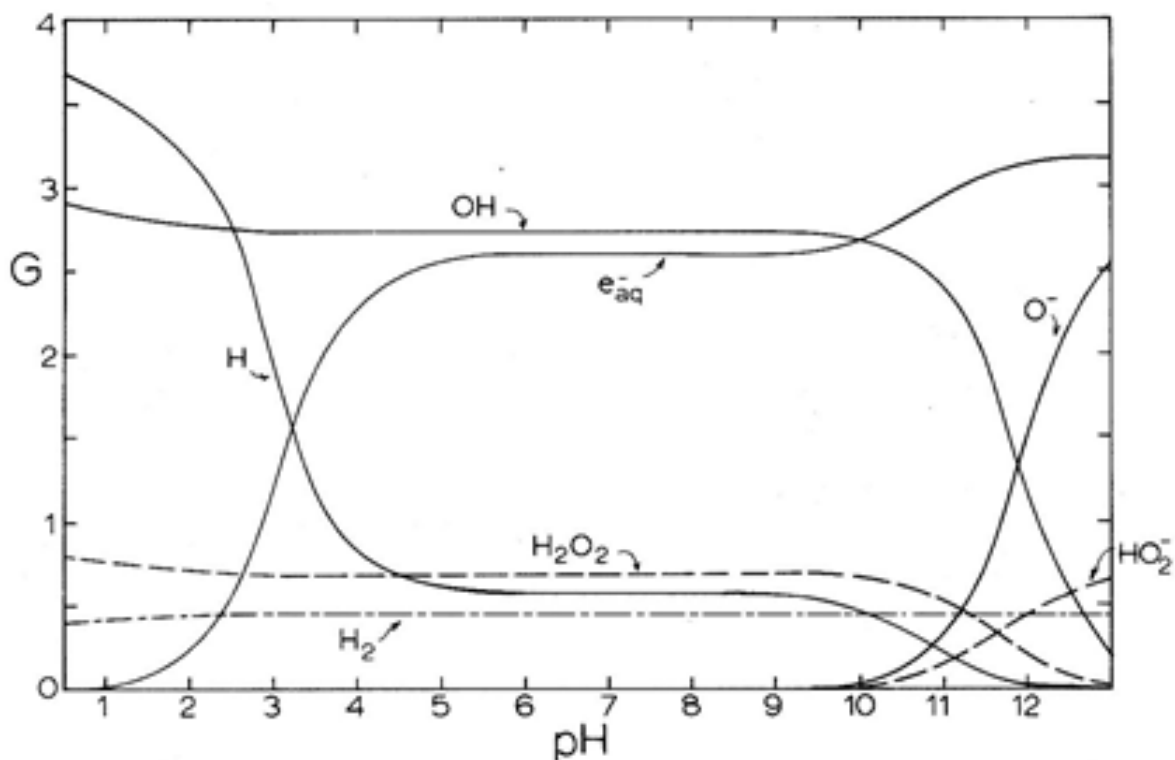


**Figure 2.10.6 pH dependency of water radiolysis products [Spinks and Woods, 1990]**

CO and CO<sub>2</sub> were found as main products by Podruzina [Podruzina, 2005] and Rieger [Rieger, 2008] in pure water. Therefore the reaction products could be different from those found by Rieger and Podruzina. Furthermore the water compositions will influence the graphite corrosion. E.g. hypochlorites will be formed in saturated salts which increase the corrosion rate a little bit.

The work of Brodda et al. [Fachinger et al, 2012] shows the production of water soluble organics, but no methane, as preferential products from leaching of spent HTR fuel pebbles at low pH values and high salt concentrations. This could be related to the different leaching conditions but also to the irradiation history and storage conditions of the fuel pebbles.

No data were found for radiolysis induced graphite oxidation at high pH values and in cements minerals. Therefore detailed investigations would be required if this becomes of importance.

Furthermore the influence of  $\beta$ - and  $\alpha$ -irradiation has to be considered, especially for HTR fuel elements. However radionuclides are also incorporated into i-graphite and water may get into areas where  $\alpha, \beta$ -radiation could become dominant. Investigations of beta- and alpha-radiolysis induced corrosion were planned at FZJ at the end of the last decade but were never performed because financing of the HTR program ceased.

#### **2.10.5 Long term scenario Water intrusion and Coated Particle damage in HTR fuel pebbles**

A number of studies have been performed by Brodda, Zhang, Grambow, den Exter, Visser-Tinova and Fachinger related to the behavior of spent HTR fuel elements and coated particles from the German high temperature reactor program. This fuel consists of graphite pebbles instead of compacts but the general design is the same; coated particles (C.P.) embedded in a porous graphite matrix. Most of the studies were performed with salt brines but some general principles will be the same.

The following scenario shown in Figure 2.10.7 should be considered if water ingress cannot be ruled out [Fachinger et. al., 2006]:

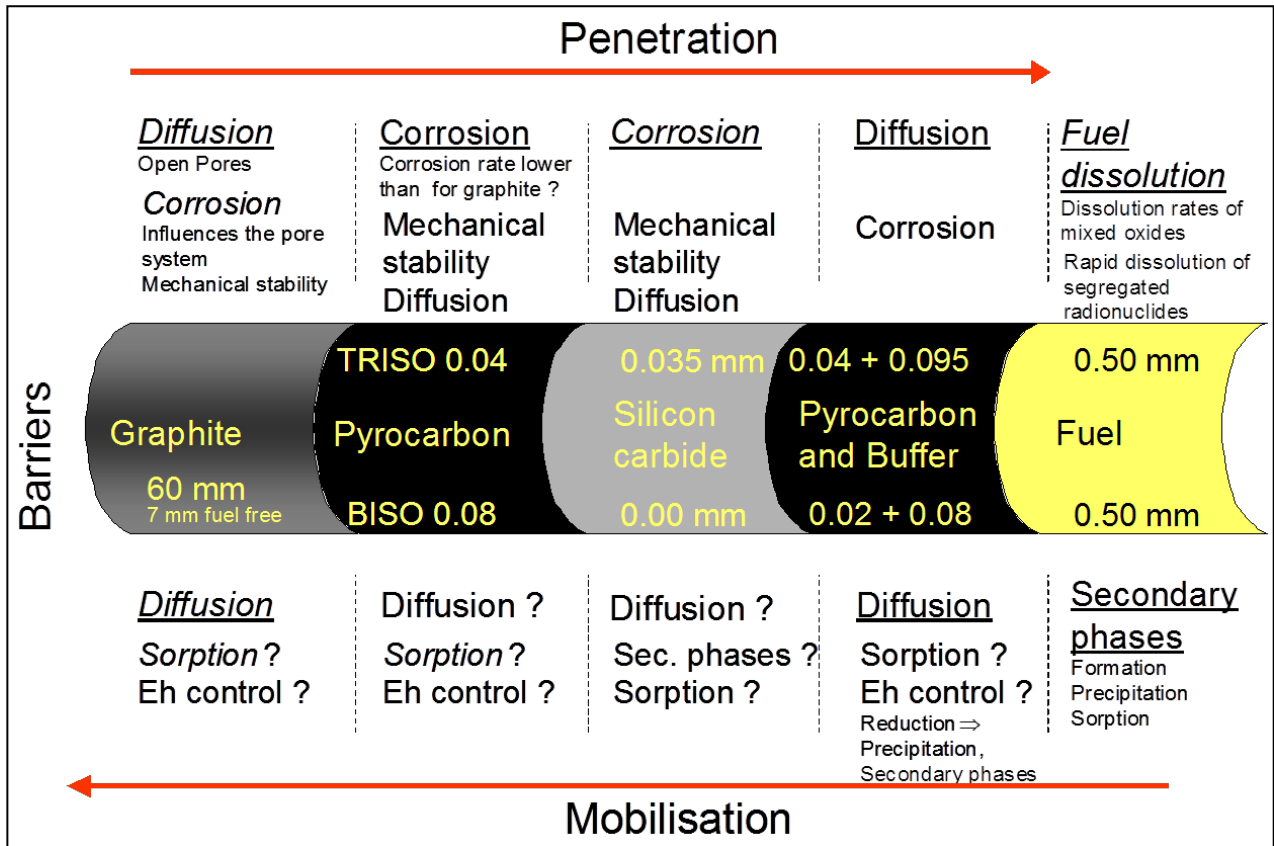


**Figure 2.10.7 Water ingress scenario**

The graphite matrix has a porosity of about 20%. Studies reported in [Rieger, 2008] have shown that the pores will be filled with water. Furthermore the work indicates that about 15% of the pore volume will be filled. These are pores larger than 0.7  $\mu\text{m}$  if the volume is compared to the size distribution of the pore volume.

Therefore the total pore surface of the graphite is accessible to oxidation. The alkaline conditions in the disposal concept as described will lead to the precipitation of carbonates which will reduce the pore volume. This will reduce the amount of water in the pores but will not completely block the pores for water diffusion.

The intrusion model means also that the C.P.s are directly in contact with the aqueous phase. The thin layer of pyrolytic carbon (PyC) will be corroded as well as the graphite matrix. This will lead to pitting corrosion of the PyC in the contact area if the same order of magnitude of the corrosion rates for pyrolytic carbon is assumed. This is shown by REM (SEM – scanning electron microscope) investigations of Rieger [Rieger, 2008].

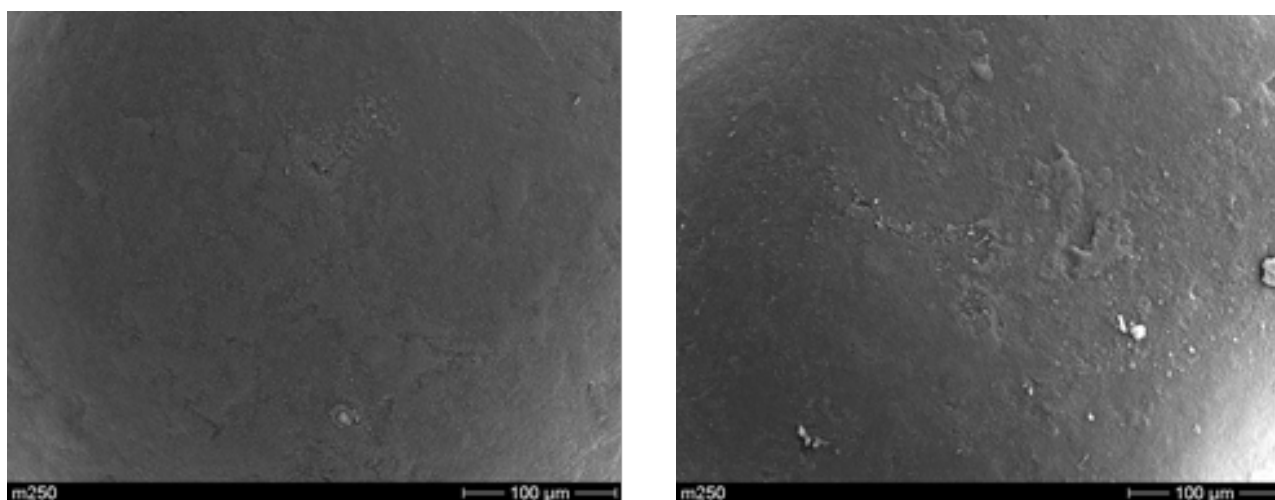


**Figure 2.10.8** PyC surface of a coated particle before and after irradiation (Dose 3.5 MGy) [Rieger, 2008)

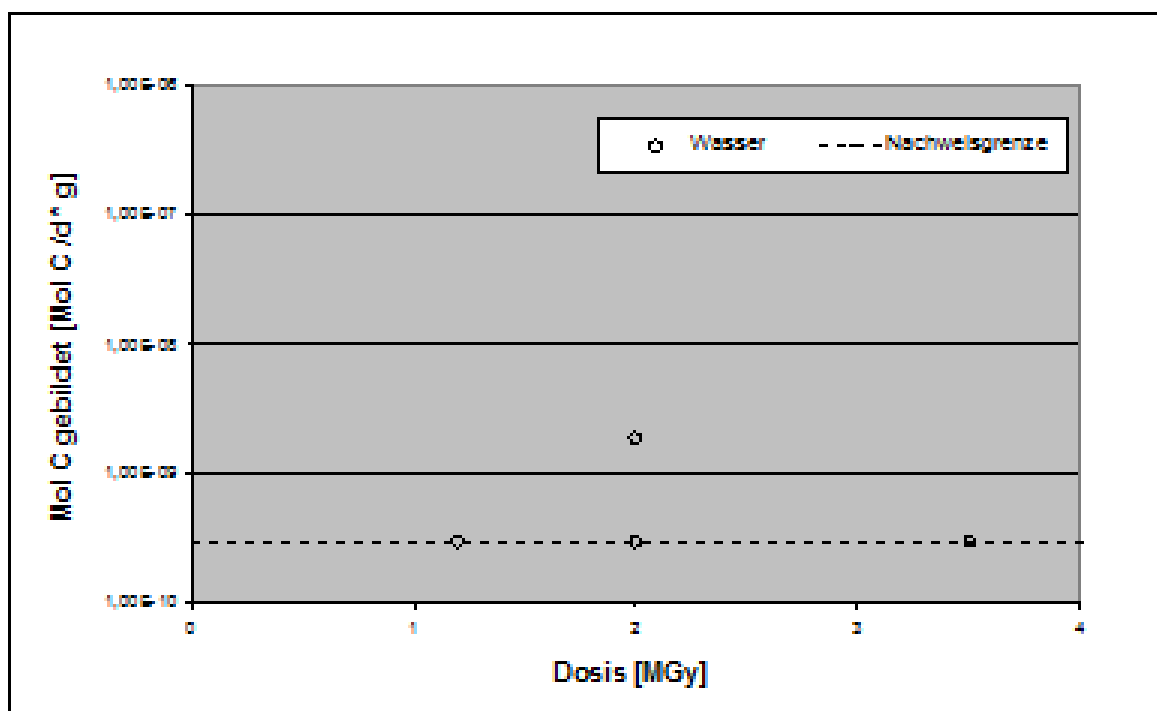


**Figure 2.10.9** Radiation induced corrosion of PyC

However, corresponding corrosion rate measurements show an extremely slow corrosion process and the carbon release was below the detection limit with exception of one case. The detection limit is given with  $\sim 1e-6$  mol C/m<sup>2</sup>d. This is related to the small surface area

of the C.P.s (~ 100 C.P.s in one experiment). The measurements of Podruzina [in Fachinger et al. 2006] lead to estimated life times of the PyC layer in the range of some ten thousand years.

After failure of the PyC layer, the aqueous phase will contact the SiC layer. Corrosion of SiC has been studied by den Exter (Table 2.10.1) and Visser-Tinova at NRG. The results indicate that SiC corrosion is slightly faster at high pH than in neutral or acidic conditions. The longevity of the SiC coating could be expected in the range of some thousands of years.

**Table 2.10.1 Corrosion rates of SiC in different environments [Fachinger et al., 2006]**

Aqueous phase	Temp (°C)	R g/m <sup>2</sup> /day	Lifetime (years)
Granite water	25	2.03E-06	1.29E+05
Granite water	50	3.84E-06	6.80E+03
Granite water	90	9.64E-06	2.70E+03
Q-Brine	25	4.55E-06	5.75E+04
Q-Brine	50	7.54E-06	3.47E+04
Q-Brine	90	1.68E-05	1.56E+04
Q-Brine	180	4.09E-05	6.39E+03
Clay pore pH 9	25	4.56E-06	5.73E+04
Clay Pore pH 9	50	8.07E-06	3.24E+04
Clay Pore pH 9	90	2.30E-05	1.14E+04
Clay Pore pH 12	25	8.85E-06	2.92E+04
Clay Pore pH 12	50	1.61E-05	1.62E+04
Clay Pore pH 12	90	3.70E-05	7.07E+03
Clay Pore pH 3	25	3.76E-06	6.96E+04
Clay Pore pH 3	50	4.45E-06	5.88E+04
Clay Pore pH 3	90	1.09E-05	2.39E+04

Therefore a complete failure of the coating layer cannot be ruled out in some ten thousands of years. The failure could also be speeded up by an internal pressure increase because of helium formation by alpha-decay (2.5 MPa in 100000 years) [Nabielek et al., 2010] because complete dissolution of the SiC layer is not required before fracturing.

The fuel kernels will come into contact with the aqueous phase after failure of the C.P. Surrounding conditions enabling graphite corrosion will be definitely different for natural ground water conditions. The graphite corrosion can only occur when oxidative species are generated by irradiation. This effect will be increased after failure of the coating by alpha-radiolysis. This will lead to a slow dissolution of the kernel.

### **2.10.6 Conclusions**

The kinetic and mechanistic models, as well as the natural analogues of graphite deposits in nature, show that the graphite has an extreme long life time. The work of Rieger, in particular, indicates that significant graphite corrosion requires high dose rates which could not be expected from i-graphite, not even spent HTR fuel. However, a disposal site should guarantee that the dose rates from other waste packages near i-graphite is low; this will ensure graphite corrosion is not an issue that requires consideration when evaluating the performance of the disposal site.

The graphite corrosion can be related to release of C-14 from that part of C-14 which is fixed in the matrix graphite. However loose bound C-14 at the graphite surface and in defect structures will be released faster than the matrix bound C-14. Therefore a quantification of the ratio between loose bound and matrix bound graphite has to be performed in order to quantify the C-14 release under disposal conditions.

### 3 Summary

Work Package 5 of the EC CAST project considers irradiated graphite and related  $^{14}\text{C}$  behaviour. The objective of this Work Package is to understand the factors determining release of  $^{14}\text{C}$  from irradiated graphite under disposal conditions (to include surface disposal facilities and geological disposal facilities). This is to be achieved by:

- Determining the  $^{14}\text{C}$  inventory and concentration distribution in i-graphites, and factors that may control these;
- Measuring the rate and speciation of  $^{14}\text{C}$  release to solution and gas from i-graphites in contact with aqueous solutions; and
- Determining the impact of selected waste treatment options on  $^{14}\text{C}$  releases and relating this to the nature of  $^{14}\text{C}$  in i-graphite.

To ensure current knowledge and understanding of irradiated graphite and  $^{14}\text{C}$  release is captured in the CAST project, Task 5.1 is being undertaken in the first year of CAST. This task has the aim of reviewing the EC project CARBOWASTE and other relevant R&D activities to establish the current understanding of inventory and release of  $^{14}\text{C}$  from i-graphites.

The European Commission project ‘Treatment and Disposal of Irradiated Graphite and other Carbonaceous Waste (CARBOWASTE)’ was launched in 2008 under the Euratom Seventh Framework Programme (FP7- 211333) and terminated in 2013 [Banford et al., 2008; von Lensa et al., 2011]. The 30-partner consortium addressed the retrieval, characterisation, treatment, reuse and disposal of i-graphite, including other carbonaceous waste such as non-graphitised carbon materials or pyrocarbon.

The safety and environmental assessments related to irradiated graphite disposal as undertaken in the CARBOWASTE project confirmed there is sufficient understanding to justify site-specific studies on the disposal of graphite wastes in surface or geological disposal facilities, and that there is sufficient underpinning understanding at a generic level

to be confident that graphite waste can be disposed in a manner such that relevant radiological protection regulations can be attained.

Residual uncertainties for irradiated graphite disposal, which could be progressed via future research, were identified as part of the assessment studies undertaken in CARBOWASTE. Such future research could assist in optimisation studies for an SDF or a GDF. Output from the CARBOWASTE project emphasised that, even in the absence of such future work, there is a sufficient understanding of irradiated graphite now to conclude with confidence, on the basis of work undertaken in the EC CARBOWASTE project, that irradiated graphite waste can be safely disposed in a wide range of disposal systems.

The current report is an output of Task 5.1, and represents Deliverable 5.5 of the CAST project. This report presents contributions from various CAST organisations on respective current i-graphite research activities. Links to precedent work, e.g. as undertaken as part of the CARBOWASTE project, are presented where relevant. Each organisation report is written to be 'stand-alone'; the common report reference list provides a good indication of the wealth of information currently accessible relating to i-graphite. The following text provides summaries of i-graphite knowledge, on the basis of research activities reported in Section 2.

### **Irradiated graphite characterisation – examples of current studies**

Both **LEI** and **IEG NASU** have undertaken work in relation to respective **RBMK** reactors and associated  $^{14}\text{C}$  inventories. As part of LEI's work, experimental measurements of C-14 inventory in the RBMK-1500 reactor graphite were performed by Centre for Physical Sciences and Technology (CPST) within the frame of CARBOWASTE Project. A short leaching test for RBMK graphite was performed at the very end of the CARBOWASTE project too. LEI also studied the relation between treatment and disposal on the performance of RBMK-1500 graphite disposed of in a crystalline rocks. An independent programme of graphite sampling from the graphite stack of Unit 1 was developed by Ignalina Nuclear Power Plant staff, and sampling was accomplished at the end of 2013 year. This work also included some leaching experiments for several radionuclides.

**FZJ** has reviewed characterisation data on the speciation of  $^{14}\text{C}$  in **MTR** and **HTR** i-graphites and relevant information from CarboDISP, decommissioning projects in Germany and the ASSE test repository. FZJ will leach samples, which have undergone decontamination treatments, and untreated samples to confirm a labile  $^{14}\text{C}$  fraction, rather than slow diffusion of  $^{14}\text{C}$  from within the graphite. Leach tests have been systematically started mainly with **RFR** graphite. Additional tests have been performed with **AVR** graphite, as it shows a quite high specific  $^{14}\text{C}$  activity. Diffusion tests have been started also for the irradiated **RFR** graphite. Extensive water-uptake tests have been performed, showing clearly that virgin graphite exhibits little water-ingression and quasi-hydrophobic behaviour. In contrast, irradiated-graphite, as well as heat-treated graphite, behaves in a hydrophilic manner with high and quick water-uptake.

**CIEMAT** has investigated graphite samples from three types of reactors:

- **MTR** reactors: Samples from JEN-1 (Spain) and samples from TRIGA (Romania);
- **UNGG** reactor: Samples from Vandellos-1 (Spain) and from SLA-2 (France);
- **Magnox** reactor: Samples supplied from Magnox Limited.

A range of characterization techniques has been deployed. To investigate the hydrogen content of graphite, two procedures have been used: thermal decomposition and solvent extraction. Graphite decontamination by chemical treatment with liquid agents has been progressed.

#### **Thermal annealing of irradiated graphite – example of current study**

**IPNL** work concludes that thermal annealing of graphite in inert atmosphere does not induce any migration of implanted  $^{13}\text{C}$  up to  $1600^\circ\text{C}$ , even if the structure of the graphite is initially disordered; at  $1600^\circ\text{C}$  slight diffusion occurs. Annealing induces a reordering of the structure. When the graphite is simultaneously annealed and irradiated, the reordering is all the more important as the deposited energy is high. This tends to stabilize  $^{13}\text{C}$  into the reordered structure. Thus, irradiation with  $\text{Ar}^{3+}$  induces a strong re-ordering of the graphite even at room temperature, compared to  $\text{He}^{2+}$  irradiation or annealing alone.

Extrapolation by IPNL of their results to  $^{14}\text{C}$  and  $^{14}\text{N}$  precursor suggests that:

- $^{14}\text{N}$  tends to migrate to the free surfaces where it is partially released under the effect of temperature ( $500^\circ\text{C}$ ). Therefore, most of the  $^{14}\text{C}$  formed by activation of the remaining  $^{14}\text{N}$  might be located close to free surfaces (open pores).
- The sole influence of heat at **UNGG** reactor temperatures ( $200 - 500^\circ\text{C}$ ) did not promote  $^{14}\text{C}$  release. On the contrary, both  $^{14}\text{N}$  and  $^{14}\text{C}$  should have been released through radiolytic corrosion when located close to free surfaces.
- The results strengthen the conclusions of previous work arguing that the remaining  $^{14}\text{C}$  inventory in French irradiated graphites has been mainly produced through the activation of  $^{13}\text{C}$ .

### **Exfoliation of irradiated graphite – example of current study**

Work undertaken by **ENEA** in the CAST project considers i-graphite from **Latina** NPP. Graphite has been exfoliated to extract  $^{14}\text{C}$  intercalated between the graphene layers. Three different organic solvents with good solvency properties and water-miscibility have been tested, initially on non-irradiated virgin graphite and then on 15 samples of nuclear i-graphite from Latina NPP moderator. Characterization by means of Scanning Electron Microscopy SEM and Laser Raman Spectrometry has been performed to evaluate the degree of the exfoliation process. A preliminary characterization of the i-graphite samples, in order to estimate the content of radiocarbon  $^{14}\text{C}$ , has been carried out.

### **Leaching of irradiated graphite – examples of current studies**

**RWM** is progressing studies on the leaching of irradiated graphite. As an example of current knowledge, drawing on the UK programme, the following summarises understanding of  $^{14}\text{C}$  releases from graphite on immersion in water. Note that the relevance of this understanding to other CAST Work Package 5 participants will vary, depending on the specifics of respective national programmes, the relative importance of i-graphite within any national programme, national regulations and proposed approaches to i-graphite management, which could include e.g. disposal (surface, geological) or treatment.

- **Release rates and extent of release**

In general, only a small fraction of the total carbon-14 inventory (up to  $\sim 1\%$ ) is released on leaching in solution over timescales of up to 3 to 4 years. The total fractional releases and rates of release over experimental timescales are dependent on the source

of irradiated graphite. This may be related to different irradiation histories, operating temperatures, nature of graphite and extent of radiolytic oxidation

The majority of release occurs to the solution phase; small amounts of gaseous phase releases have been measured. Leaching studies show an initial fast release followed by an approach to a steady state with a very low incremental release rate. Crushing may increase the accessibility of carbon-14 to water but volatile carbon-14 may be lost during crushing. Even when harsh acidic conditions are applied, <30% of the carbon-14 inventory is released over experimental timescales. This points to the likelihood that there are two forms of carbon-14 in irradiated graphite: leachable (with the leachability depending on accessibility to leachant) and non-leachable (inaccessible, probably part of graphite matrix).

- **Speciation**

There is evidence from separate studies that  $^{14}\text{C}$  is released to the solution phase in organic as well as inorganic ( $^{14}\text{CO}_2$ /carbonate) forms under alkaline conditions. Evidence from French and UK studies show that carbon-14 is released to the gas phase under high-pH conditions. Gas phase releases include both volatile  $^{14}\text{C}$ -hydrocarbon/organics (probably  $^{14}\text{CH}_4$ ) and  $^{14}\text{CO}$ .  $^{14}\text{CO}_2$  is also purged from solution at near-neutral pH. The form of gaseous carbon-14 release is affected by redox conditions with a lower redox seeming to favour  $^{14}\text{C}$ -hydrocarbon/organic compounds.

- **Location and form of carbon-14**

There is evidence that carbon-14 has a homogeneously distributed part throughout the graphite matrix that arises primarily from the activation of carbon-13, and a heterogeneously distributed part that is enriched in hotspots and on surfaces. The distribution of carbon-14 is dependent on irradiation and operational history and the extent of radiolytic oxidation that will remove surface carbon and the extent of reordering due to graphite annealing

The chemical form of carbon-14 is primarily elemental and it is bound covalently in the graphite structure. Thus the removal of the bulk of the carbon-14 would only occur by oxidation with conversion to either  $^{14}\text{CO}$  or  $^{14}\text{CO}_2$  but the graphite matrix is extremely resistant to oxidation at GDF temperatures and is unlikely to undergo oxidation once GDF conditions have become anaerobic after closure.

- **Mechanisms of release**

Experimental evidence shows release of carbon from unirradiated graphite is dependent in part on the presence of oxygen; water is required to catalyse the reaction in some way at low temperatures. Release of  $^{14}\text{CO}_2$  as a major product is consistent with a principal mechanism of release being an oxidation process similar to that for graphite at elevated temperatures. The mechanisms of formation of hydrocarbon and/or other VOC species is uncertain but may result from the association of hydrogen with active carbon sites.

### **Release of $^{14}\text{C}$ compounds from i-graphite in alkaline environment**

The main objective of **INR** is to update the inventory of  $^{14}\text{C}$  in the irradiated graphite arising from **TRIGA** 14MW thermal column and to define the associated source term.

On the basis of work undertaken in Romania:

- The experimental results of different tests on C14 release in alkaline solutions published in the literature indicate the presence of  $^{14}\text{C}$  bearing CO and CH<sub>4</sub>. Release kinetics are specific to each species and depend on the properties of graphite, the history and conditions of irradiation.
- The amount of  $^{14}\text{C}$  released into the environment depends on the chemical form in which graphite is released. The  $^{14}\text{C}$ -organic species show a tendency to release as the gaseous form, for example, methane, while the inorganic  $^{14}\text{C}$  is prone to precipitate on the solid matrix of the repository barriers to form, for example, calcium carbonate.
- Most of the experimental tests indicated that the total release of  $^{14}\text{C}$  in hyperalkaline solutions is dominated by inorganic species (CO<sub>2</sub>) which is mostly in the liquid phase.
- The proposed mechanism for explaining release carbon species from i-graphite is the water catalyzed oxidation with oxygen dissolving to form CO<sub>2</sub>,
- there is no clear understanding of the processes leading to the formation of the range of species that may be released on leaching of irradiated graphite.

### **Graphite corrosion**

An understanding of the corrosion behaviour of bulk graphite will enable the prediction of C-14 release from that part of C-14 which is fixed in graphite matrix. This is directly related to the bulk graphite corrosion and is slower than the release of loose bound C-14 on surfaces as well as from disturbed structures. Graphite is a stable material in nature which is proven by its natural occurrence. Only strong oxidative environments will lead to measurable graphite corrosion rates. Work of **FNAG** shows that kinetic and mechanistic studies undertaken to understand the corrosion behaviour of graphite under disposal conditions, as well as the natural analogues of graphite deposits in nature, show that the graphite has an extreme long life time. Work to date indicates that significant graphite corrosion requires high dose rates, which could not be expected from i-graphite, not even spent HTR fuel. However, a disposal site should guarantee that the dose rate from other waste packages disposed near i-graphite is low.

The graphite corrosion can be related to the release of  $^{14}\text{C}$  in comparison to that part of  $^{14}\text{C}$  which is fixed in the matrix graphite. However, loose-bound  $^{14}\text{C}$  at the graphite surface and in defect structures will be 'lost' from graphite faster than the matrix-bound  $^{14}\text{C}$ . Therefore a quantification of the ratio between loose-bound and matrix-bound graphite has to be performed in order to quantify possible  $^{14}\text{C}$  release under disposal conditions.





## References

ADEOGUN, A.C. 2014. Carbon-14 project phase 2 : Inventory (Tasks 1 & 2) Amec report AMEC/200047/003 Pöyry report Pöyry/3900936/Phase 2 v3 (draft).

ALMENAS, K., KALIATKA, A. AND USPURAS, E. IGNALINA RBMK-1500. A SOURCE BOOK. EXTENDED AND UPDATED VERSION, LITHUANIAN ENERGY INSTITUTE, KAUNAS, 1998.

ASSOCIATION of GERMAN ENGINEERS 1990 (VDI) - The society for energy technologies (PUBL.), "AVR - Experimental High Temperature Reactor 21 years of successful operation for a future energy technology".

AVR 2008, Arbeitsgemeinschaft Versuchs-Reaktor AVR GmbH: Si-cherheitsbericht Abbau des AVR Atomversuchskernkraft-werks, E-11026, Stand 29.04.2008.

BANFORD, A., ECCLES, H., GRAVES, M.J., VON LENZA, W., and NORRIS, S. 2008. CARBOWASTE—An Integrated Approach to Irradiated Graphite. Nuclear Future 4, no. 05.

BASTON, G.M.N., CHAMBERS, A.V., COWPER, M.M., FAIRBROTHER H.J., MATHER, I.D., MYATT, B.J., OTLET, R.L., WALKER, A.J. and WILLIAMS, S.J. 2006. A preliminary study of the possible release of volatile carbon 14 and tritium from irradiated graphite in contact with alkaline water, Serco Assurance Report SA/ENV-0654.

BASTON, G.M.N., MARSHALL, T.A., OTLET, R.L., WALKER, A.J., MATHER, I.D. and WILLIAMS, S.J. 2012. Rate and speciation of volatile carbon-14 and tritium releases from irradiated graphite, Mineralogical Magazine 76(8), 3293-3302.

BASTON, G.M.N., PRESTON, S., OTLET, R.L., WALKER, A.J., CLACHER, A., KIRKHAM, M. and SWIFT, B.T. 2014. Carbon 14 release from Oldbury graphite, AMEC Report AMEC/5352 Issue 2.

CAPONE, M., COMPAGNO, A., CHERUBINI, N, DODARO, A. and GUARCINI, T. CARBOWASTE, 2013, Chemical decontamination by organic solvents treatments ultrasound assisted on LT-NPP i-graphite, CARBOWASTE Technical Report T-4.3.3.a, 31/01/2013.

CARLSSON, T., KOTILUOTO, P., VILKAMO, O., KEKKI, T., AUTERINEN, I. and RASILAINEN, K. 2014. Chemical aspects on the final disposal of irradiated graphite and aluminium - A literature survey, VTT Technology 156, ISBN 978-951-38-8095-8.

CLEAVER, J., McCRORY, S., SMITH, T.E. and DUNZIK-GOUGAR, M.L. 2012. Chemical characterisation and removal of C-14 from irradiated graphite, Paper presented at WM2012 Conference, Phoenix, Arizona, 26 February – 1 March 2012.

COBOS, J., GUTIERREZ, L., RODRIGUEZ, N., IGLESIAS, E., PIÑA, G. AND MAGRO, E CARBOWASTE T3.2.4 Irradiated graphite samples bulk analyses at CIEMAT, 2008.

CONSTANTIN, A., DIACONU, D., BUCUR, C. 2013. Performance assessment of C-14 (gas and liquid phase) and Cl-36 (liquid phase) for disposal of irradiated graphite from MTR, CARBOWASTE Report T6.4.5.

CRESPO, E., LUQUE, J, FERNÁNDEZ-RODRÍGUEZ, C., RODAS, M., DÍAZ-AZPIROZ, M., FERNÁNDEZ-CALIANI, J. C. and BARRENECHEA, J. F. 2004

"Significance of graphite occurrences in the Aracena Metamorphic Belt, Iberian Massif". Geological Magazine / Volume 141 / Issue 06 / November 2004, pp 687-697.

DIACONU, D., IORDACHE, M., CONSTANTIN, A., IORGULIS, C., ARSENE, C., 2013. Characteristics of the Irradiated Graphite from the TRIGA Thermal Column, EURADWASTE 2013, Vilnius, October 14-17, 2013.

DRUTEIKIENE, R., DUSKESAS, G., GUDELIS, A. AND GVOZDAITE. R. TECHNICAL REPORT T-6.1.8. 2013. Leach Behaviour of RBMK-1500 Graphite. CARBOWASTE Project.

EDFE, 2014. Information on graphite weight loss levels for AGRs, <http://newsroom.edfenergy.com/News-Releases/Information-on-graphite-weight-loss-levels-for-Advanced-Gas-cooled-Reactors-AGRs-2ba.aspx>, 11/07/2014.

FACHINGER, J., 2008. Inventory of Reactor Graphite and Treatment for Disposal (gehalten auf der RADWAP 2008, Würzburg, 2008), <http://www.fz-juelich.de/ief/ief-6/datapool/page/404/Fachinger%20-%20Inventory%20of%20Reactor%20Graphite%20and%20Treatment%20for%20Disposal.pdf>.

FACHINGER, J., den EXTER, M., GRAMBOW, B., HOLGERSSON, S., LANDESMAN, C., TITOV, M. and PODRUHZINA, T. 2006. Behaviour of spent HTR fuel elements in aquatic phases of repository host rock formations. HTR-2004. Nuclear Engineering and Design, Volume 236, Issues 5–6, March 2006, Pages 543–554.

FACHINGER, J., ZHANG, Z. X. and BRODDA, B. G. 2012. Graphite corrosion and hydrogen release from HTR fuel elements in Q-Brine. Comprehensive Nuclear Materials, Pages 539–561, Volume 5: Material Performance and Corrosion/Waste Materials.

GASCÓN, J.L. ET AL. CARBOWASTE T-4.3.5-d Report on decontamination of irradiated graphite by chemical treatment with liquid agents. 2013.

GIRKE, N.A., STEINMETZ, H.-J., BOSBACH, D., BUSHUEV, A.V. and ZUBAREV, V.N. 2011. Carbon-14 and tritium content in contaminated reactor graphite after long-term storage, Paper presented at WM2011, Phoenix, Arizona.

GRAMBOW, B., NORRIS, S., PETIT, L., Petit, L., BLIN, V., COMTE, J. and de VISSER – TÝNOVÁ, E. 2013. CARBOWASTE Project Work Package 6, Disposal Behaviour of Irradiated Graphite & Carbonaceous Wastes -Final Report.

Graphit Kropfmühl AG; <http://www.gk-graphite.com/graphitanwendungen.....>“

GRAY, W.J. 1982. A study of the oxidation of graphite in liquid water for radioactive waste storage applications, Rad. Waste Management 3, 137-149.

GRAY, W.J. and MORGAN W.C. 1988. Leaching of 14C and 36Cl from Hanford reactor graphite, Pacific Northwest laboratory Report PNL-67699.

GRAY, W.J. and MORGAN, W.C. 1989. Leaching of 14C and 36Cl from irradiated French graphite, Pacific Northwest laboratory Report PNL-6989.

HANDY, B.J. 2006. Experimental study of C 14 and H 3 release from irradiated graphite spigot samples in alkaline solutions, NNC Report 11996/TR/001, Issue 1.

- HEARD, P.J., PAYNE, L., WOOTTON, M.R. and FLEWITT, P.E.J. 2014. Evaluation of surface deposits on the channel wall of trepanned reactor core graphite samples, *J. Nucl. Mats.* 91-97, 445.
- HOU, X. 2005. Rapid analysis of <sup>14</sup>C and <sup>3</sup>H in graphite and concrete for decommissioning of nuclear reactor, *Applied Radiation and Isotopes* 62 (2005) 871–882.
- IAEA, 2000. Irradiation damage in graphite due to fast neutrons in fission and fusion systems, International Atomic Energy Agency IAEA-TECDOC-1154.
- IAEA, 2006, IAEA-TECDOC-1521 Characterization, Treatment and Conditioning of Radioactive Graphite from Decommissioning of Nuclear Reactors, September 2006.
- IAEA, 2010, IAEA-TECDOC-1647 Progress in Radioactive Graphite Waste Management, 2010.
- IORGULIS, C, DIACONU, D, GUGIU, D, ROTH, C. 2013. Isotopes accumulation in the thermal column of TRIGA reactor, NUCLEAR 2013 Conference, Pitesti, May 16-18, 2013, ISSN 2066-2955.
- ISOBE, M., NUMATA, K., TAKAHASHI, R., SASOH, M., HIROSE, E. and SAKURAI, J. 2007. Distribution coefficient of C-14 released from irradiated graphite in Tokai plant, Atomic Energy Society of Japan Autumn Meeting (in Japanese), N57.
- ISOBE, M., YAMAMOTO, T., TAKAHASHI, R., SASOH, M., KURASAWA, S. and NAKANE, Y. 2008a. Leaching behaviour of radioactive nuclide from irradiated graphite in Tokai plant, Atomic Energy Society of Japan Autumn Meeting (in Japanese), I45.
- ISOBE, M., YAMAMOTO, T., TAKAHASHI, R., SASOH, M., NAKANE, Y. and SAKAI, H. 2008b. Chemical form of organic C-14 leaching from irradiated graphite in Tokai plant, Atomic Energy Society of Japan Autumn Meeting (in Japanese), L28.
- ISOBE, M., YAMAUCHI, T., TAKAHASHI, R., SASOH, M. and NAKANE, Y. 2009. Leaching behaviour of C 14 from irradiated graphite in Tokai plant, Atomic Energy Society of Japan Autumn Meeting (in Japanese), M20.
- JACKSON, C.P. and YATES, H. Key Processes and Data for the Migration of <sup>14</sup>C Released from a Cementitious Repository - SERCO Report SERCO/TAS/002925/002 Issue 2.2, April 2011.
- KNIZIA, K. and SIMON, M. Betriebserfahrungen mit dem THTR-300 und Zukunftsaussichten fuer Hochtemperaturreaktoren; *atomwirtschaft-atomtechnik*, 1988, S. 435-441
- MARSDEN, B.J., HOPKINSON, K.L and WICKHAM, A.J. 2002. The chemical form of carbon-14 within graphite, Serco Assurance Report SA/RJCB/RD03612001/R01 Issue 4.
- MARSDEN, B. J. and WICKHAM, A. J., 2006. Characterization, Treatment and Conditioning of Radioactive Graphite from Decommissioning of Nuclear Reactors. IAEA-TECDOC-1521.
- MARSHALL, T.A., BASTON, G.M.N., OTLET, R.L., WALKER, A.J. and Mather, I.D. 2011. Longer term release of carbon-14 from irradiated graphite, Serco Report SERCO/TAS/001190/001 Issue 2.

McDERMOTT, L., 2011. Characterisation and chemical treatment of irradiated UK graphite waste, PhD Thesis, University of Manchester.

MOORMANN, R. 2008. "A safety re-evaluation of the AVR pebble bed reactor operation and its consequences for future HTR concepts", Forschungszentrum Jülich , Jül-4275, [http://juser.fz-juelich.de/record/1304/files/Juel\\_4275\\_Moormann.pdf](http://juser.fz-juelich.de/record/1304/files/Juel_4275_Moormann.pdf), 2008.

NARKUNAS, E., SMAIZYS, A., POSKAS, P., DRUTEIKIENE, R., DUSKESAS, G., GARBARAS, A., GUDELIS, A., GVOZDAITE, R., LUJANIENE, G., PLUKIENE, R., PLUKIS, A. AND PUZAS, A. TECHNICAL REPORT T-3.4.2. 2013a. Assessment of Isotope-Accumulation Data from RBMK-1500 Reactor. CARBOWASTE Project.

NARKUNAS, E., POSKAS, P., BLACK, G., JONES, A., IORGULIS, C., DIACONU, D., PETIT, L. AND PONCET, B. TECHNICAL REPORT T-3.4.3. 2013b. Modelling of Isotope Release Mechanism Based on Fission Product Transport Codes. CARBOWASTE Project.

NARKUNIENE, A., POSKAS, P. AND KILDA, R. TECHNICAL REPORT T-6.4.4. 2012. Study of the Relation between Treatment and Disposal on the Performance of RBMK-1500 Graphite in Crystalline Rock. CARBOWASTE Project.

NDA, 2010a. Nuclear Decommissioning Authority, Geological disposal: Gas status report, NDA/RWMD/037.

NDA, 2010b. Nuclear Decommissioning Authority, Geological disposal. An overview of the generic Disposal System Safety (DSSC), NDA Report NDA/RWMD/010.

NDA, 2012. Nuclear Decommissioning Authority, Geological disposal. Carbon-14 project phase 1 report, NDA Report NDA/RWMD/092.

NABIELEK, H., VAN DER MENWE, H., FACHINGER, J., VERFONDERN, K., VON LENZA, W., GRAMBOW, B. and de VISSER -TÝNOVÁ, E. 2010. *Ceramic Coated Particles for Safe Operation in HTRs and in Long-Term Storage* (pages 193–202). In *Ceramics in Nuclear Applications*, editors Katoh, Y., Cozzi, A., Singh, D. and Salem, J. Print ISBN: 9780470457603, Online ISBN: 9780470584002.

PAYNE, L., HEARD, P. and SCOTT, T. 2014. The use of magnetic sector secondary ion mass spectrometry to investigate <sup>14</sup>C distribution in Magnox reactor core graphite, poster presented at IGD-TP conference, Manchester, UK 2014, submitted for publication *Min. Mag.*

PIÑA, G., JONES, A., VULPIUS, D., COMTE, J., NARKUNAS, E. AND VON LENZA, W. CARBOWASTE D-3.0.0 Summary Report on Work Package 3, 2013.

PIÑA, G., RODRIGUEZ, M., GASCON, J.L., MAGRO, E. AND LARA, E. CARBOWASTE D.3.1.5-CWRRT Final Report on Statistical Evaluation & Conclusions, 2013.

PIÑA, G., RODRIGUEZ, M., VULPIUS, D., COMTE, J., BRENNETOT, R., DODARO, A., DUSKEAS, G., BRUNE, C., VISSER – TYNOVA, E., VAN HECKE, K., LANDESMAN, C. AND JONES, A. CARBOWASTE T-3.1.6 Topical Report on Characterization Methods, 2013.

PIÑA, G. ET AL. CARBOWASTE T-3.5.1 Topical Report with the characteristics of the legacy irradiated graphite, 2013.

PIÑA, G., ARSENE, C., CAPONE, M., GASCÓN, J. L., JONES, A., MCDERMOTT, L., VULPIUS, D. CARBOWASTE, 2013, Decontamination Factors by Decontamination Agents under Normal Pressure, CARBOWASTE D-0113-4.3.5, 20/01/2013.

PODRUZHINA, T. 2005. Graphite as radioactive waste: Corrosion behaviour under final repository conditions and thermal treatment, Forschungszentrum Jülich, Jül 4166.

PONCET, B. and PETIT, L. 2013. Method to assess the radionuclide inventory of irradiated graphite waste from gas-cooled reactors, J. Radioanal. Nucl. Chem. (2013) 1– 13.

RIEGER, T. 2007. "Strahleninduzierte Oxidation von graphitischen Werkstoffen - Verhalten bei Wasserzutritt im Endlager". (Diplomarbeit RWTH Aachen 2007).

RIEGER, T. 2008. "Strahleninduzierte Oxidation von graphitischen Werkstoffen - Verhalten bei Wasserzutritt im Endlager", IB-IEF-6/001, FZJ, Institut für Energieforschung-6 Jülich.

SILBERMANN, G. 2013. Effets de la température et de l'irradiation sur le comportement de <sup>14</sup>C et de son précurseur <sup>14</sup>N dans le graphite nucléaire. Etude de la décontamination thermique du graphite en présence de vapeur d'eau, PhD thesis, Oktober 15<sup>th</sup> 2013, Université de Lyon LYCEN T 2013-12.

SILBERMANN, G., MONCOFFRE, N., TOULHOAT, N., BÉRERD, N., PERRAT - MABILON, A., LAURENT, G., RAIMBAULT, L., SAINSOT, P., ROUZARD, J.-N. and DELDICQUE, D. 2014. Temperature effects on the behavior of carbon 14 in nuclear graphite, Nuclear Instruments and Methods in Physics Research B 332 (2014) 106–110.

SMITH, T.E., McCRORY, S. and DUNZIK-GOUGAR, M.L. 2013. Limited oxidation of irradiated graphite waste to remove surface carbon-14, Nuclear Engineering and Technology 45, 211-218.

SPINKS, J. W. T. and WOODS, R. J. 1990. An Introduction to Radiation Chemistry, ISBN-13: 978-0471614036 ISBN-10: 0471614033.

TAKAHASHI, R., TOYAHAH, M., MARUKI, S., UEDA, H. and YAMAMOTO, T. 2001. Investigation of morphology and impurity of nuclear grade graphite, and leaching mechanism of Carbon 14, in Proceedings, Nuclear Graphite Waste Management, Manchester, UK, 18-20 October 1999, IAEA.

VENDÉ, L. 2012. Comportement des déchets graphite en situation de stockage: relâchement et répartition des espèces organiques et inorganiques due carbone 14 et du tritium en milieu alcalin, Thèse de Doctorate no. 2012EMNA0018, l'Ecole des Mines, de Nantes, L'Université Nantes, Angers et Le Mans, submitted 26 October 2012, accessed at [www.theses.fr/2012EMNA0018/abes](http://www.theses.fr/2012EMNA0018/abes) 10 January 2014.

VON LENZA, W., VULPIUS, D., STEIMETZ, H.-J., GIRKE, N., BOSBACH, D., THOMASKE, B., BANFORD, A.W., BRADBURY, D., GRAMBOW, B., GRAVE M.J., JONES, A.N., PETIT, L. and PINA, G. 2011. Treatment and disposal of irradiated graphite and other carbonaceous waste, ATW, International Journal for Nuclear Power, April/May 2011; ISSN 1431-5254. ([http://www.carbowaste.eu/lw\\_resource/datapool/\\_pages/pdp\\_10/CW1103-AtW-final.pdf](http://www.carbowaste.eu/lw_resource/datapool/_pages/pdp_10/CW1103-AtW-final.pdf)).

VULPIUS, D., BAGINSJI, K., FISCHER, C. and THOMASUSKE, B. 2013. Location and chemical bond of radionuclides in neutron-irradiated nuclear graphite, J. Nuclear Materials 438, 163-177.

VULPIUS, D., VON LENZA, W., JONES, A., GUY, C., COMTE, J., PIÑA, G., DODARO, A., DUŠKESAS, G. AND IORDACHE, M. CARBOWASTE D-3.3.1 First Radionuclide Inventory Data on Untreated Graphite /Evaluation for Direct Disposal, 2010.

WAREING, A., ABRAHAMSEN, L., BANFORD, A. AND METCALFE, M. CARBOWASTE, 2013, Synthesis of CARBOWASTE Work Package Findings, CARBOWASTE Technical Report T-1.7.3, 22/05/2013.

WHITE, I.F., SMITH, G.M., SAUNDER, L.J., KAYE, C.J., MARTIN, T.J., CLARKE, G.H. and WAKERLEY, M.W. 1984. Assessment of management modes for graphite from reactor decommissioning, CEC Report EUR 9232.

Wikipedia, <http://de.wikipedia.org/wiki/Graphit>

WOHLER, J. and RAUTENBERG, J.; Ergebnisse des THTR 300 Leistungsbetriebs; 1987 Kerntechnik 51 (1987), No 3.

YAMASHITA, Y. 2012a. A study on migration behaviour of C-14 in graphite waste, presentation to AMEC and NDA RWMD on 12 September 2012.

YAMASHITA, Y. 2012b. A study on the analysis methods of C-14 chemical species, presentation to AMEC and NDA RWMD on 12 September 2012.

ZIEGLER, J.F., BIERSACK, J.P. and ZIEGLER, M.D. SRIM, The Stopping and Range of Ions in Matter. SRIM Co (2008).

ZLOBENKO, B., SHABALIN, B., SKRIPKIN, V., FEDORENKO Y. and YATZENKO, V. Report on graphite categories in the RBMK reactor, CAST-2014-D5.3, 2014.